Sphalerons and Electroweak Baryogenesis

Cand. Scient. Thesis

by

Solveig Skadhauge

The Niels Bohr Institute

University of Copenhagen

August 1996

Contents

Introduction

The Universe we live in consist mainly of matter. Locally this is evident from observations, since the amount of antimatter, present in for instance cosmic rays, is so small that it can be considered zero. The region of pure matter can be estimated to be of size of the present horizon. Indeed if antimatter was present in a considerable amount, it would collide with matter, causing large gamma bursts to be emitted. These are not detected and it is confident that the amount of antimatter can be neglected. If the asymmetry is just local, matter and antimatter has to be separated with a size given by the current horizon. This corresponds to causally disconnected region in the Early Universe. Therefore it is not possible to have a mechanism for separating matter and antimatter on the large scale needed[1].

The totally asymmetric Universe today, corresponds to a tiny asymmetry in the early Universe. Analysis of the primordial nucleosynthesis gives a ratio of baryon density to entropy density of

$$\Delta = \frac{n_b}{s} = 4 \times 10^{-11} \Leftrightarrow 10^{-10} \tag{0.1}$$

Above a temperature of twice the mass of the fermion q the process $\gamma \leftrightarrow q\bar{q}$ is in equilibrium, and one can deduce that in the early Universe there was one extra baryon per billion baryon-antibaryon pair.

The symmetric description of antiparticles and particles in the physical theories, lead us to wonder how there can be an asymmetry. It seems very subtle to explain the small asymmetry. One could assume that the initial condition of the Universe was asymmetric with respect to the number of baryons and antibaryons. From a physical point of view, this is not appealing, we would like to be able to explain it by means of a physical theory, and the dynamics of the early Universe. In this way the baryon asymmetry could be considered a remnant of the early Universe.

In 1966 Sakharov [4] was the first to discussed the possibility of generating a baryon asymmetry of the Universe in terms of particle theory. During the past decades much work have been done in explaining this asymmetry. Various scenarios have been proposed at different time periods and energy scales. I will mainly consider the scale of ~ 100 GeV. At this scale the electroweak phase transition took place, and one might hope that it will provide us with the possibility of generating an asymmetry.

The baryon number is to a very high degree a conserved quantum number at the low energy scale, present in today's Universe. As we shall see the electroweak baryon number is not conserved on the quantum level due to the chiral anomaly. In fact the baryon violating processes are fast at high temperatures, offering an opportunity to explain the asymmetry, since these are naturally a needed ingredient in a baryogenesis mechanism.

[1] Inflationary model may give a locally asymmetric Universe

An important implication of the high rate is that any asymmetry created before the electroweak phase transition is washed out, unless special conditions are satisfied.

The standard model is known to fit experiments very well at the energy scale we can probe now. An interesting question is whether it is capable of explaining the observed baryon asymmetry. If not a new theory will have to be proposed. Choosing a baryogenesis scenario, and fitting it to the observed asymmetry, gives the possibility to put constraints on the parameters of a theory. In this sense we may consider the baryon asymmetry as a test of a theory at high energies, since a "real" physical theory should be able to predict it. What we can observe as remnants from the early Universe is a nice addition to high energy experiments.

In this thesis I give an overview of the current status of electroweak baryogenesis studies. My own work has been concerning an area related to this subject, which is determining the sphaleron barrier of the $SU(2)$ Higgs theory. The sphaleron configuration and its connection to baryon violating processes in the electroweak theory is described in detail, while the electroweak phase transition and baryogenesis scenarios will be treated on a more heuristic level.

Chapter 1

Basics of electroweak theory

In this chapter the electroweak theory is described with emphasis on aspects of interest for baryogenesis.

1.1 Weinberg-Salam theory

The Weinberg-Salam theory unifies the electromagnetic and weak interaction. The theory describes the electroweak sector of the standard model, and is a $SU(2)_L \times U(1)_Y$ gauge theory, with spontaneous symmetry breaking. The symmetry breaking is obtained by a coupling to a Higgs field Φ, which is a doublet complex field conventionally written as

$$\Phi(x) = \begin{pmatrix} \phi^+(x) \\ \phi^0(x) \end{pmatrix} , \qquad Y(\Phi) = 1 , \tag{1.1}$$

where $\phi^+(x)$ and $\phi^0(x)$ are complex scalar fields, and Y is the weak hypercharge. Throughout this paper we will use the metric $g_{\mu\nu} = \mathrm{diag}(1, \Leftrightarrow 1, \Leftrightarrow 1, \Leftrightarrow 1)$. The bosonic part of the Weinberg-Salam Lagrangian is given by

$$\mathcal{L}_\mathrm{b} = \frac{1}{2g^2}\,\mathrm{Tr} F_{\mu\nu}F^{\mu\nu} \Leftrightarrow \frac{1}{4} f_{\mu\nu}f^{\mu\nu} + (D_\mu\Phi)^\dagger(D^\mu\Phi) \Leftrightarrow V(\Phi^\dagger\Phi) , \tag{1.2}$$

where $F_{\mu\nu} = \partial_\mu A_\nu \Leftrightarrow \partial_\nu A_\mu + [A_\mu, A_\nu]$ is the $SU(2)$ field strength tensor, and $f_{\mu\nu} = \partial_\mu a_\nu \Leftrightarrow \partial_\nu a_\mu$ is the $U(1)$ field tensor. The $SU(2)$ gauge fields can be expanded in terms of the Lie algebra elements by $A_\mu(x) = \Leftrightarrow igT^\alpha A^\alpha_\mu$, where $\alpha = 1, 2, 3$ is the SU(2) colour index, also known as weak isospin. The covariant derivative is given by

$$D_\mu = \partial_\mu I \Leftrightarrow igT^\alpha A^\alpha_\mu \Leftrightarrow ig'\frac{Y}{2}a_\mu . \tag{1.3}$$

The gauge group is not simple, and we need two coupling constants, g for $SU(2)$ and g' for $U(1)$. Normally we will take half the Pauli-matrices as generators for the Lie algebra, $T^\alpha = \frac{1}{2}\sigma^\alpha$. The weak hypercharge operator Y, can be written in terms of the electric charge Q and the third component of the weak isospin T_3, by the relation $Y = 2(Q \Leftrightarrow I_3)$. The potential for the Higgs field is described by a quartic self coupling,

$$V(\Phi^\dagger\Phi) = \lambda(\Phi^\dagger\Phi \Leftrightarrow \frac{v^2}{2})^2 \tag{1.4}$$

The Higgs field is needed to give mass to the gauge fields in a gauge invariant way. When then Higgs field acquires a vacuum expectation value v, the symmetry of the Lagrangian is spontaneously broken, since the vacuum is no longer gauge invariant. But the Lagrangian is still gauge invariant as it should. The $SU(2)_L$ symmetry is completely broken, by the vacuum expectation value of the Higgs field

$$\langle\Phi\rangle_0 = \langle 0|\Phi|0\rangle = \begin{pmatrix} 0 \\ \frac{v}{\sqrt{2}} \end{pmatrix} . \tag{1.5}$$

Now defining

$$W_\mu^\pm = \frac{1}{\sqrt{2}}(A_\mu^1 \mp iA_\mu^2) , \tag{1.6}$$

we get the fields for the charged W particles. The Weinberg angle θ_W is given by

$$\cos(\theta_W) = \frac{g^2}{\sqrt{g^2+g'^2}} . \tag{1.7}$$

From this we may write the neutral Z field, and the photon field B_μ,

$$Z_\mu = \sin(\theta_W)a_\mu \Leftrightarrow \cos(\theta_W)A_\mu^3 , \qquad B_\mu = \cos(\theta_W)a_\mu + \sin(\theta_W)A_\mu^3 . \tag{1.8}$$

It is easily seen that the covariant derivative gives rise to a mass term for the gauge fields. Using 1.5

$$(D_\mu\Phi)^\dagger(D^\mu\Phi) = \tfrac{1}{2}v^2\left(\frac{g^2}{2}W_\mu^- W^{+\mu} + \tfrac{1}{4}(g^2+g'^2)Z_\mu Z^\mu\right) , \tag{1.9}$$

where we get $M_W = \frac{1}{2}vg$ and $M_Z = \frac{1}{2}v\sqrt{g^2+g'^2}$. The photon field is left massless.

The fermionic content of the standard model consists of 3 generations with 2 doublets each, one quark doublet and one lepton doublet. The first generation is

$$\begin{pmatrix} u \\ d \end{pmatrix}, \begin{pmatrix} e \\ \nu_e \end{pmatrix} . \tag{1.10}$$

The quark doublet further comes in three different colors, arising from the $SU(3)$ gauge group of the standard model. In total there are 24 fermions. A crucial point of the electroweak theory, is the gauge fields does not couple to the full fermion field, but to the chiral fermions,

$$u_L = \tfrac{1}{2}(1 \Leftrightarrow \gamma_5)u , \qquad u_R = \tfrac{1}{2}(1+\gamma_5)u , \tag{1.11}$$

where u_L is the left handed field, and u_R is the right handed field. The coupling to these components of the fermion fields is not equal, in fact for the case of the $SU(2)$ gauge field the right handed part totally decouples. For simplicity the fermionic Lagrangian is only written for the quark doublet ψ of the first generation, with analog contribution from the other doublets,

$$\psi_L = \begin{pmatrix} u_L \\ d_L \end{pmatrix} . \tag{1.12}$$

We will also collect the right handed fields in doublets, even though they transform as singlets under the $SU(2)$ group. The fermionic part of the Weinberg-Salam Lagrangian is given by

$$\begin{aligned} \mathcal{L}_{\mathrm{f}} &= \bar\psi_L i\gamma^\mu D_\mu\psi_L + \bar\psi_R i\gamma^\mu(\partial_\mu \Leftrightarrow ig'\frac{Y}{2}a_\mu)\psi_R \\ &\Leftrightarrow f^{(u)}(\bar\psi_L\tilde\Phi u_R + \bar u_R\tilde\Phi^\dagger\psi_L) \Leftrightarrow f^{(d)}(\bar d_R\Phi^\dagger\psi_L + \bar\psi_L\Phi d_R) . \end{aligned} \tag{1.13}$$

Here $\tilde{\Phi} = i\sigma_2\Phi^*$. An implicit sum over the three $SU(3)$ colors is meant for the quarks doublets. Also the fermions acquire a mass, due to the Yukawa coupling to the Higgs field

$$m_u = \frac{1}{\sqrt{2}} f^{(u)} v \ , \qquad m_d = \frac{1}{\sqrt{2}} f^{(d)} v \ . \tag{1.14}$$

Note that the Lagrangian 1.13 is an approximation, since the quarks with electric charge $\Leftrightarrow\frac{1}{3}$ is mixed with the Kobayashi-Maskawa matrix K

$$\begin{pmatrix} d' \\ s' \\ b' \end{pmatrix} = K \begin{pmatrix} d \\ s \\ b \end{pmatrix} \tag{1.15}$$

The mixing of the quarks can give rise to CP violation, if K has a complex phase.

The full Lagrangian for the electroweak theory is

$$\mathcal{L} = \mathcal{L}_f + \mathcal{L}_b + \mathcal{L}_c + \mathcal{L}_g \tag{1.16}$$

where $\mathcal{L}_c$ contains the counterterms that have to be added when the theory is renormalized, and $\mathcal{L}_g$ is a gauge fixing term, that makes it possible to define a propagator for the gauge fields. Since we are not going to use these terms, they will not be described in any detail.

The Lagrangian is invariant under the gauge transformations

$$A_\mu(x)U(x)A_\mu(x)U^{-1}(x) \Leftrightarrow (\partial_\mu U(x))U^{-1}(x) \ , \tag{1.17}$$

$$\Phi(x) \to U(x)\Phi(x) \ , \tag{1.18}$$

$$\psi(x) \to U(x)\psi(x) \ , \tag{1.19}$$

where $U(x) \in SU(2)$. And a $U(1)$ gauge transformation

$$a_\mu(x) \to a_\mu(x) \Leftrightarrow i\partial_\mu\alpha(x) \ , \quad \Phi(x) \to e^{i\alpha(x)}\Phi(x) \ , \quad \psi(x) \to e^{i\alpha(x)}\psi(x) \ . \tag{1.20}$$

where $\alpha(x)$ is a arbitrary scalar function. The only unknown parameter of the Weinberg-Salam theory is the Higgs self coupling λ.

1.2 The vacuum structure of $SU(2)$

For the purpose of studying electroweak baryogenesis, it is a good approximation to neglect the $U(1)$ gauge fields in the Weinberg-Salam theory. This is equivalent to putting the Weinberg angle to zero, since in this limit the $U(1)$ fields totally decouple. As we shall see, baryon number violating processes are associated with a transition of the $SU(2)$ gauge fields between topologically different vacuum states. The $U(1)$ gauge group has a topologically trivial vacuum structure with a unique vacuum state, and for this reason it will only enter the dynamics of baryon violating processes. Hence for the rest of this chapter we will restrict ourself to a $SU(2)$ gauge theory. In the present section the Higgs field and the fermions are disregarded as well.

The vacuum structure of the $SU(2)$ gauge theory turns out to be rather complicated, in the sense that there is a discrete set of classically vacua, that cannot be transformed

continuously into one another, without passing through non vacuum states. To see this we rotate to Euclidean time ($x_0 \to \Leftrightarrow ix_4$), so that space time equals R^4. The Euclidean Lagrangian in the pure $SU(2)$ theory is

$$\mathcal{L} = \frac{1}{2g^2}\,\mathrm{Tr}F_{\mu\nu}F^{\mu\nu}\ . \tag{1.21}$$

Hence the vacuum condition for a pure Yang-Mills theory reads

$$\forall x \in R^4\ :\quad F_{\mu\nu}(x) = 0 \tag{1.22}$$

If $F_{\mu\nu}(x)$ vanishes in some open connected neighbourhood of x, then $A_\mu(x)$ is a pure gauge, i.e.

$$F_{\mu\nu}(x) = 0 \Leftrightarrow \exists U(x):\ A_\mu(x) = \partial_\mu U(x)U^{-1}(x)\ . \tag{1.23}$$

Indeed if $F_{\mu\nu}(x) = 0$ in a region around x_0, then the integral of A_μ along a curve C, starting at x_0 and ending at x, does not depend on the curve. The path ordered integral

$$U(x) = P\exp(\int_C A_\mu(x')dx'_\mu) \tag{1.24}$$

is independent of C. This U will therefore satisfy the pure gauge form for A_μ. It is easily seen that the opposite statement is true, since if A_μ is a pure gauge then the field strength tensor obviously vanishes. This shows that a vacuum state is a pure gauge in the whole Euclidean space. Therefore a vacuum state can be represented by the matrix $U(x) \in SU(2)$ defined for all x in R^4.

Given a $U \in SU(2)$, it can be written in terms of the Lie algebra $su(2)$, which is spanned by the Pauli matrices.

$$U = e^{i\epsilon_\alpha\sigma_\alpha} = \cos(|\epsilon|)I + i\frac{\epsilon_\alpha\sigma_\alpha}{|\epsilon_\alpha|}\sin(|\epsilon|) = a_0 I + i\vec{a}\vec{\sigma} \tag{1.25}$$

and since $\det U = 1$ we have

$$a_0^2 + a_1^2 + a_2^2 + a_3^2 = 1\ , \tag{1.26}$$

showing that U can be represented by a point on the three sphere S^3. This implies that $SU(2)$ is topologically equivalent to S^3. Generally, a configuration having a finite Euclidean action, must approach a pure gauge at infinity. Choosing the boundary conditions such that $U \to 1$ at spatial infinity,

$$\lim_{|x|\to\infty} U(x) = 1\ , \tag{1.27}$$

$$\lim_{|x|\to\infty} A_\mu(x) = 0\ , \tag{1.28}$$

allows us to compactify Euclidean space R^4 to S^3. Hereby $U(x)$, representing a vacuum state, defines a map from S^3 to itself,

$$U:\ S^3 \to SU(2) \sim S^3\ . \tag{1.29}$$

The vacuum states can be characterized as laying in $\pi_3(S^3) = Z$, where Z is the set of integer numbers. The degenerate vacuum states are physically equivalent but topologically distinct. Topologically the vacuum states can be divided into different homotopy classes,

classified by the integer winding number, that counts the number of times S^3 is mapped onto itself. The winding number n is given by

$$n(U) = \frac{1}{24\pi^2}\int d^3x\epsilon_{ijk}\ \mathrm{Tr}(\partial_i U)U^{-1}(\partial_j U)U^{-1}(\partial_k U)U^{-1}\ . \tag{1.30}$$

An example is given, where we choose the temporal gauge $A_0 = 0$. There is still the freedom of choosing a time independent gauge transformation $\partial_0 U(x) = 0$, since this will leave A_0 invariant,

$$A_0(x) \to A_0'(x) = U^{-1}(x)A_0(x)U(x) \Leftrightarrow \partial_0 U(x)U^{-1}(x) = 0\ . \tag{1.31}$$

The vacuum states will be described by a time independent potential satisfying

$$A_i(\vec{x}) = \Leftrightarrow \partial_i U(\vec{x})U^{-1}(\vec{x})\ . \tag{1.32}$$

For instance, with λ an arbitrary scale parameter, and

$$U(\vec{x}) = e^{i\pi\vec{\sigma}\cdot\vec{x}/(x^2+\lambda^2)^{\frac{1}{2}}}\ , \tag{1.33}$$

the corresponding pure gauge vacuum is a $n = 1$ vacuum state.

Generally, to a four dimensional configuration with finite Euclidean action, we can assign the topological charge Q of the configuration

$$Q = \frac{1}{16\pi^2}\int d^4x\ \mathrm{Tr}F_{\mu\nu}\tilde{F}^{\mu\nu}\quad ,\ \tilde{F}^{\mu\nu} = \tfrac{1}{2}\epsilon^{\mu\nu\rho\sigma}F_{\rho\sigma}\ , \tag{1.34}$$

where $\tilde{F}_{\mu\nu}$ is the dual tensor. It is clearly a gauge invariant quantity. The topological charge can be written as a total derivative, since

$$\mathrm{Tr}F_{\mu\nu}\tilde{F}^{\mu\nu} = \partial_\mu K^\mu\ , \tag{1.35}$$

where

$$K^\mu = 2\epsilon^{\mu\nu\rho\sigma}\ \mathrm{Tr}(A^\nu\partial^\rho A^\sigma + 2/3A^\nu A^\rho A^\sigma)\ . \tag{1.36}$$

This can easily be seen. Using $F_{\mu\nu} = [D_\mu, D_\nu]$ we get

$$\begin{aligned}
\mathrm{Tr}F_{\mu\nu}\tilde{F}^{\mu\nu} &= \tfrac{1}{2}\epsilon^{\mu\nu\rho\sigma}\ \mathrm{Tr}(\partial_\mu A_\nu \Leftrightarrow \partial_\nu A_\mu + [A_\mu, A_\nu])(\partial_\rho A_\sigma \Leftrightarrow \partial_\sigma A_\rho + [A_\rho, A_\sigma]) \\
&= \tfrac{1}{2}\epsilon^{\mu\nu\rho\sigma}\ (4\ \mathrm{Tr}(\partial_\mu A_\nu\partial_\rho A_\sigma) + 4\ \mathrm{Tr}A_\mu A_\nu(\partial_\rho A_\sigma) + 4\ \mathrm{Tr}(\partial_\mu A_\nu)A_\rho A_\sigma) \\
&= 2\epsilon^{\mu\nu\rho\sigma}\ (\ \mathrm{Tr}\partial_\mu A_\nu\partial_\rho A_\sigma + 2\ \mathrm{Tr}(\partial_\mu A_\nu)A_\rho A_\sigma)\ .
\end{aligned} \tag{1.37}$$

Because of the cyclic property of the trace we have

$$\partial_\mu K_\mu = 2\epsilon^{\mu\nu\rho\sigma}\ \mathrm{Tr}\left[(\partial_\mu A_\nu)(\partial_\rho A_\sigma) + 2(\partial_\mu A_\nu)A_\rho A_\sigma\right]\ , \tag{1.38}$$

which completes the proof. Note that expanding the field strength tensor in the Lie algebra elements, $F_{\mu\nu} = \Leftrightarrow igF^\alpha_{\mu\nu}T^\alpha$, we have that $F^\alpha_{\mu\nu} = \partial_\mu A^\alpha_\nu \Leftrightarrow \partial_\nu A^\alpha_\mu + g\epsilon_{\alpha\beta\gamma}A^\beta_\mu A^\gamma_\mu$. Then K_μ, in terms of the Lie algebra elements, reads

$$K_\mu = \Leftrightarrow\frac{1}{2}g^2\epsilon_{\mu\nu\rho\sigma}(A^a_\nu F^a_{\rho\sigma} \Leftrightarrow \frac{1}{3}g\epsilon_{abc}A^a_\nu A^b_\rho A^c_\sigma)\ . \tag{1.39}$$

Using 1.35 and 1.34 the topological charge becomes

$$Q = \frac{1}{16\pi^2}\int d^4x \partial_\mu K_\mu \ . \tag{1.40}$$

The Chern-Simons number N_{CS} is defined by

$$N_{CS} = \frac{1}{16\pi^2}\int d^3x K^0 = \frac{1}{8\pi^2}\int d^3x \epsilon_{ijk}\ \mathrm{Tr}(A^i\partial^j A^k + \frac{2}{3}A^iA^jA^k) \ . \tag{1.41}$$

A large gauge transformation is one that cannot be continuously deformed into the identity, and it will change the Chern-Simons number by an integer amount, since we have that a gauge transformation with $U \in SU(2)$ changes N_{CS} as

$$N_{CS} \to N_{CS} + \frac{1}{24\pi^2}\int d^3x \epsilon_{ijk}\ \mathrm{Tr}(\partial_i U)U^{-1}(\partial_j U)U^{-1}(\partial_k U)U^{-1} = N_{CS} + n(U) \ . \tag{1.42}$$

The local, or small, gauge transformations are those that can be continuously transformed into the identity, and they will leave N_{CS} invariant. Calculating the Chern-Simons number for the vacuum states, one finds that it equals the winding number. Between two neighbouring vacuum states there must be an energy barrier, since they cannot be transformed into one another without passing through non-vacuum states. In the next chapter we will shown that the barrier is finite[1], allowing the gauge field to make transitions between the vacuum states. The Chern-Simons number may be regarded as a parameter for the configuration space. Performing a large gauge transformation changes the Chern-Simons number by an integer amount, while the energy is invariant. The configuration space therefore has a periodic energy barrier with respect to the Chern-Simons number with period 1. The vacuum states are situated at the integer points.

For an evolution of a gauge field configuration, we can define the topological charge as a function of time by

$$Q(t) = \frac{1}{16\pi^2}\int_0^t dt \int d^3x \partial_\mu K^\mu \ . \tag{1.43}$$

This is not a Lorentz invariant quantity since it depend on the time. Transforming to a gauge where $\vec{K}$ vanish at infinity we get

$$Q(t) = \frac{1}{16\pi^2}\left[\int d^3x K^0\right]_0^t + \int_0^t dt \int_S \vec{K} dS = N_{CS}(t) \Leftrightarrow N_{CS}(0) \ . \tag{1.44}$$

The topological charge is gauge invariant, implying that the difference between $N_{CS}(t)$ and $N_{CS}(0)$ is gauge invariant, even under large gauge transformation. Let us consider vacuum transitions, where the gauge fields evolve from a vacuum configuration at $t = 0$ with winding number $n(0)$ and ending in another with $n(t)$. Then choosing the temporal gauge $A_0 = 0$, we have equation 1.44 is satisfied, and

$$Q = n(t) \Leftrightarrow n(0) \ . \tag{1.45}$$

The topological charge for a vacuum transition will be an integer number.

[1] In the $SU(2)$ Higgs theory

1.3 Instantons

Let us estimate the probability for quantum tunnelling through the energy barrier between adjacent vacua $|n\rangle$ and $|n+1\rangle$. In a semi-classical approximation the tunnelling amplitude T_t is given in terms of the Euclidean action, with use of the Feynman-Kac formula

$$T_t = \langle n|e^{-H/T}|n+1\rangle = \int \mathcal{D}A_\mu e^{-S_E} \ , \tag{1.46}$$

where T is the temperature, and the fields are integrated over closed loops of length $1/T$. For $T \to 0$ we expect the integral to be dominated by a solution that minimizes the Euclidean action.

The instanton [50] solution provides us with such a configuration. It is a solution to the 4-dimensional Euclidean field equations, and hence minimizes the action. Again denoting Euclidean time x_4, it can be written as

$$A_\mu = \frac{\tau^2}{\tau^2+\lambda^2}(\partial_\mu U)U^{-1} \ , \tag{1.47}$$

where $\tau^2 = x_4^2 + \vec{x}^2$, and

$$U = \frac{x_4 + i\vec{x}\vec{\sigma}}{\tau} \ . \tag{1.48}$$

The arbitrary constant λ, defines the instanton size. The size is not fixed since the Euclidean action

$$S_E = \frac{1}{2g^2}\int d^4x \ \mathrm{Tr}F_{\mu\nu}F_{\mu\nu} \tag{1.49}$$

is invariant when scaling the fields $A^\nu(x) \to \nu A(\nu x)$. The instanton is self dual $\tilde{F}_{\mu\nu} = F_{\mu\nu}$, and it follows immediately from the Bianchi identity $D_\mu \tilde{F}_\mu = 0$, that the field equation $D_\mu F_\mu = 0$ is satisfied. We have that for $x_4 \to \Leftrightarrow\infty$ the instanton configuration is equal to a pure gauge vacuum with winding number n, and for $x_4 \to \infty$ it is a vacuum state with winding number $n+1$. Hence the topological charge is

$$Q = n(t = \Leftrightarrow\infty) \Leftrightarrow n(t=\infty) = 1 \ . \tag{1.50}$$

The instanton interpolates between the two different vacuum states, and we must have that for the intermediate state $F_{\mu\nu} \neq 0$. Therefore the instanton has an energy bump, which is not classically allowed. It describes the tunnelling between two neighbouring vacua.

A general bound on the action can be obtained using the inequality

$$\mathrm{Tr}(F_{\mu\nu} \Leftrightarrow \tilde{F}_{\mu\nu})^2 \geq 0 \ . \tag{1.51}$$

In Euclidean space we have $\tilde{F}_{\mu\nu}\tilde{F}_{\mu\nu} = F_{\mu\nu}F_{\mu\nu}$, giving

$$\mathrm{Tr}F_{\mu\nu}F_{\mu\nu} \geq \ \mathrm{Tr}F_{\mu\nu}\tilde{F}_{\mu\nu} \ . \tag{1.52}$$

Inserting the topological charge, we get the bound

$$S_E \geq \frac{8\pi}{g^2}Q \ . \tag{1.53}$$

The instanton being self dual, satisfies the equality in 1.51, and the action is

$$S_E = \frac{8\pi}{g^2} \ . \tag{1.54}$$

Using equation 1.46, the transition rate for quantum tunnelling between two inequivalent vacua [2] is suppressed by a very small number

$$T_t \propto \exp(\Leftrightarrow\frac{16\pi^2}{g^2}) \sim 10^{-160} \tag{1.55}$$

The quantum tunnelling probability between the vacuum states is so small that it can be neglected.

Now adding a Higgs doublet to the theory the action reads

$$S_E = \int d^4x(\frac{1}{2g^2}\ \mathrm{Tr}F_{\mu\nu}F^{\mu\nu} + (D_\mu\Phi)^\dagger(D_\mu\Phi) + \lambda(\Phi^\dagger\Phi \Leftrightarrow \frac{v^2}{2})^2) \ . \tag{1.56}$$

The vacuum configurations are now given by

$$A_\mu = \partial_\mu U U^{-1} \ , \tag{1.57}$$

$$\Phi = \frac{v}{\sqrt{2}} U \begin{bmatrix} 0 \\ 1 \end{bmatrix} \ . \tag{1.58}$$

Also the Higgs field can be characterised by a winding number, if $\rho(x) = (\phi_1\phi_1^* + \phi_2\phi_2^*)^{\frac{1}{2}} \neq 0$ throughout space. This condition allows us to write the Higgs field in the matrix form

$$\Phi(x) = \begin{bmatrix} \Phi_2 & \Phi_1 \\ \Leftrightarrow\Phi_1^* & \Phi_2^* \end{bmatrix} = \rho(x)\tilde{U}(x) \ , \tag{1.59}$$

where $\tilde{U} \in SU(2)$. The winding number of this matrix represents the winding number of the Higgs field.

$$N_H = n(\tilde{U}) \ . \tag{1.60}$$

We see that for a vacuum transition, this implies that for the Higgs field somewhere on the path there exist a point where $\Phi(x) = 0$. Otherwise $\tilde{U}$ is defined everywhere and will change continuously as the field evolve, yielding a constant winding number. In particular the instanton interpolating between vacuum states will have $\Phi = \frac{v}{\sqrt{2}}$ for $x_4 \to \pm\infty$, and for some x_4 there most be a zero point of the Higgs field. But scaling the Higgs field $\Phi(x) \to \Phi^s(x) = \Phi(sx)$, the action for the potential term will scale as

$$S_E(\Phi^s(x)) = \frac{1}{s^4} S_E(\Phi(x)) \ . \tag{1.61}$$

The solution that minimizes the Euclidean action, and having topological charge equal to one, will therefore have the Higgs field at the vacuum expectation value everywhere, except at one point, where it is zero. This solution, being singular, is not a physical configuration, and in this sense, the instanton solution does not exist in the $SU(2)$ Higgs theory. There is no physical solution that minimizes the action, but it is possible to find configurations with an Euclidean action arbitrarily close to $\frac{8\pi}{g^2}$, and it is concluded that the quantum transition rate between different vacuum sectors is unchanged.

[2] This rate applies only for zero temperature.

1.4 The chiral anomaly

In this section we will look at anomalies in the electroweak theory. With an anomaly we understand a classical symmetry which is not preserved at the quantum level. This can come about since in the quantum theory the path integral includes fields that do not obey the classical field equations. The non-conservation of the baryonic current is due to the asymmetric coupling to chiral fermions in the SU(2) sector, and is therefore related to the chiral anomaly. For this reason we will now derive the anomaly of the axial current. The interaction between the fermions and the gauge fields is described by the Lagrangian

$$\mathcal{L} = i\bar{\psi}_L \gamma_\mu D^\mu \psi_L \ . \tag{1.62}$$

It is invariant under a global chiral transformation

$$\psi(x) \to e^{i\alpha\gamma_5}\psi \ , \qquad \bar{\psi}(x) \to \bar{\psi}(x) e^{i\alpha\gamma_5} \ , \tag{1.63}$$

and we have the classically conserved Nöther current

$$j^5_\mu = \bar{\psi}\gamma_\mu\gamma_5\psi \tag{1.64}$$

Note that this is true only for massless fermions. But under a local chiral transformation, with $\alpha = \alpha(x)$ the Lagrangian will change as

$$\delta\mathcal{L} = \Leftrightarrow\bar{\psi}\gamma_\mu\gamma_5\psi\partial^\mu\alpha(x) \ . \tag{1.65}$$

Therefore

$$\delta S[\bar{\psi}, \psi, A_\mu] = \Leftrightarrow\int d^4x \alpha(x)\partial_\mu j^\mu_5(x) \ . \tag{1.66}$$

It would be natural to expect that the expectation value,

$$\langle\partial^\mu j^5_\mu(x)\rangle = \frac{\int \mathcal{D}\bar{\psi}\mathcal{D}\psi\mathcal{D}A_\mu \partial^\mu j^5_\mu(x) e^{iS[\bar{\psi},\psi,A_\mu]}}{\int \mathcal{D}\bar{\psi}\mathcal{D}\psi\mathcal{D}A_\mu e^{iS[\bar{\psi},\psi,A_\mu]}} \tag{1.67}$$

would be zero even in the quantum theory, since otherwise the functional measure cannot be invariant under the formally unitary transformation given by 1.63, with $\alpha \to \alpha(x)$. As shown in the following, this however is not true.

We will follow the derivation of Fujikawa [6, 47], who first showed that the chiral anomaly can be obtained non-perturbatively in the path integral approach. This is done by observing that the functional measures $\mathcal{D}\psi$ and $\mathcal{D}\bar{\psi}$ of the fermionic fields are not invariant under an infinitesimal chiral transformation. During the calculation we rotate to Euclidean space, where the Lagrangian reads

$$\mathcal{L} = \Leftrightarrow i\psi_L\gamma_\mu D_\mu\psi_L \ . \tag{1.68}$$

The idea is to expand the fermionic fields over a complete orthotogonal basis, consisting of the eigenstates of the covariant derivative operator $\not{D}_\mu$. After the Wick rotation the operator $\not{D}_\mu$ is hermitian in the Hilbert space of (doublet) spinors, and the eigenstates will form a complete set,

$$\psi(x) = \sum_n a_n\phi_n(x) \ , \quad \bar{\psi} = \sum_n \phi^\dagger_n(x)\bar{b}_n \ , \tag{1.69}$$

where $\{\phi_n\}$ is a set of eigenfunctions for the covariant derivative operator,

$$\Leftrightarrow i\gamma_\mu D_\mu \phi_n(x) = \lambda_n \phi_n(x) \ , \tag{1.70}$$

with the orthonormality property

$$\int d^4x \phi_n^\dagger \phi_m = \delta_{nm} \ . \tag{1.71}$$

The path integral is defined as the integral where $\psi(x)$ is varied over all possible spinors, therefore

$$\int \mathcal{D}\bar{\psi}\mathcal{D}\psi = \prod_m d\bar{b}_m \prod_n da_n \ . \tag{1.72}$$

It is clear that $\mathcal{A}_\mu$ will not change under the chiral transformation. Performing a local chiral transformation of the spinors, we have

$$\psi'(x) = e^{i\alpha(x)\gamma_5}\psi = \sum_n e^{i\alpha(x)\gamma_5} a_n \phi_n(x) = \sum_m a'_m \phi_m(x) \ . \tag{1.73}$$

Using relation 1.71 the new coefficient is extracted,

$$a'_m = \int d^4x \phi_m^\dagger(x) \sum_n e^{i\alpha(x)\gamma_5} a_n \phi_n(x) = \sum_n \int d^4x \phi_m^\dagger(x) e^{i\alpha(x)\gamma_5} a_n \phi_n(x) = \sum_n C_{mn} a_n \ . \tag{1.74}$$

With this definition, C_{mn} is infinite in its labels, but assuming that there is only a finite number of of eigenfunctions, it becomes a finite matrix. Similarly we get

$$\bar{b}'_m = \sum_n \int d^4x \bar{b}_n \phi^\dagger(x) e^{i\alpha(x)\gamma_5} \phi_n(x) = \sum_n \bar{b}_n C_{nm} \ . \tag{1.75}$$

The coefficients $\bar{b}_n$ and a_n are Grassmann variables and we have, for x and y Grassmann n-vectors, and A a complex matrix.

$$x = Ay \Rightarrow d^n x = (\det A)^{-1} d^n y \ . \tag{1.76}$$

For the functional measure 1.72 we can formally write

$$\prod_n d\bar{b}'_n \prod_m da'_m = (\det C)^{-2} \prod d\bar{b}_n \prod da_m \tag{1.77}$$

For an infinitesimal local chiral transformations $\alpha(x)$, the Taylor expansion of the Matrix C reads

$$C = I + \hat{\alpha} + \mathcal{O}(\alpha^2) \ , \qquad \hat{\alpha} = \int d^4x i \phi_n^\dagger(x) \alpha(x) \gamma_5 \phi_m(x) \ . \tag{1.78}$$

Then

$$(\det C)^{-2} = e^{-2 \ \mathrm{tr} \log C} = e^{-2 \ \mathrm{tr} \hat{\alpha} + \mathcal{O}(\alpha^2)} = e^{-2i \int d^4x \alpha(x) \sum_n \phi_n^\dagger(x) \gamma_5 \phi_n(x)} \tag{1.79}$$

The sum $\sum_n \phi_n^\dagger(x)\gamma_5\phi_n(x)$ is not well defined and to evaluate the expression a gauge invariant regularization should be imposed. This can be done by providing a cutoff M in the eigenvalues λ_n, since these are gauge invariant,

$$\sum_n \phi_n^\dagger(x) \gamma_5 e^{-\left(\frac{\lambda_n}{M}\right)^2} \phi_n(x) \ , \quad M \to \infty \ . \tag{1.80}$$

Putting back $\Leftrightarrow i\gamma_\mu D_\mu = \Leftrightarrow \not{D}$ and using the Dirac notation $\phi_n(x) = \langle x|n\rangle$ we get

$$\begin{aligned}\sum_n \phi_n^\dagger(x)\,\gamma_5 e^{-\left(\frac{-i\not{p}_\mu}{M}\right)^2}\phi_n(x) &= \sum_n \langle n|x\rangle\,\gamma_5 e^{\left(\frac{\not{p}_\mu}{M}\right)^2}\langle x|n\rangle \\ &= \mathrm{Tr}\left(|x\rangle\,\gamma_5 e^{\left(\frac{\not{p}_\mu}{M}\right)^2}\langle x|\right)\ , \end{aligned} \tag{1.81}$$

where trace is taken over the whole Hilbert space. The state $|n\rangle$ can be Fourier expanded in plane waves

$$\sum_n \phi_n^\dagger(x)\,\gamma_5 e^{\left(\frac{\not{p}_\mu}{M}\right)^2}\phi_n(x) = \mathrm{Tr}\int \frac{d^4p}{(2\pi)^4}\gamma_5 e^{-ipx} e^{\left(\frac{\not{p}_\mu}{M}\right)^2} e^{ipx}\ , \tag{1.82}$$

where the trace is now over the doublet spinor indices. In order to evaluate this, we write $\not{D}_\mu^2$ as

$$\begin{aligned}\not{D}_\mu^2 &= \gamma_\mu\gamma_\nu D_\mu D_\nu = \tfrac{1}{2}\{\gamma_\mu,\gamma_\nu\}D_\mu D_\nu + \tfrac{1}{2}[\gamma_\mu,\gamma_\nu]D_\mu D_\nu \\ &= \delta_{\mu\nu}D_\mu D_\nu + \tfrac{1}{4}[\gamma_\mu,\gamma_\nu]D_\mu D_\nu \Leftrightarrow \tfrac{1}{4}[\gamma_\nu,\gamma_\mu]D_\mu D_\nu \\ &= D^2 + \tfrac{1}{4}[\gamma_\mu,\gamma_\nu][D_\mu,D_\nu] = D^2 + \tfrac{1}{4}[\gamma_\mu,\gamma_\nu]F_{\mu\nu} \\ &= D^2 \Leftrightarrow \frac{i}{2}\sigma_{\mu\nu}F_{\mu\nu}\ , \end{aligned} \tag{1.83}$$

where $\sigma_{\mu\nu} = \frac{i}{2}[\gamma_\mu,\gamma_\nu]$. Now, for a function $f(x)$ we have

$$\begin{aligned} e^{-ipx}D^2 e^{ipx}f(x) &= e^{-ipx}D_\mu(ip_\mu e^{ipx}f(x) + e^{ipx}D_\mu f(x)) \\ &= e^{-ipx}(\Leftrightarrow p^2 e^{-ipx}f(x) + 2ip_\mu e^{-ipx}D_\mu f(x) + e^{-ipx}D_\mu D_\mu \\ &= (\Leftrightarrow p^2 + 2ip_\mu D_\mu + D^2)f(x) \end{aligned} \tag{1.84}$$

and

$$e^{-ipx}[D_\mu,D_\nu]e^{-ipx}f(x) = [D_\mu,D_\nu]f(x)\ . \tag{1.85}$$

In total we have

$$e^{-ipx}\not{D}_\mu^2 e^{ipx} = (\Leftrightarrow p^2 + 2ip_\mu D_\mu + \not{D}^2)\ . \tag{1.86}$$

From the Taylor expansion of the exponential function we get

$$e^{-ipx}e^{\left(\frac{\not{p}_\mu}{M}\right)^2}e^{ipx} = \sum_{n=0}^{\infty}\frac{1}{n!}e^{-ipx}\left(\frac{\not{D}_\mu}{M}\right)^n e^{ipx} = \sum_{n=0}^{\infty}\frac{1}{n!}\left(e^{-ipx}\,\frac{\not{D}_\mu}{M}\,e^{ipx}\right)^n\ , \tag{1.87}$$

hence

$$e^{-ipx}e^{\left(\frac{\not{p}_\mu}{M}\right)^2}e^{ipx} = e^{-\frac{p^2}{M^2}}e^{\frac{\not{D}^2+2ip_\mu D_\mu}{M^2}}\ . \tag{1.88}$$

Plugging this into formula 1.82, and expanding the in powers on M, we obtain

$$\begin{aligned}&\sum_n \phi_n^\dagger(x)\,\gamma_5 e^{\left(\frac{\not{p}_\mu}{M}\right)^2}\phi_n(x) \\ &\quad= \int\frac{d^4p}{(2\pi)^4}e^{-\frac{p^2}{M^2}}\ \mathrm{Tr}\,\gamma_5\left(1 + \frac{\not{D}^2+2ip_\mu D_\mu}{M^2} + \frac{(\not{D}^2+2ip_\mu D_\mu)^2}{2!M^4} + \mathcal{O}\left(\frac{1}{M^6}\right)\right)\end{aligned} \tag{1.89}$$

The gaussian integral of the exponential gives

$$\int \frac{d^4p}{(2\pi)^4} e^{-\frac{p^2}{M^2}} = \frac{M^4}{(2\pi)^2} \ . \tag{1.90}$$

In the limit of $M \to \infty$ the term with $\mathcal{O}(\frac{1}{M^6})$ will vanish. In this limit the two first terms would be divergent, but we have $\mathrm{Tr}\gamma_5 = 0$ and $\mathrm{Tr}\gamma_5\sigma_{\mu\nu} = 0$. The third term gives rise to a finite integral. The only nonzero contribution coming from the term with $tr(\gamma_5\sigma_{\mu\nu}\sigma_{\rho\sigma}) = \epsilon_{\mu\nu\rho\sigma}$. This gives

$$\begin{aligned} \sum_n \phi_n^\dagger(x)\, \gamma_5 e^{\left(\frac{\not{p}_\mu}{M}\right)^2} \phi_n(x) &= \Leftrightarrow \frac{1}{(2\pi)^2}\frac{1}{8}\mathrm{tr}(\gamma_5\sigma_{\mu\nu}\sigma_{\rho\epsilon})\ \mathrm{Tr}F_{\mu\nu}F_{\rho\epsilon} \\ &= \Leftrightarrow \frac{1}{16\pi^2}\ \mathrm{Tr}F_{\mu\nu}\tilde{F}_{\mu\nu} \ . \end{aligned} \tag{1.91}$$

Using 1.79 we finally obtain

$$\int \mathcal{D}\bar{\psi}\mathcal{D}\psi \to \int \mathcal{D}\bar{\psi}\mathcal{D}\psi e^{\frac{i}{8\pi^2}} \int d^4x\alpha(x)\ \mathrm{Tr}F_{\mu\nu}\tilde{F}^{\mu\nu} \ . \tag{1.92}$$

This will contributribute to the change of the effective action under a local chiral transformation, Rotating back to Minkowski space, and using 1.66 we get

$$\delta S^{eff} = \Leftrightarrow \frac{1}{8\pi^2} \int d^4x\alpha(x)\ \mathrm{Tr}F_{\mu\nu}\tilde{F}^{\mu\nu} \Leftrightarrow \int d^4x\alpha(x)\partial_\mu j_5^\mu(x) \ . \tag{1.93}$$

The local chiral transformation is just a change of variables, and we must have $\langle \delta S^{eff} \rangle = 0$. This gives the anomalous axial current

$$\partial_\mu j_5^\mu = \Leftrightarrow \frac{1}{8\pi^2}\ \mathrm{Tr}F_{\mu\nu}\tilde{F}^{\mu\nu} \ . \tag{1.94}$$

We see that it is indeed possible to have a non vanishing anomaly.

1.5 The baryon number

The baryon number B, defined as the number of baryons b minus the number of antibaryons $\bar{b}$, is not a conserved quantity in the electroweak theory, as was realized by 't Hooft in 1976 [5]. This is an entirely non-perturbative effect. Considering massless fermions we have the interaction Lagrangian

$$\mathcal{L} = \sum_i i\bar{\psi}_L^{(i)}\gamma_\mu D^\mu \psi_L^{(i)} \ , \tag{1.95}$$

where i is a doublet index. Generally the fermion number N^i for a doublet (i) is given by

$$N_f^{(i)} = \int d^3x \bar{\psi}^\dagger \psi \tag{1.96}$$

The baryon number is defined to be $\frac{1}{3}$ for a quark, giving $B^{(i)} = 1/3N_f^{(i)}$. The theory has $n_L = 12$ classically conserved Abelian currents, where 9 of them are associated with

the conservation of the number of quarks and come from the symmetry given by the transformation

$$\begin{aligned} \psi &\rightarrow e^{i\alpha(B)}\psi \ , \\ \bar{\psi} &\rightarrow \bar{\psi}e^{i\alpha(B)} \ , \end{aligned} \tag{1.97}$$

Similarly we have 3 conserved currents, by substituting the lepton number L in 1.97, where $L = 1$ for a lepton. We define the current $J_\mu^{(i)}$ for the doublet $\psi^{(i)}$

$$J_\mu^{(i)} = \bar{\psi}_L^{(i)}\gamma_\mu\psi_L^{(i)} = \bar{\psi}^{(i)}\gamma_\mu\psi^{(i)} \Leftrightarrow \frac{1}{2}\bar{\psi}^{(i)}\gamma_\mu\gamma_5\psi^{(i)} \tag{1.98}$$

If $\psi(i)$ is a lepton doublet then $J_\mu^{(i)}$ is the leptonic current, if it a quark doublet $J_\mu^{(i)}$ equals three times the baryonic current. The corresponding charge is the fermion number

$$N_f^{(i)} = \int d^3x J_0^{(i)} \ . \tag{1.99}$$

The currents 1.98 are not conserved in the quantum theory, by using equation 1.94 we get

$$\partial^\mu J_\mu^{(i)} = \frac{1}{16\pi^2}\ \mathrm{Tr}F_{\mu\nu}\tilde{F}^{\mu\nu} \quad , \ \tilde{F}^{\mu\nu} = \frac{1}{2}\epsilon^{\mu\nu\rho\sigma}F_{\rho\sigma} \ , \tag{1.100}$$

where the total baryonic current is obtained by summing over the three different generation of quarks, and their colour index, which cancels with the factor of 1/3 for the definition of the baryon number for a quark. Similarly the leptonic current is given by the sum over the three lepton generations. In total we may write

$$\partial^\mu J_\mu^B = \partial^\mu J_\mu^L = \frac{N_f}{16\pi^2}\ \mathrm{Tr}F_{\mu\nu}\tilde{F}^{\mu\nu} \ , \tag{1.101}$$

where N_f is the number of generations. The lepton and baryon currents have the same anomaly, and it is clear that the electroweak theory still preserves $B \Leftrightarrow L$.

From the equation 1.100 we get

$$\begin{aligned} \partial^0 N_f^{(i)} &= \int d^3x \partial^0 J_0^{(i)} && (1.102) \\ &= \Leftrightarrow \int d^3x \partial^i J_i^{(i)} + \int d^3x \frac{1}{16\pi^2}\ \mathrm{Tr}F_{\mu\nu}\tilde{F}^{\mu\nu} && (1.103) \\ &= \int d^3x \frac{1}{16\pi^2}\ \mathrm{Tr}F_{\mu\nu}\tilde{F}^{\mu\nu} \ , && (1.104) \end{aligned}$$

where we assumed that the currents vanish at infinity. We see that it is possible to change the number of fermions if the gauge fields evolve in such a way that

$$\int_0^t dt \int d^3x \frac{1}{16\pi^2}\ \mathrm{Tr}F_{\mu\nu}\tilde{F}^{\mu\nu} \neq 0 \ . \tag{1.105}$$

This is the topological charge of equation 1.44. The change of the fermion number is therefore related to the topological charge by

$$\Delta N_f^{(i)} = Q(t) \ . \tag{1.106}$$

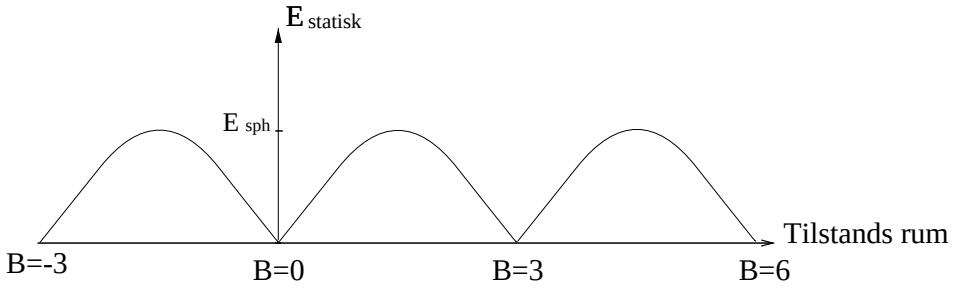

Figure 1.1: The barrier between different vacuum sectors when neglecting the fermions. I instanton tunnelling. S sphaleron transition. Here E_{sph} is the energy of the sphaleron.

For vacuum transitions $Q(t)$ is an integer, given by the difference in the winding numbers. In the temporal gauge we get

$$\Delta N_B = \Delta N_L = N_f(N_{CS}(t) \Leftrightarrow N_{CS}(0)) \ . \tag{1.107}$$

Relation 1.35 allow us to define a conserved current

$$\tilde{J}^B_\mu = J^B_\mu \Leftrightarrow \frac{N_f}{16\pi^2} K_\mu = J^B_\mu \Leftrightarrow \frac{1}{8\pi^2} \epsilon_{\mu\nu\rho\sigma} \ \mathrm{Tr}(A^\nu \partial^\rho A^\sigma + \frac{2}{3} A^\nu A^\rho A^\sigma) \ . \tag{1.108}$$

giving the conserved charge

$$B \Leftrightarrow \frac{N_F}{16\pi^2} \int d^3x K_0 = B \Leftrightarrow N_F N_{CS} \ . \tag{1.109}$$

This current, though, is not gauge invariant under large gauge transformation, and no physical meaning can be given to it.

We see that associated with a process where the *bosonic* fields jumps between different vacuum sectors, there will be a change in the baryon number. If the gauge fields evolve from one vacuum, say with $N_{CS} = 0$, to a neighbouring one with $N_{CS} = +(\Leftrightarrow)1$, then the baryon number will change with $+(\Leftrightarrow)3$. Even though it is the asymmetry of the fermions we are interested in explaining, they can be neglected in a first approximation, since the violation of the fermion number is governed by the bosonic fields. Neglecting the fermions and the $U(1)$ gauge group is a widely used approximation when studying baryogenesis. Baryon number violation has never been detected experimentally, but at low energies and temperatures, the only possibility for an evolution of the bosonic fields between different vacua, is by quantum tunnelling. It was shown in section 1.3 that these processes are highly suppressed. The baryon number is a good quantum number at low temperatures.

The form of the energy barrier between the topologically distinct vacua, and especially the height, is therefore of importance when studying baryogenesis, since it will determining the transition rate between the vacuum sectors. In the next chapter the sphaleron solution is describes, which represents the top of the barrier when neglecting the fermions. The height of the barrier is therefore given by the energy of the sphaleron. At high temperature, there are large thermal fluctuations, and one might expect that the gauge fields has sufficient energy to pass the barrier classically, as shown in figure 1.1. Processes where the gauge field evolves classically are known as sphaleron transitions. When including the fermion the pictures looks a bit different, as is described in chapter 4.

Chapter 2

The sphaleron configuration

The sphaleron configuration of the $SU(2)$ Higgs model and its properties are described in this chapter. The sphaleron configuration is thought as being representing the top of the barrier between two neighbouring topological distinct vacua, and is therefore important when discussing baryon violating processes. It was first found by Dashen, Hasslacher and Neveu (DHN) [7], but the relation of the sphaleron to the topology of configuration space and baryon violation was founded by Klinkhammer and Manton (KM) [9].

2.1 Static configurations

We want to investigate the barrier between topologically distinct vacua, in the case where the fermions are neglected. A point on the barrier, for a given Chern-Simons number, is the minimum classical static energy of the bosonic fields. The top of the barrier is represented by the maximum energy configuration on a minimal[1] energy path from one vacua to a neighbouring one. Assuming that we have such a configuration, it will be a non-trivial static solution to the Euler-Lagrange equations. This property is realized by the sphaleron configuration, as we will show in the following sections. For static configurations A_0 can consistently be set to zero. Given the Lagrangian 1.2, the energy functional for static configurations is

$$E = \int d^3x \tfrac{1}{4}F_{ij}^{\alpha}F_{ij}^{\alpha} + \tfrac{1}{4}f_{ij}f_{ij} + (D_i\Phi)^{\dagger}(D_i\Phi) + \lambda(\Phi^{\dagger}\Phi \Leftrightarrow \frac{v^2}{2}) \; , \tag{2.1}$$

where $f_{ij} = \partial_i a_j \Leftrightarrow \partial_j a_i$ is the field tensor for the $U(1)$ gauge field. The field equations reads

$$(D_j F_{ij})^a = \Leftrightarrow \tfrac{1}{2} ig[\Phi^{\dagger}\sigma^a D_i\Phi \Leftrightarrow (D_i\Phi)^{\dagger}\sigma^a\Phi] \; , \tag{2.2}$$

where $(D_j F_{ij})^a = \partial_j F_{ij}^a + g\epsilon^{abc}A_j^b F_{ij}^c$. For the $U(1)$ field we get

$$\partial_j f_{ij} = \Leftrightarrow \tfrac{1}{2} ig'[\Phi^{\dagger}D_i\Phi \Leftrightarrow (D_i\Phi)^{\dagger}\Phi] \; , \tag{2.3}$$

and for the Higgs field

$$D_i D_i \Phi = 2\lambda(\Phi^{\dagger}\Phi \Leftrightarrow \tfrac{1}{2}v^2)\Phi \; . \tag{2.4}$$

Let us see how the energy varies when the fields are scaled with the parameter s.

$$A^s(x) = sA(sx) \; , \qquad \Phi^s(x) = \Phi(sx) \; . \tag{2.5}$$

[1] Strictly speaking this should be the infimum

The contribution to the energy from the pure Yang-Mills term, when using the gauge group $SU(2)$, scales as

$$\begin{aligned} E(A(x)) &= \Leftrightarrow\frac{1}{2g^2}\int d^3x\ \mathrm{Tr}(F_{ij}^2(x)) \ = \ \Leftrightarrow\frac{1}{2g^2}\int d^3(sx)\ \mathrm{Tr}(F_{ij}^2(sx)) && (2.6)\\ &= \Leftrightarrow\frac{1}{2g^2}\int d^3xs^3\ \mathrm{Tr}(\frac{\partial}{\partial sx_i}A_j(sx)\frac{\partial}{\partial sx_j}A_i(sx)+[A_i(sx),A_j(sx)])^2 && (2.7)\\ &= \Leftrightarrow\frac{1}{2g^2}\int d^3xs^3\ \mathrm{Tr}(s^{-2}F_{ij}^s(x))^2 \ = \ \frac{1}{s}E(A^s(x))\ . && (2.8)\end{aligned}$$

There is no non-trivial static solution in pure Yang Mills theory, since the energy varies monotonically with the scaling parameter. The only static solution is the vacuum. However, the energy from the interaction term scales oppositely,

$$E(A(x),\Phi(x))=\int d^3xs^3((\frac{\partial}{\partial sx_i}+A_i(sx))\Phi(sx))^2=sE(A^s(x),\Phi^s(x)) \qquad (2.9)$$

and the pure scalar field energy scales as

$$E(\Phi(x))=\int d^3xs^3\lambda(\Phi(sx)^\dagger\Phi(sx)\Leftrightarrow\frac{v^2}{2})^2=s^3E(\Phi^s(x))\ . \qquad (2.10)$$

When scaling the Higgs field down the energy is lowered. We see that in the coupled gauge Higgs model the energy diverges both as $s\to\infty$ and $s\to 0$. There is a fixed s that minimizes the energy, in contrast to both the pure Yang-Mills theory and the pure scalar theory. We can therefore talk about the height of the barrier. The size, and hence the energy, of a non-trivial static configuration is determined. Note that in turn, it was found in section 1.3, that the instanton solution to the four dimensional Euclidean field equations, due to scaling properties, is not physically existing in this theory.

2.2 Non-contractible loops in Weinberg-Salam theory

In this section we will study the topology of the configuration space in the Weinberg-Salam theory without fermions. We want to consider only physically different states, and collect the configurations in gauge orbits. We regard all configurations, which can be obtained from a given configuration by a gauge transformation[2], as equivalent. Consider the manifold consisting of all finite energy, static field configurations $\{A_\mu(x),\Phi(x)\}$ and let E be the functional on the manifold, defined by the classical energy of the configuration. This manifold has a unique vacuum, since we work with gauge orbits. The question is whether there exist non-contractible loops on the manifold passing through the vacuum. A non-contractible loop is one that cannot be continuously transformed into a point. We collect the loops at the vacuum configuration in homotopy classes. For a given loop C there will exists some maximum energy when going around the loop. We define E_H as being the infimum of the maximum energies for loops in a non-contractible homotopy class H

$$E_H=\inf_{C\in H}\max_C E\ . \qquad (2.11)$$

[2]Including large gauge transformations

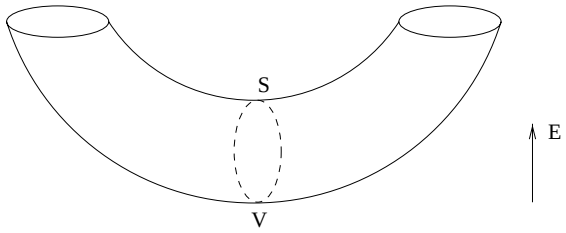

Figure 2.1: Configuration space collected in gauge orbits, with the energy (E) vertically. The dashes curve is the non-contractible loop going through the sphaleron solution (S).

Note that a solution to this equation will have a negative energy mode, since the vacuum have less energy. A priori it is not known whether there exist non-contractible loops in the Weinberg-Salam theory, and if so, we cannot be sure of the existence of a configuration that will have exactly the energy E_H, since the manifold in question is infinite dimensional, and the minimum might not be realized. If however such a solution exist, the energy of the configuration will be the height of the barrier between topologically distinct vacua. The non-contractible loops in the manifold where we have gauge orbits corresponds to a path of configurations between topologically distinct vacua. The sphaleron configuration satisfies 2.11[3]. A solution to equation 2.11 will be a saddle-point of the energy functional, and therefore a solution to the classical field equations. Being a saddlepoint it is classically unstable, but since it satisfies equation 2.11, it is clear that it can only have one unstable direction. Indeed if there were two unstable directions, it would be possible to construct a lower energy configuration in the same homotopy class, by continuously deforming the configuration along one of the unstable directions, which contradicts the assumption $E = E_H$. The negative energy direction of the sphaleron correspond to the directions of the Chern-Simons number. This picture of the configuration space is schematically shown in figure 2.1.

As was shown by N. Manton [8], it is indeed possible to construct non-contractible loops in the Weinberg-Salam theory. In the following we will give an explicit example of a non-contractible loop. For this purpose we write the four real components of the complex Higgs doublet as a four vector

$$\Phi = \begin{bmatrix} \Phi_1 + i\Phi_2 \\ \Phi_3 + i\Phi_4 \end{bmatrix} , \qquad \Phi_{\mathcal{R}\mathrm{e}} = \begin{bmatrix} \Phi_1 \\ \Phi_2 \\ \Phi_3 \\ \Phi_4 \end{bmatrix} . \tag{2.12}$$

It is convenient to work with spherical coordinates. The gauge should be fixed completely, and by choosing the polar gauge $A_r = 0$ there is no further local gauge freedom. To obtain a finite energy solution, the Higgs field must approach its vacuum value at infinity. Assuming that the limiting Higgs field Φ^{∞}_{RE}, is a smooth function of the polar angles φ, θ, the requirement reads

$$|\Phi^{\infty}_{\mathcal{R}\mathrm{e}}(\varphi, \theta)| = \frac{v}{\sqrt{2}} . \tag{2.13}$$

[3]For $M_H < 12M_W$

By making a global gauge transformation, we impose that it should be in the form

$$\Phi^{\infty}(\varphi, \theta = 0) = \frac{v}{\sqrt{2}} \begin{bmatrix} 0 \\ 1 \end{bmatrix} . \tag{2.14}$$

This gives the unique vacuum state

$$\Phi_{\rm vac}(x) = \frac{v}{\sqrt{2}} \begin{bmatrix} 0 \\ 1 \end{bmatrix} , \qquad A_{\rm vac}(x) = 0 . \tag{2.15}$$

We want to construct a closed loop at this vacuum state. Note that the remaining global $U(1)$ gauge freedom cannot affect the homotopy class of this loop, since it is a continuous transformation. The asymptotic Higgs field maps three dimensional space at infinity, to the Higgs vacuum manifold, which by equation 2.13, is equivalent to the three sphere S^3 (with radius $\frac{v}{\sqrt{2}}$). Hence $\Phi^{\infty}_{\mathcal{R}\rm e}$ can be regarded as a map from the two sphere S^2 to S^3. Let $\tau \in [0, \pi]$ be a parameter for the loop C, for $\tau = 0$ and $\tau = \pi$ all of S^2 is mapped into the vacuum state. Going around the loop C we therefore go through a continuous family of maps given by $\Phi^{\infty}_{\mathcal{R}\rm e}$. By associating a point (τ, θ, φ) with the point $p(\tau, \theta, \varphi)$ on S^3, given by

$$p(\tau, \theta, \varphi) = \Big(\sin\tau \sin\theta \cos\varphi, \sin\tau \sin\theta \sin\varphi, \sin^2\tau \cos\theta + \cos^2\tau, \sin\tau \cos\tau(\cos\theta \Leftrightarrow 1)\Big) , \tag{2.16}$$

this family of maps is then equivalent to a single map $\Upsilon(p) = \Phi^{\infty}_{\mathcal{R}\rm e}(\tau(p), \theta(p), \varphi(p)$ from S^3 to itself. Naturally it has to be checked that this map, and the inverse maps $\tau(p)$, $\theta(p)$, $\varphi(p)$ are well defined. Every point in the domain of S^3 is reached by at least one point (τ, θ, φ), and the maps $\theta(p)$ and $\varphi(p)$ are unique points in S^2. Further more the map $\tau(p)$ is unique, when restricted to the interval $]0, \pi[$, except for the point (0,0,1,0). Even for this point though, the mapping is unambiguous. In fact when $p = (0, 0, 1, 0)$, θ has to be 0, and the gauge fixing implies that for all τ the point $\theta = 0$ is mapped to $(0, 0, 1, 0)$. The map $\Upsilon : S^3 \mapsto S^3$ is indeed well defined.

Recall that maps from S^3 to S^3 can be classified by an integer number, equivalent to the winding number of the map ($\pi_3(S^3) = Z$). A map with non-zero degree is provided by the identity map, which has winding number one. This gives a asymptotic Higgs field

$$\Phi^{\infty} = \begin{bmatrix} \sin\tau \sin\theta e^{i\varphi} \\ e^{-i\mu}(\cos\mu + i \sin\mu \cos\theta) \end{bmatrix} . \tag{2.17}$$

Now, the gauge field will have to approach a pure gauge asymptotically, in order to give a finite energy configuration. It is natural to define

$$A^{\infty}_{\theta} = \Leftrightarrow\!\!\!\partial_{\theta} \hat{U} \hat{U}^{-1} , \qquad A^{\infty}_{\varphi} = \Leftrightarrow\!\!\!\partial_{\varphi} \hat{U} \hat{U}^{-1} , \tag{2.18}$$

where

$$\hat{U} = \begin{bmatrix} (\Phi^{\infty}_2)^* & \Phi^{\infty}_1 \\ \Leftrightarrow(\Phi^{\infty}_1)^* & \Phi^{\infty}_2 \end{bmatrix} . \tag{2.19}$$

This will insures that the covariant derivative term in the energy, given by equation 2.1 vanishes asymptotically as it must. A non-contractible loop in the manifold can now be constructed as

$$\Phi = [1 \Leftrightarrow h(r)] \begin{bmatrix} 0 \\ \exp(\Leftrightarrow i\mu) \cos\mu \end{bmatrix} + h(r) \Phi^{\infty} , \tag{2.20}$$

$$A_\theta = f(r)A_\theta^\infty \ , \qquad A_\varphi = f(r)A_\varphi^\infty \ , \qquad A_r = 0 \ . \tag{2.21}$$

The energy will be finite for suitable choices of f and h, and these must satisfy the boundary conditions $f(0) = h(0) = 0$ and $f \to 1, h \to 1$ as $r \to \infty$.

As already mentioned the non-contractible loops defines a path from one vacuum to a topologically distinct one, when the gauge fixing is relaxed. Indeed if we imposed the condition that at spatial infinity the configuration should be the unitary vacuum, and $\tau = 0$ is the unitary vacuum then the configuration for $\tau = \pi$ would be a pure gauge $A_i(x) = \Leftrightarrow\partial_i U(x)U^{-1}(x)$, where $U(x)$ cannot be continuously transformed into the unit matrix.

This shows the existence of non-contractible loops in the $SU(2)$ Higgs theory, and it makes it likely that there exist non-trivial static solution to the field equations. The only obstacle to this is that, since the manifold is infinite dimensional, the solutions to equation 2.11 might "escape" to infinity. Finding a non-trivial static solution analytically is not an easy task, but by making certain ansätze for the configurations and minimizing the energy functional, it is possible to construct an approximation to the solution to equation 2.11, and obtain an upper bound for the energy.

2.3 The $SU(2)$ Higgs sphaleron

We are searching for a non-trivial static solution to the field equations. In order to be able to perform analytic calculations, we put restrictions on the possible forms of the Higgs and gauge fields. The ansatz must be such that we get a finite energy solution, and compatible with the classical field equations. First we restrict ourselves to $SU(2)$. This, as already mentioned is equivalent to the Weinberg-Salam theory for $\theta_W = 0$. A simple ansatz can be made by assuming fields of the form

$$A_i^\alpha \sigma^\alpha = \Leftrightarrow\frac{2i}{g} f(gvr)\partial_i U^\infty (U^\infty)^{-1} \ , \tag{2.22}$$

$$\Phi = \frac{v}{\sqrt{2}} h(gvr) U^\infty \begin{bmatrix} 0 \\ 1 \end{bmatrix} \ , \tag{2.23}$$

where f and h are function of the radial distance r, and

$$U^\infty = \frac{1}{r}\begin{bmatrix} x_3 & x_1 + ix_2 \\ \Leftrightarrow x_1 + ix_2 & x_3 \end{bmatrix} \ . \tag{2.24}$$

These fields are compatible with the classical equations of motion, given by equation 2.2 and 2.4. We see that for $h \to 1$ and $f \to 1$ when $\xi \to \infty$ the fields will approach their vacuum values at spatial infinity, as they should to obtain finite energy. A more general ansatz will be considered later. The energy is given by formula 2.1, where the term with f_{ij} is zero, since we disregard the $U(1)$ gauge group. The energy density is spherically symmetric as shown in appendix A. Introducing the dimensionless radial distance $\xi = gvr$, the energy functional becomes

$$E = \frac{2M_W}{\alpha}\int_0^\infty \left[4(f')^2 + \frac{8}{\xi^2}[f(1 \Leftrightarrow f)]^2 + \tfrac{1}{2}\xi^2(h')^2 + [h(1 \Leftrightarrow f)]^2 + \frac{1}{4}\frac{\lambda}{g^2}\xi^2(h^2 \Leftrightarrow 1)^2\right] d\xi \ , \tag{2.25}$$

where the prime denote differentiation with respect to ξ. We are searching for functions f and h that minimizes the energy, and from variational calculus this can be obtained by

$$\frac{d}{d\xi}\frac{dE}{df'} \Leftrightarrow \frac{dE}{df} = 0 \ . \tag{2.26}$$

The field equations for the dynamical variables are

$$8f'' \Leftrightarrow \frac{8}{\xi^2}2[f(1 \Leftrightarrow f](1 \Leftrightarrow 2f) + h^2 2(1 \Leftrightarrow f) = 0 \tag{2.27}$$

and

$$\frac{d}{d\xi}(\xi^2 h') = 2h(1 \Leftrightarrow f)^2 + \frac{\lambda}{g^2}\xi^2 h(h^2 \Leftrightarrow 1) \ . \tag{2.28}$$

If these equations are satisfied, the field equations 2.2 and 2.4 are satisfied. The configuration given by 2.22, 2.23 and with f and h solution to the above differential equations, is what we will call the sphaleron solution in $SU(2)$ Higgs theory. The negative energy direction is outside the class of configurations satisfying the ansatz 2.22 and 2.23, making the sphaleron a local minimum of the energy functional 2.25. It is still only a saddlepoint of the full energy functional. As we shall see later it is possible to lower the energy by non-charge conjugation invariant perturbations.

It is not easy to solve the pair of non-linear coupled differential equations analytically, but by searching for solutions numerically it was found by DHN [7] that there is only one solution. The functions f and h are shown in figure 2.2 Asymptotically the fields will behave as

$$f(\xi) = a\xi^2 \qquad \text{for } \xi \to 0 \ , \tag{2.29}$$

$$f(\xi) = 1 \Leftrightarrow c\exp(\Leftrightarrow\tfrac{1}{2}\xi) \qquad \text{for } \xi \to \infty \ , \tag{2.30}$$

$$h(\xi) = b\xi \qquad \text{for } \xi \to 0 \ , \tag{2.31}$$

$$h(\xi) = 1 \Leftrightarrow \tfrac{d}{\xi}\exp(\Leftrightarrow\sqrt{2\lambda/g^2}\xi) \qquad \text{for } \xi \to \infty \ , \tag{2.32}$$

where a,b,c and d are constants that can be determined by solving the differential equations 2.27 and 2.28. We see that the energy density is exponentially decreasing, and hence the sphaleron is localized. The Higgs field is zero at the core of the sphaleron, as it must be in order to change the winding number. In this sense the sphaleron can be regarded as interpolating between the two different vacua. The vacua of the broken and the symmetric phase. From equation 2.25 we see that the energy can be written in the form

$$E_{sph} = \frac{M_W}{\alpha}B(\frac{\lambda}{g^2}) \ . \tag{2.33}$$

The factor B dependents on the Higgs mass. An upper bound on the sphaleron energy can be found by assuming a simplified form for the functions f and h. This was done by KM [9], by basically letting the functions be given by the asymptotic behaviour and requiring that they are continuously differentiable. In this way they obtained the bound 3.12 at $\lambda = 0$ and the highest value 5.44 for $\lambda \to \infty$. It is seen that B varies slowly as a function of the Higgs mass. A better bound was found in ref. [15], by solving the differential equations numerically, They found $B = 3.04$ at $\lambda = 0$, and $B = 3.64$ for $M_H = M_W$.

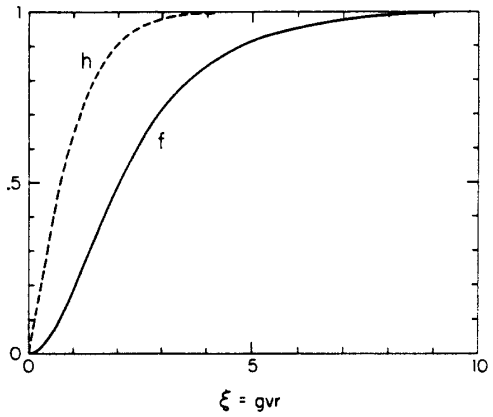

Figure 2.2: The functions f and h for $\lambda = g^2$. Reproduced from ref. [27]

The diameter of the sphaleron was estimated to be $2 \Leftrightarrow 3\ M_W^{-1}$. The sphaleron energy is therefore roughly given by 10 TeV.

We have shown that the sphaleron solution exist in the pure $SU(2)$ theory, and one expects that it possible to continuously deform the solution to the full Weinberg-Salam theory without fermions. To see the effects of the $U(1)$ gauge group on the sphaleron, we consider the case of small Weinberg angle Θ_W. The $SU(2)$ and Higgs fields can be approximated by their values for $\Theta_W = 0$. The $U(1)$ field a_i, though, will be non-zero. The change in energy can then be written as

$$\Delta E = \int d^3x \frac{1}{4} f_{ij} f_{ij} \Leftrightarrow a_i j_i \ , \tag{2.34}$$

where

$$j_i = \Leftrightarrow \frac{1}{2} i g' (\Phi^\dagger D_i \Phi \Leftrightarrow D_i \Phi)^\dagger \Phi \ , \qquad D_i = \partial_i \Leftrightarrow \frac{1}{2} i g \sigma^a A_i^a \ . \tag{2.35}$$

In the energy change 2.34 we have neglected the second order term in a_i from the covariant derivative. Using the field equation 2.3 we have

$$\int d^3x a_i j_i = \frac{1}{2} \int d^3x f_{ij} f_{ij} \tag{2.36}$$

therefore the energy change will be negative,

$$\Delta E = \Leftrightarrow \frac{1}{4} \int d^3x f_{ij} f_{ij} \ . \tag{2.37}$$

The current $\vec{j}$ is found by inserting 2.22 and 2.23

$$\vec{j} = \frac{1}{2} g' v^2 \frac{h^2(\xi)(1 \Leftrightarrow f(\xi))}{r^2} (\Leftrightarrow x_2, x_1, 0) \ . \tag{2.38}$$

This acts as a source for a, and the energy density of the sphaleron is no longer spherically symmetric, but only axially symmetric. For $\Theta_W \neq 0$ the sphaleron will have a magnetic moment. In ref. [10] the sphaleron energy at the physical mixing angle $\Theta_W = 0.5$ was obtained. The energy was found to differ from the pure $SU(2)$ Higgs sphaleron by less than 1%. Indeed the $SU(2)$ sphaleron is a good approximation to the electroweak sphaleron.

2.4 Topological charge of the sphaleron

To find the topological charge of the sphaleron, we choose a gauge where $\int \vec{K} dS = 0$, to have no contribution from the surface term. Using formula 1.44, and assuming that the sphaleron configuration is obtained from an evolution of a vacuum configuration at $t = \Leftrightarrow\infty$, we get

$$Q = \frac{1}{16\pi^2} \int d^3x K^0 + n \ , \qquad n \in Z \ . \tag{2.39}$$

First we perform a rigid rotation and a gauge transformation by changing $U^\infty \to U$,

$$U = \begin{bmatrix} 0 & 1 \\ 1 & 0 \end{bmatrix} U^\infty \begin{bmatrix} 0 & i \\ \Leftrightarrow i & 0 \end{bmatrix} = i\vec{\sigma} \cdot \hat{\vec{x}} \ . \tag{2.40}$$

in the formulae 2.22 and 2.23. The sphaleron solution is then written as

$$A_i^a = \Leftrightarrow \frac{2f}{gr^2} \epsilon_{iab} x_b \ , \tag{2.41}$$

$$\Phi = \frac{v}{\sqrt{2}} hi\vec{\sigma} \cdot \vec{x} \begin{bmatrix} 0 \\ 1 \end{bmatrix} \ . \tag{2.42}$$

Further more we make a gauge transformation through

$$\begin{aligned} U(\vec{x}) &= \exp(\tfrac{1}{2} i\Theta(r) \vec{\sigma} \cdot \hat{\vec{x}}) \\ &= \cos\frac{\Theta(r)}{2} + i\vec{\sigma} \cdot \hat{\vec{x}} \sin\frac{\Theta(r)}{2} \ . \end{aligned} \tag{2.43}$$

Provided that $\Theta(0) = 0$ and that $\Theta(r)$ goes sufficiently fast to π as $r \to \infty$, the integral of $\vec{K}$ is zero. The gauge field configuration becomes

$$A_i^a = \frac{[1 \Leftrightarrow 2f(gvr)] \cos\Theta(r) \Leftrightarrow 1}{gr} \epsilon_{iab} \hat{x}_b + \frac{[1 \Leftrightarrow 2f(gvr)] \sin\Theta(r)}{gr} (\delta_{ia} \Leftrightarrow \hat{x}_i \hat{x}_a) + \frac{1}{g} \frac{d\Theta}{dr} \hat{x}_i \hat{x}_a \ . \tag{2.44}$$

The topological charge in this gauge is equal to the Chern-Simons number and can now be obtained from the formula

$$N_{CS}(\text{sphaleron}) = \Leftrightarrow \frac{g^2}{16\pi^2} \int d^3x \epsilon_{ijk} \left(A_i^a \partial_j A_k^a + \frac{1}{3} g \epsilon_{abc} A_i^a A_j^b A_k^c \right) \ . \tag{2.45}$$

In appendix A this integral is calculated. The topological charge density turns out to be spherically symmetric, and the sphaleron has half integer topological charge

$$Q(\text{sphaleron}) = \tfrac{1}{2} + n \ , \qquad n \in Z \ . \tag{2.46}$$

The sphaleron lies halfway between the topologically distinct vacua. This fit well with the picture of the sphaleron as representing the barrier height, as shown in figure 1.1.

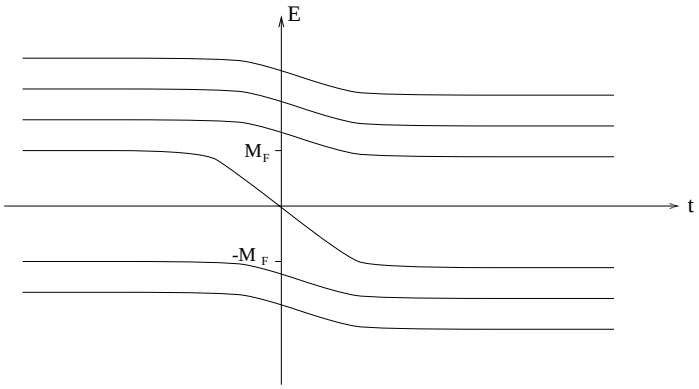

Figure 2.3: The Dirac energy levels of the fermions as a function of time, when the gauge fields perform a vacuum transition.

2.5 Fermionic level crossing

As the bosonic fields evolve from one vacuum to another topological distinct one, the Dirac energy levels of the fermions will shift. We can view the baryon violation, as the consequence of one fermionic energy level crossing zero, turning an antifermion into a fermion or vice versa. This simple picture is shown in figure 2.3. Assuming that the gauge fields passes through the sphaleron, then the zero crossing take place at the sphaleron configuration, since the fermions have a zero mode there.

We want to show that the fermions have a normalizable zero mode in the background of the sphaleron solution. Let us consider the case of a fermion doublet with degenerate mass M_F, given in terms of the Yukawa coupling m. Using the representation of the Dirac matrices

$$\gamma_i = \begin{bmatrix} 0 & \sigma_i \\ \Leftrightarrow\sigma_i & 0 \end{bmatrix} , \tag{2.47}$$

we can reduce the spinors to two components, and the zero energy Dirac equations in the background of the sphaleron solution becomes

$$i\sigma^i(\partial_i \Leftrightarrow ig\sigma^a A_i^a)\psi_L \Leftrightarrow m\Phi\psi_R^{(1)} \Leftrightarrow m\tilde{\Phi}\psi_R^{(2)} = 0 , \tag{2.48}$$

$$i\sigma^i\partial_i\psi_R^{(1)} + m\Phi^\dagger\psi_L = 0 , \tag{2.49}$$

$$i\sigma^i\partial_i\psi_R^{(2)} + m\tilde{\Phi}^\dagger\psi_L = 0 , \tag{2.50}$$

where Φ and $\vec{A}$ are given by equation 2.42 and 2.41, and ψ_L is a left handed doublet, and $\psi_R^{(1)}, \psi_R^{(2)}$ are right handed singlets. The following ansatz for the fermions will be made

$$\psi_{L,ab} = \epsilon_{ab}u(r) , \qquad \psi_{R,ab}^{(1)} = \Phi_{0a}\epsilon_{ab}w(r) , \qquad \psi_{R,ab}^{(2)} = \tilde{\Phi}_{0a}\epsilon_{ab}w(r) , \tag{2.51}$$

where $\Phi_0 = \left[\begin{smallmatrix} 0 \\ 1 \end{smallmatrix}\right]$. With this ansatz we get

$$\frac{1}{r}(\partial_r u(r) + \frac{2f(\xi)}{r}u + M_F h(\xi)w(r)) = 0 , \tag{2.52}$$

$$\frac{1}{r}(\partial_r w(r) + M_F h(\xi)u(r) = 0 , \tag{2.53}$$

since the equations 2.49 and 2.50 are identical. Let us look at the case were $M_F = 0$. The equation in $u(r)$ is easily integrated

$$u(r) = N \exp(\Leftrightarrow 2 \int_0^{r_0} \frac{f(gvr)}{r}) dr \tag{2.54}$$

From the asymptotic behaviour of the function f, see equation 2.29, we have

$$\begin{aligned} u(r) &= \exp(\Leftrightarrow \xi^2) \qquad \text{for } \xi \to 0 \ , \\ u(r) &= r^{-2} \qquad \text{for } \xi \to \infty \ . \end{aligned} \tag{2.55}$$

We see that each left handed fermion doublet has a zero modes in the sphaleron background. In the case of $M_F \neq 0$ the equations 2.52 and 2.53 can be rewritten as two decoupled second order differential equation for $w(r)$ and $u(r)$, and the solutions yields a normalizable zero mode [12]. For the physical case of a fermion doublet with nondegenerate masses, one cannot use the spherically symmetric ansatz for the fermions fields, but only an axially symmetric ansatz. It is shown in ref. [13] that the zero modes is still normalizable [13]. When the gauge fields passe through the sphaleron, one fermionic energy level will therefore cross zero, and the baryon number is violated.

2.6 General spherical symmetric ansatz

The most general spherical symmetric ansatz can be written, in the temporal gauge, as

$$A_i^a = \frac{1 \Leftrightarrow f_A(r)}{gr} \epsilon_{aij} \hat{r}_j + \frac{f_B(r)}{gr} (\delta_{ij} \Leftrightarrow \hat{r}_i \hat{r}_a) + \frac{f_C(r)}{gr} \hat{r}_i \hat{r}_a \ , \tag{2.56}$$

$$A_0^a = 0 \ , \tag{2.57}$$

$$\Phi = \frac{v}{\sqrt{2}} \left(H(r) + i \vec{\sigma} \cdot \hat{r} K(r) \right) \begin{bmatrix} 0 \\ 1 \end{bmatrix} \ . \tag{2.58}$$

The sphaleron solution found previously in section given equation 2.41 and 2.42, is identical to this ansatz for $f = \frac{1}{2}(1 \Leftrightarrow f_A)$, $h = K$ and the last three functions vanishing identically. Under charge conjugation the function f_A and H are left invariant, while f_B, f_C, K changes sign. The latter terms are therefore charge conjugation odd. This ansatz give rise to the spherical symmetric energy density [16]

$$\begin{aligned} E &= \frac{M_W}{\alpha} \int dx \Big(\frac{1}{2x^2} (f_A^2 + f_B^2 \Leftrightarrow 1)^2 + (f_A' + \frac{f_B f_C}{x})^2 + (f_B' \Leftrightarrow \frac{f_A f_C}{x})^2 \\ &+ (K^2 + H^2)(1 + f_A^2 + f_B^2 + \frac{1}{2} f_C^2) + 2 f_A (K^2 \Leftrightarrow H^2) \Leftrightarrow 4 f_B H K \\ &\Leftrightarrow 2x f_C (K' H \Leftrightarrow K H') + 2x^2 (H'^2 + K'^2) + \frac{1}{2} \left(\frac{M_H}{M_W} \right)^2 x^2 (H^2 + K^2 \Leftrightarrow 1)^2 \Big) \ , \end{aligned} \tag{2.59}$$

where $x = M_W r$. The gauge is not complete fixed by this ansatz, indeed the form of the ansatz is invariant under the transformation

$$U(r) = \exp(i \Theta(r) \vec{\sigma} \cdot \vec{x}) \ , \tag{2.60}$$

where $\Theta(r)$ is an arbitrary radial function. This gauge freedom, allows us to fix one of the functions. For the sphaleron solution to be possible, the length of Higgs field should

not be fixed. Using the radial gauge $x_j A_j^a = 0$, setting $f_C = 0$, the field equations can be obtained from 2.59, given four coupled differential equations. Searching for solutions to these differential equations for small Higgs masses only the sphaleron solution of the previous section is found [14], showing that there is only one static solution besides the vacuum state. In the next section we will discus the case of large Higgs masses.

An important point for allowing the interpretation of the sphaleron solution as the top of the barrier, is that it has only one negative mode. As mentioned earlier the sphaleron is not a local minimum of the energy functional 2.59. We will consider small perturbations of the sphalerons solution with charge conjugation odd fluctuations, i.e. f_B, f_C and K, since we know that within the charge conjugation invariant ansatz the energy cannot be lowered. Hence the change in energy has the form

$$\begin{aligned} E(f_A, f_B, f_C, K, H) &= E_{sph} + \delta E(0, f_B, f_C, 0, H) \\ &= E_{sph} + \frac{M_W}{\alpha} \int dx \Psi^\dagger \Omega \Psi \ , \end{aligned} \tag{2.61}$$

where $\Psi = (\delta f_B, \delta f_C, \delta K)$, and Ω can be obtained from equation 2.59. This can be written as an eigenvalue equation for the 3 by 3 matrix Ω, and it has been shown [15, 16] by a numerically study of the eigenvalues for Ω, that for small Higgs masses the sphaleron only has one unstable direction. Assuming that there is no asymmetric negative mode, the sphaleron will satisfies equation 2.11 and is therefore indeed the top of the barrier. For large Higgs masses some of the positive energy modes cross zero and the sphaleron acquire more negative modes. This property gives rise to new static solutions, and the sphaleron is no longer the top of the barrier.

2.7 Bisphalerons

For large Higgs masses the sphaleron bifurcates and the structure of the configuration space becomes very rich. To see this we will choose the gauge $K = 0$, and the classical equations of motion become

$$\Leftrightarrow x^2 f_A'' = x^2 H^2 (1 \Leftrightarrow f_A) + 2x f_B' f_C + f_B (x f_C' \Leftrightarrow f_C) \ , \tag{2.62}$$

$$x^2 f_B'' = x^2 H^2 f_B + 2x f_A' f_C + f_A (x f_C' \Leftrightarrow f_C) \ , \tag{2.63}$$

$$x^2 H'' = \Leftrightarrow 2xH' + \tfrac{1}{2} H (f_A^2 + f_B^2 + \tfrac{1}{2} f_C^2) \Leftrightarrow f_A H + \tfrac{1}{2} \frac{M_H}{M_W} x^2 H (H^2 \Leftrightarrow 1) \ . \tag{2.64}$$

Since f_C' is not present in the energy functional, we get the constraint equations

$$f_C = x \frac{\Leftrightarrow f_A' f_B + f_A f_B'}{x^2 H^2/2 + f_B^2 + f_A^2} \ , \tag{2.65}$$

$$x f_C' = 2 f_B \Leftrightarrow f_C (1 + 2x \frac{H'}{H}) \ . \tag{2.66}$$

Using the spherical symmetric ansatz it is possible to choose two set of boundary conditions to the differential equations and obtain a finite energy static solutions. The term $H^2(1 \Leftrightarrow f_A)^2$ in the energy functional vanish at the origin for either $H(0) = 0$ or $f_A = 1$. The first set

$$f_A(0) = \Leftrightarrow 1 \ , \qquad f_A(\infty) = 1 \ ,$$

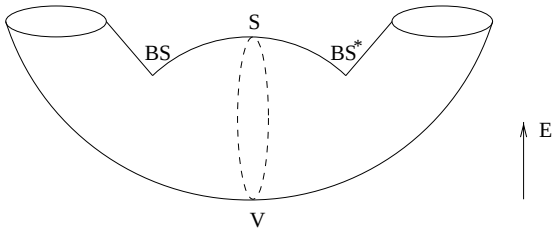

Figure 2.4: Configuration space collected in gauge orbits for $M_H > 12M_W$ with the energy (E) vertically. The sphaleron solution (S) is no longer the lowest energy state for non-contractible loops. The lowest energy state is now degenerate and given by the bisphalerons (BS and BS^*).

$$\begin{aligned} f_B(0) &= 0 \ , & f_B(\infty) &= 0 \ , \\ H(0) &= 0 \ , & H(\infty) &= 1 \ , \end{aligned} \tag{2.67}$$

is consistent with the sphaleron solution. The second set

$$\begin{aligned} f_A(0) &= 1 \ , & f_A(\infty) &= 1 \ , \\ f_B(0) &= 0 \ , & f_B(\infty) &= 0 \ , \\ H'(0) &= 0 \ , & H(\infty) &= 1 \ , \end{aligned} \tag{2.68}$$

gives rise to new solutions called bisphalerons or deformed sphalerons. When $M_H < 12M_W$ these solutions are identical to the sphaleron solution [15, 11]. The condition $H'(0) = 0$ is forcing H to rapidly approach 0 when M_H approach $12M_W$ from above, but in general the Higgs field is non-zero throughout space. It is possible, though, to construct a non-contractible loop[4] through the bisphalerons [15], and somewhere on the path the Higgs field will be zero, since this is a necessary conditions for having a non-contractible loop. The bisphalerons are not charge conjugation invariant, since f_B will be non vanishing, and comes in charge conjugate pairs. They have lower energy than the sphaleron, and the topological charge is not a half integer. The configuration space, where the configurations are collected in gauge orbits, develops a "hill" with the sphaleron at the top, and the bisphalerons are now degenerate solutions to equation 2.11, as shown in figure 2.4.

For higher values of M_H the sphaleron will acquire more negative energy directions, and branches of bisphalerons emerge, the next branch starting at $M_H = 137M_W$. This is just the start of an infinite sequence. As the Higgs mass approach infinity the number of static solutions rises logarithmically. The nth branch of bisphalerons will have n negative modes. The first branch of bisphalerons have only one negative mode, and hence for $m_H > 12M_W$ the minimal energy path from one vacuum to another is passing through the bisphalerons and not the sphaleron. The energy of the lowest bisphaleron differs only little from the sphaleron energy, for $M_H \to \infty$ the difference is about 8%.

[4] In gauge orbit configuration space

2.8 The sphaleron barrier

The barrier between the topological distinct vacua has been studied from different approaches. For $M_H < 12M_W$ this barrier is called the sphaleron barrier for natural reasons. One way is to minimize the function

$$H = E + \frac{M_W}{\alpha}\eta N_{CS} \ , \tag{2.69}$$

where η is a Lagrange multiplier. In ref. [16, 14] this was done using the general spherical symmetric ansatz. This method will yield the extremal path. It will always pass through the sphaleron and the bisphalerons if they exits, causing the barrier to bifurcate for Higgs masses above $12M_W$, and the barrier is not monotonic as a function of N_{CS}. Therefore this approach will not give the minimal energy path for large Higgs masses.

Another approach was considered in ref. [17], where the path was constructed from a gradient method. Also here the general spherical symmetric ansatz was used. Having a configuration C, the new configuration $\tilde{C}$ is found by going in the negative gradient direction

$$\tilde{C} = C \Leftrightarrow \delta C \ , \tag{2.70}$$

where δC is in the steepest descent direction. Starting at the sphaleron or bisphaleron the corresponding barrier is then obtained. The sphaleron barrier having a maximum energy larger than the bisphaleron barrier. The barriers obtained in this way is smooth and monotonic, but we have two different barriers, giving obtained from the bisphalerons, that yields the minimal energy path. The path going through the bisphaleron is not symmetric around $N_{CS} = \frac{1}{2}$, but they can be obtained from one another by the transformation $E \to E$ and $N_{CS} \to 1 \Leftrightarrow N_{CS}$. In this sense one barrier corresponds to the path taken by the gauge fields when a fermion is created, and the other barrier when an antifermion is created.

For $M_W = M_H$ the two sphaleron barriers obtained from the extremal and gradient methods are both symmetric and differs very little, although the extremal path is steeper than the gradient path, but they both end at the sphaleron configuration.

Summarizing the properties of the sphaleron, it can be characterized as a charge conjugation invariant, static solution to the classical field equations. The Higgs field is zero at the core of the solution, and the sphaleron has half integer topological charge. The solution exist for all values of the Higgs mass, but only for small Higgs masses does it represent the top of the barrier between topological distinct vacua. The physical interest in the sphaleron is due to the last property, which makes the connection to baryon violating processes.

Chapter 3

Lattice simulation of the sphaleron barrier

The finite energy barrier between topologically inequivalent vacua for the $SU(2)$ Higgs theory, also called the sphaleron barrier, is simulated on a lattice for $M_W = M_H$ using the Hamiltonian formulation.

A configuration with a given Chern-Simons number is generated, this configuration will have to high temperature and hence energy. It is subsequently cooled down by a modified gradient method, in order to keep the Chern-Simons number fixed. In this process the energy is minimized, and the potential barrier will be reached after sufficiently long time of cooling. In particular, by choosing $N_{CS} = \frac{1}{2}$, the sphaleron configuration is obtained.

Due to recent lattice simulations of the baryon violation rate, it is of interest to determine the lattice effects on the sphaleron, especially how the energy changes with the lattice parameters. This work is mainly concerning these aspects of the sphaleron. These simulations offers the opportunity to study configurations with an arbitrary Chern-Simons number, allowing to determine the form of the barrier.

The computer code used for the simulations was kindly provided to me by Alexander Krasnitz. Some modifications of the program were done by myself.

3.1 Continuum Hamiltonian formulation

To study the sphaleron barrier, we need only to consider classical physics, since it is determined by the minimum classical energy. Here the Hamiltonian formulation of the $SU(2)$ Higgs model is used. In this chapter we will use the Higgs potential

$$V(\Phi^\dagger\Phi) = \Leftrightarrow\lambda(\Phi^\dagger\Phi \Leftrightarrow v^2)^2 \ . \tag{3.1}$$

With these conventions the classical masses are given by $m_H = 2v\sqrt{\lambda}$ and $m_W = \frac{1}{\sqrt{2}}gv$. The Hamiltonian is obtained from the Lagrangian by a Legendre transformation

$$H = \pi^i\dot{\Phi} + \Pi^\alpha_\mu \dot{A}^\alpha_\mu \Leftrightarrow \mathcal{L} \ , \tag{3.2}$$

where the conjugate momenta are

$$\pi = \frac{\partial\mathcal{L}}{\partial\dot{\phi}} \ , \qquad \Pi^\alpha = \frac{\partial\mathcal{L}}{\partial_\mu \dot{A}^\alpha_\mu} = \dot{A}^\alpha_\mu = E^\alpha_\mu \ . \tag{3.3}$$

We will work in the temporal gauge $A_0 = 0$, and one finds

$$H = \frac{1}{2}E_i^\alpha E_i^\alpha + \frac{1}{4}F_{ij}^\alpha F_{ij}^\alpha + |\pi^2| + (D_i\Phi)^\dagger(D_i\Phi) + \lambda(\Phi^\dagger\Phi \Leftrightarrow v^2)^2 \ . \tag{3.4}$$

Let x generally denote any canonical coordinates. The Hamiltonian equation of motion are given by the Possion brackets

$$\dot{x} = \{H, x\} \ . \tag{3.5}$$

For the pure Yang-Mills theory these reads

$$\dot{A}_i^\alpha = E_i^\alpha \ , \qquad \dot{E}_i^\alpha = \Leftrightarrow D^j F^{ji} \tag{3.6}$$

3.2 Lattice formulation

One way of doing non-perturbative calculations is by means of lattice gauge field theory simulations. When putting the system on a lattice, it is in principle possible to directly compute expectation values. But normally the number of possible configuration on the lattice is too big for a direct calculation. Nevertheless it might be indirectly estimated with a Monte-Carlo technique, where the configurations are generated with a probability according to their weight in the expectation value. A continuum limit can then be obtained by letting the lattice spacing approach zero, while fine tuning the coupling constants.

Lattice simulation has turn out to be a powerful tool for studying non-perturbative physics, and has been used to calculated the transition rate between topological distinct vacua in the electroweak theory, from which the baryon violation rate is extracted. Here the sphaleron is studied on a lattice, and we would like to determine the effect of this discretization. It will be important for the estimating the lattice artifacts on the baryon violation rate.

Let us consider a lattice $\{\ x \mid x \in aZ^3\}$, were we denote a site by x, and a is the distance between two neighbouring sites. Our goal is to obtain a lattice Hamiltonian, which for small lattice spacings a converges to the continuum Hamiltonian given by equation 3.4. We will denote $x + a\hat{e}_i$, where $\hat{e}_i$ is a unit vector in the i direction, as $x + i$.

First we will consider a pure $SU(2)$ theory. In a lattice formulation, it is no longer convenient to work with the gauge-fields themselves. Instead one works with the parallel transporters or link matrices $U_{x,i} \in SU(2)$. The link matrices are related to the gauge fields by

$$U_{x,i} = \exp(\Leftrightarrow aA_i(x)) = \exp(iag\frac{\sigma^\alpha}{2}A_i^\alpha(x)) \ , \tag{3.7}$$

where we use the notation that $U_{x,i}$ is the parallel transporter from site $x + i$ to x. The gauge fields can then be represented by an assignment of $U_{x,i}$ on each link on the lattice. The link matrices obey the relation $U_{x+i,-i}^{-1} = U_{x,i}$. Since the gauge group $SU(2)$ is unitary, we have that $U_{x+i,-i}^\dagger = U_{x,i}$. One defines the plaquette $U_\Box$ at a site x and in the directions i, j by the smallest possible loop on the lattice

$$U_\Box = U_{x,i,j} = U_{x,i}U_{x+i,j}U_{x+i+j,-i}U_{x+j,-j} \ . \tag{3.8}$$

A standard form for the magnetic part of the Hamiltonian is given in terms of the plaquettes by

$$\sum_\Box (1 \Leftrightarrow \frac{1}{N}\mathcal{R}\mathrm{e}\ \mathrm{Tr}U_\Box) = \sum_{x,i\leq j} (1 \Leftrightarrow \frac{1}{2}\mathcal{R}\mathrm{e}\ \mathrm{Tr}U_{x,i,j}) \ , \tag{3.9}$$

where $N = \mathrm{Tr}I = 2$. In the following we will shown that it converges to the continuum magnetic part of the Hamiltonian, if the coupling constant is chosen correctly. Using

$$A_i(x+j) = A_i(x) + a\partial_j(x) + \mathcal{O}(a^2) \ , \tag{3.10}$$

and the Cambell-Baker-Hausdorff formula

$$e^A e^B \simeq e^{A+B+\frac{1}{2}[A,B]} \ , \tag{3.11}$$

where we have left out higher order terms in A, B. Hence

$$U_{x,i,j} = \exp \Leftrightarrow a^2(F_{ij}(x) + \mathcal{O}(a)) \ . \tag{3.12}$$

Since the matrix in the exponential is hermitian, the real trace of the plaquette reads

$$\begin{aligned} \mathcal{R}\mathrm{e}\ \mathrm{Tr}U_{x,i,j} &= \tfrac{1}{2}\ \mathrm{Tr}(U_{x,i,j} + U^\dagger_{x,i,j}) \\ &= \mathrm{Tr}I + \frac{a^4}{2}\ \mathrm{Tr}(F_{ij}(x))^2 + \mathcal{O}(a^5) \ . \end{aligned} \tag{3.13}$$

In the limit $a \to 0$ formula 3.9 becomes

$$\begin{aligned} \sum_{\square}(1 \Leftrightarrow \frac{1}{N}\mathcal{R}\mathrm{e}\ \mathrm{Tr}U_{x,i,j}) &= \sum_{x,i,j} \frac{a^4}{4N}\ \mathrm{Tr}(F_{ij}(x))^2 + \mathcal{O}(a^5) \\ &\to \frac{1}{a^3}\int d^3x(\frac{a^4}{4N}\ \mathrm{Tr}(F_{ij}(x))^2 + \mathcal{O}(a^5)) \\ &= \int d^3x \frac{a}{4N}\ \mathrm{Tr}(F_{ij}(x))^2 + \mathcal{O}(a^2) \ . \end{aligned} \tag{3.14}$$

Comparing to the continuum Hamiltonian we see that choosing $g^2 a = 4$ will give the wished property of the lattice Hamiltonian. In the present simulation $a = 1$, giving $g = 2$.

The representation of the electric field on the lattice is again an assignment $E_{x,i}$ on each link. The electric field can be chosen such that they generate right covariant derivative. For the pure Yang-Mills theory we therefore have the standard Kogut-Susskind Hamiltonian

$$H_{YM} = \tfrac{1}{2}\sum_l E^\alpha_l E^\alpha_l + \sum_{\square}\left(1 \Leftrightarrow \tfrac{1}{2}\mathcal{R}\mathrm{e}\ \mathrm{Tr}U_{\square}\right) \ . \tag{3.15}$$

The equations of motion for the lattice system are given by

$$\dot{U}_l = \{H, U_l\} = \Leftrightarrow \frac{\partial H}{\partial E^\alpha_l} \ , \tag{3.16}$$

$$\dot{E}^\alpha_l = \{H, E^\alpha_l\} = \frac{\partial H}{\partial U_l} \ , \tag{3.17}$$

where we denote a link (x, i) by the subscript l. One finds

$$\dot{E}^\alpha_l = \Leftrightarrow \frac{i}{2}\ \mathrm{Tr}\left(\sigma^\alpha U^\dagger_l \sum_{\square_l} U_{\square_l}\right) \ . \tag{3.18}$$

The sum is over the four plaquettes that contain U_l and start at x, as shown in figure

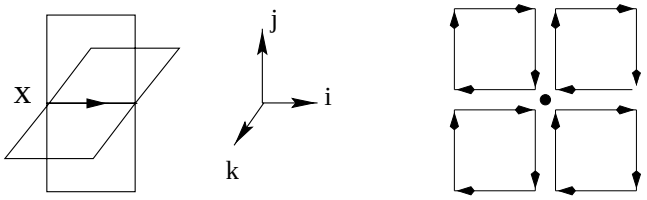

Figure 3.1: Left the matrix $\sum_{\Box_{x,i}} U_\Box$ uses for the time derivative of the electric field $E_{x,i}$. Right the matrix used for the calculating the magnetic field. The lines of the plaquettes are shifted for clarity.

3.1. For the plaquettes we have the equations of motion

$$\dot{U}_l = \Leftrightarrow i E_l^\alpha U_l \sigma^\alpha \ . \tag{3.19}$$

To represent the scalar field we assign a complex doublet field Φ_x on each lattice site. The potential term is easily formulated on the lattice,

$$V(|\Phi|^2) = \lambda(\Phi_x^\dagger \Phi_x \Leftrightarrow v^2)^2 \ . \tag{3.20}$$

The covariant derivative term can be expressed as

$$D_i\Phi(x) \to \Phi_{x+i} \Leftrightarrow U_{x,i}\Phi_x \simeq \Phi(x + a\hat{e}_i) \Leftrightarrow (1 \Leftrightarrow aA_i(x))\Phi(x) = a(\partial_i + A_i)\Phi(x) \ . \tag{3.21}$$

The canonical momenta of the Higgs field are substituted by π_x, living on each site. In total the Hamiltonian for the $SU(2)$ Higgs system becomes

$$H = H_{YM} + \sum_x |\pi_x|^2 + \sum_{x,j} |\Phi_{x+j} \Leftrightarrow U_{x,j}\Phi_x|^2 + \lambda V(|\Phi_x|^2) \ . \tag{3.22}$$

It is possible to formulate the concept of local gauge invariance on a lattice. A local gauge transformation is given by

$$\Phi_x \to V_x \Phi_x \ , \qquad U_{x,i} \to V_x U_{x,i} V_{x+i} \ , \tag{3.23}$$

where $V_x \in SU(2)$.

When calculating the energy of a configuration, we are only interested in the static energy given by

$$E_{stat} = \sum_\Box (1 \Leftrightarrow \tfrac{1}{2}\mathcal{R}\mathrm{e}\ \mathrm{Tr}U_\Box) + \sum_{x,i,j} (\Phi_{x+i} \Leftrightarrow U_{x,i}\phi_x)^\dagger (\Phi_{x+i} \Leftrightarrow U_{x,i}\Phi_x) + \sum_x \lambda(\Phi_x^\dagger \Phi_x + v^2)^2 \tag{3.24}$$

The static energy density at a site x can be written as the symmetric expression

$$\begin{aligned} \mathcal{E}(x)_{stat} &= 3 \Leftrightarrow \sum_k \sum_{i,j\neq k} \frac{1}{8}\,\mathrm{Tr}U_{x,i,j} + \lambda(\Phi_x^\dagger \Phi_x \Leftrightarrow v^2)^2 \\ &+ 6\Phi_x^\dagger \Phi_x + \sum_i \tfrac{1}{2}(\Phi_{x-i}^\dagger \Phi_{x-i} + \Phi_{x+i}^\dagger \Phi_{x+i}) \\ &\Leftrightarrow \sum_i \left\{ (U_{x-i,x}\Phi_x)^\dagger \Phi_{x-i} + (U_{x,x+i}\Phi_{x+i})^\dagger \Phi_x \right\} \ , \end{aligned} \tag{3.25}$$

where the matrix $\sum_{i,j\neq k} U_{x,i,j}$ is shown is figure 3.1. This formula is used for calculating the energy density.

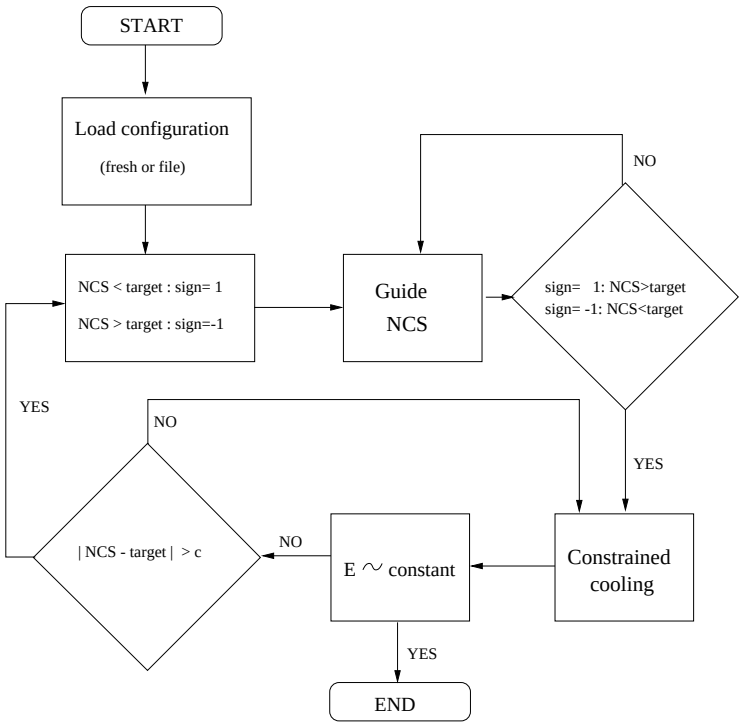

Figure 3.2: Flow diagram of the program. c is an input parameter.

3.3 Description of the program

First I will give an overview of the program used. The following sections provide more detailed information of the most important algorithms. A flow diagram of the program is shown in figure 3.2. Since we are only interested in the static properties of a configuration, the conjugate momenta of the fields are not needed. A configuration consists of the set of $\{U_{x,i}\}$ assigned on every link of the lattice, and $\{\Phi_x\}$ on every site. A finite lattice with N points in each space direction is used. Periodic boundary condition are imposed, giving every site a neighbour in each direction. We start with a configuration close to a vacuum state, deviation from the vacuum is needed since this is a stable configuration. The initial configuration is generated such that all Higgs doublets are put to the vacuum value, and all link variables, except around one site, are put to the identity matrix. The last three link variables are set to random $SU(2)$ matrices. This configuration is then guided in the direction of a target value N_{CS}^{target} of the Chern-Simons number. During the guidance N_{CS} is measured, allowing to determine when N_{CS} passes its target value, and the guidance is stopped. Then the configuration undergoes constrained cooling, where it looses energy, and the value of N_{CS} is close to constant. The static energy of the configuration is calculated at regular intervals. The whole point is to obtain a configuration that has constant energy even though the constrained cooling algorithm is used. Such a configuration minimizes the static energy, and is a point on the potential barrier. The constrained cooling, though, is not keeping the Chern-Simons number fixed. If the configuration goes too far from N_{CS}^{target}, it is guided back again. When the guidance is used, the configuration will pick up energy, slowing down the process of reaching the barrier.

3.4 Evolution

Let us first see how the link matrices are updated. This should be performed in such a way that they preserve the $SU(2)$ form. It is convenient to write the derivative of U as

$$\dot{U}_{x,i} = i\sigma^{\alpha}\dot{U}^{\alpha}_{x,i}U_{x,i} \ . \tag{3.26}$$

In the weak field limit the expansion of the link matrices given by 3.7 is

$$\dot{U}_{x,i} = i\sigma^{\alpha}\frac{dA^{\alpha}_{x,i}}{dt}U_{x,i} = i\sigma^{\alpha}E^{\alpha}_{x,i}U_{x,i} \ , \tag{3.27}$$

and it follows that

$$\dot{U}^{\alpha}_{x,i} = E^{\alpha}_{x,i} \ . \tag{3.28}$$

The electric field is given in term of the time derivative of the link variables.

We discretize time by choosing a time step Δt, and equation 3.26 is integrated numerically with a second order Runge-Kutta algorithm

$$\begin{aligned} U_{x,i}(t+\tfrac{1}{2}\Delta t) &= U_{x,i}(t)\exp(i\sigma^{\alpha}\dot{U}^{\alpha}_{x,i}(t)\frac{\Delta t}{2}) \\ U_{x,i}(t+\Delta t) &= U_{x,i}(t)\exp(i\sigma^{\alpha}\dot{U}^{\alpha}_{x,i}(t+\tfrac{1}{2}\Delta t)\Delta t) \ . \end{aligned} \tag{3.29}$$

With this updating the new set of link variable should in principle belong to $SU(2)$. Due to the finite computer accuracy, there are small deviations from the $SU(2)$ form. Consequently a reunitarization is performed with regular intervals. The evolution of the Higgs field is also integrated numerically by the Runge-Kutta method.

3.5 Measuring the Chern-Simons number

For a given configuration $\{U, \Phi\}$ it is not possible to give a direct measurement of the Chern-Simons number on the lattice [20, 21]. One way to go around this problem is to cool the gauge fields down to a vacuum configuration, where the Chern-Simons number is known to be an integer. During the cooling it is possible to measure the change in the Chern-Simons number. The Chern-Simons number is only dependent on the gauge fields, so the Higgs field is left unchanged. Since the integer value of the Chern-Simons number is not known, the program simply uses $N_{cs}(\text{vacuum}) = 0$. A configuration close to $N_{CS} = 0.5$ can roll down to both the vacuum at $N_{CS} = 0$ and at $N_{CS} = 1$, giving two different output values. This has caused some technical problems. The gauge fields are cooled by the gradient method

$$\dot{U}_{x,i} = \Leftrightarrow\frac{\partial H_{YM}}{\partial U_{x,i}} \ . \tag{3.30}$$

The configuration is pushes in negative gradient direction of the Hamiltonian, lowering the energy. A vacuum configuration should be reached after sufficiently long time of cooling. The algorithm is stopped when the energy of the configuration is reduced by a factor 2×10^4 compared to the initial configuration, and the final configuration should be close to a vacuum state. Note that the gradient methods is equal to the equation of

motion, where we have replace second order in Δt with first order in the fictitious time used here. Using equation 3.18 the derivative of the link matrix becomes

$$\dot{U}_l = U_l^\dagger \sum_{\square_l} U_{\square_l} \ . \tag{3.31}$$

Let us consider how the change of Chern-Simon number can be calculated. In the continuum we have,

$$N_{cs}(t) \Leftrightarrow N_{cs}(0) = \Leftrightarrow \frac{g^2}{32\pi^2} \int_o^t dt \int d^3x F^\alpha_{\mu\nu} \tilde{F}^{\mu\nu\alpha} \ . \tag{3.32}$$

For smooth fields, which is always the case in the continuum, this implies

$$\frac{dN_{CS}}{dt} = \Leftrightarrow \frac{g^2}{32\pi^2} \int d^3x F^\alpha_{\mu\nu} \tilde{F}^{\mu\nu\alpha} \ . \tag{3.33}$$

Using the identity

$$F^\alpha_{\mu\nu} \tilde{F}^{\mu\nu\alpha} = \frac{1}{2} \epsilon^{\mu\nu\rho\sigma} F^\alpha_{\mu\nu} F^\alpha_{\rho\sigma} = \Leftrightarrow 4 \vec{E}^\alpha \cdot \vec{B}^\alpha \ , \tag{3.34}$$

the time derivative of the Chern-Simons number can then be expressed in terms of the electric and magnetic field as

$$\frac{dN_{cs}}{dt} = \frac{g^2}{8\pi^2} \int d^3x E^{i,\alpha}(x) B^{i,\alpha}(x) \ . \tag{3.35}$$

The problem is reduced to finding an expression for the magnetic and electric fields on the lattice. The magnetic field can be obtained from the link variables, as is evident form equation 3.12. Let us deduce the corrections terms. From Stokes theorem we have

$$\oint A_\mu dx_\mu = \int_S F_{ij} ds \ . \tag{3.36}$$

The plaquette at x is a closed loop S

$$U_{x,i,j} = \exp(\int_S \Leftrightarrow F_{ij}(x') ds) = \exp(\Leftrightarrow F_{ij} a^2 \Leftrightarrow \int_S \partial_j F_{ij} x_j a ds + ...) \ . \tag{3.37}$$

Defining the magnetic field as

$$B^{k,\alpha}_x = \Leftrightarrow \frac{i}{8} \ \mathrm{Tr}(\sigma^\alpha \sum_{i,j \neq k} U_{x,i,j}) \ . \tag{3.38}$$

where i, j, k is chosen such that $\epsilon_{ijk} = 1$, the first moment will cancel due to symmetry of the plaquettes. Hence yielding a better definition of the magnetic field. Note that the magnetic field is only assigned to a site.

The electric field is obtained from the time derivative of the link matrices, by using the equations 3.31 and 3.28 one finds

$$E^\alpha_{x,i} = \Leftrightarrow \frac{i}{2} \ \mathrm{Tr}(\sigma^\alpha \sum_{\square_l} U_\square) \ . \tag{3.39}$$

But the electric field lives on a link, and we will therefore parallel transport the field going out of x down to x giving

$$2E^{i,\alpha}_x = \frac{1}{2} \ \mathrm{Tr} \left(\sigma^\alpha U_{x,i} (E^\beta_{x,i} \sigma^\beta) U^\dagger_{x,i} \right) + E^\alpha_{x-i,i} \ . \tag{3.40}$$

Here we use the notation that $E_x^{i,\alpha}$ means the electric field assigned to a site, and $E_{x,i}^{\alpha}$ is assigned to a link. The final expression for the change of the Chern-Simons number becomes

$$\Delta N_{CS} = \Delta t \frac{1}{2\pi^2} \sum_x E_x^{i,\alpha} B_x^{i,\alpha} \tag{3.41}$$

In the continuum the topological charge dependents only on the final and the initial gauge fields configurations, but on the lattice this turns out not to be exact, since the expression for $\frac{dN_{CS}}{dt}$ is not a total time derivative. Obviously the fields are not smooth on the lattice. This means that the measurement of N_{CS} with this method, depends on the path taken to reach a vacuum, and not just on the initial configuration.

The definition of $\tilde{F}_{\mu\nu}F^{\mu\nu}$ was later changed to include next-to-nearest neighbours for the electric field, and plaquettes with 2 link matrices on each side. This was done in order to make the expression closer to a total time derivative.

3.6 Guidance of the Chern-Simons number

To make it possible to obtain a configuration with a specific Chern-Simons number, the link variables should be updated in such a way that the sign of ΔN_{CS} is known. A procedure for this is by update the link matrices with a magnetic field corresponding to a link, such that it transforms covariantly. The magnetic field obtained from formula 3.38 is only situated at a single lattice site x. In order to get the magnetic field associated with a link, we parallel transform the magnetic field from the link above and add it to the magnetic field at site x,

$$B_{x,i}^{\alpha} = \tfrac{1}{2} \operatorname{Tr}\left(\sigma^{\alpha} U_{x,i}^{\dagger} B_x^{i,\beta} \sigma^{\beta} U_{x,i}\right) + B_{x+i}^{i,\alpha} \ . \tag{3.42}$$

Updating the link matrices with this magnetic field, that is choosing $\dot{U}_{x,i}^{\alpha} = B_{x,i}^{\alpha}$, gives us $E_{x,i}^{\alpha} = B_{x,i}^{\alpha}$, see equation 3.28. Again the magnetic field $\hat{B}$ is living on a link, and we have use the same technique as last for calculating ΔN_{CS}, hence

$$\tilde{F}_{\mu\nu}F^{\mu\nu} \propto \sum_x \left(2B_x^{i,\alpha} + (PD)(B_{x+i,i}^{\alpha}) + (PU)(B_{x-i,i}^{\alpha})\right) \cdot B_x^{i,\alpha} \geq 0 \ , \tag{3.43}$$

and hereby

$$\Delta N_{CS} \propto \Delta t \tilde{F}_{\mu\nu}F^{\mu\nu} \tag{3.44}$$

where (PD) means parallel transporting the link variable down, and (PU) means parallel transporting it up. This expression is clearly positive for $\Delta t > 0$, and the value of N_{CS} is raised. Correspondently it is possible to lower the value of N_{CS} by choosing a negative time step $\Delta t < 0$. This algorithm allows us to guide a configuration in a certain direction of N_{CS}, and the magnitude of the time step determines how close to the target value the final configuration will get.

As mention earlier the Chern-Simons number depends on the path. To check that the measure for N_{CS} is reasonable, it is measured from two different path during the guiding of a configuration. One is the above described, and the other by measuring N_{CS} just before and after the guidance of N_{CS}, by the cooling algorithm described in section 3.5. Performing these measurement should give us an idea of how good the operator for $F_{\mu\nu}\tilde{F}^{\mu\nu}$ is on the lattice.

It was found that they agree extremely well for small Chern-Simons numbers, and also for configurations with $N_{CS} \simeq 0.5$ if the energy of the configuration is sufficiently high. But for configurations close to the sphaleron, the discrepancy is fairly large. This is expected since the weak field limit, used to obtain formula 3.28, is not a good approximation around the sphaleron. Here the derivative of the fields are large. For instance in the continuum the Higgs field goes to zero at the core of the sphaleron.

3.7 The constrained cooling algorithm

This algorithm is designed for cooling down the configuration with the constrain $N_{CS} \simeq$ constant.

The Higgs field is cooled down by the gradient method

$$\dot{\Phi}_x = \Leftrightarrow \frac{\partial H}{\partial \Phi_x^\dagger} \ . \tag{3.45}$$

Giving

$$\dot{\Phi}_x = \Leftrightarrow 2(3 + \lambda(\Phi_x^\dagger \Phi_x \Leftrightarrow v^2))\Phi_x + U_{x,i}\Phi_{x+i} + U_{x-i,i}^\dagger \Phi_{x-i} \ , \tag{3.46}$$

again decreasing the energy.

But for the link variables we cannot simply use the steepest descent method, since the Chern-Simons number would change. Note that having added the Higgs doublet, the electric field corresponding to the gradient method would be

$$E_{x,i}^\alpha = \frac{1}{2} \ \mathrm{Tr}\left(\Leftrightarrow i\sigma^\alpha \sum_{\Box_l} U_\Box \right) + 2\mathcal{R}\mathrm{e}\left((\Phi_{x+i})^\dagger (i\sigma^\alpha (U_{x,i})^\dagger \Phi_x) \right) \ . \tag{3.47}$$

We will modify this algorithm, by adding an extra term to the electric field

$$\hat{E}_{x,i}^\alpha = E_{x,i}^\alpha \Leftrightarrow \frac{\sum_x B_{x,i}^\alpha E_{x,i}^\alpha}{\sum_x B_{x,i}^\alpha B_{x,i}^\alpha} B_{x,i}^\alpha \ , \tag{3.48}$$

where $E_{x,i}^\alpha$ is given by equation 3.47, and $B_{x,i}^\alpha$ is given by equation 3.42. Since as already explained we can associate $\hat{\vec{E}}$ with the electric field, we have $\sum_x \hat{\vec{E}} \cdot \vec{B} = 0$ during the iteration, and hence clearly N_{CS} is constant. However, the numerical integration will not be exact, and the Chern-Simons number is not totally fixed.

3.8 Discussion

The goal of the simulations is to find the potential barrier, and to study the lattice effects on the sphaleron configuration. There are two sources of conflicting error when using a finite lattice. The finite size effect, which arises since the object studied cannot fit on the lattice, and the lattice artifacts arising when the lattice is too coarse to determine the object studied. To minimize the finite size effect one should choose a large physical volume of the lattice, whereas the lattice artifacts are lowered for small lattice spacings, yielding a smaller physical volume for a fixed number of lattice points.

Since we are interested in studying the sphaleron, the lattice size should be large compared M_W^{-1}, see section 2.3. We have the formulas

$$M_W = \frac{1}{\sqrt{2}} g v \ , \qquad M_H = 2\sqrt{\lambda} v \ , \tag{3.49}$$

with $g = 2$. Choosing λ sets the ratio between the Higgs mass and the W mass. The masses are then determined by the value for the higgs expectation value v. This allow us to set the correlation length which is given by the inverse of the smallest mass.

To determine the lattice effects on the sphaleron the following method is used. Varying v and N in such a way that the physical size is kept constant, allows us to compared the sphaleron energy for different coarseness. Let us denote the sphaleron energy for physical volume $LM_W = NaM_W$ and coarseness aM_W by $E_{sph}(LM_W, aM_W)$. The continuum sphaleron energy at a finite volume is obtained, by extrapolating the energy as a function of the coarseness. The values for $E_{sph}(LM_W, 0)$ are then extrapolated to infinite volume, giving the physical sphaleron energy $E_{sph}(\infty, 0)$. Furthermore the dependence on the Higgs mass could be studied, but because of time limitations all simulations were done for $M_W = M_H$. For this choice of Higgs mass the bisphalerons are not present. The barrier will therefore be symmetric around $N_{CS} = \frac{1}{2}$, see section 2.8. Hence only barrier points with $N_{CS} < \frac{1}{2}$ are found. It was found that the barrier is indeed symmetric, by checking for a few values.

The $SU(2)$ sphaleron has already been studied on the lattice in ref. [19], with the use of saddle point cooling. The lattice artifacts were found to be described by the formula

$$E_{sph}(LM_W, aM_W) = E_{sph}(LM_W, 0) + E_1 (aM_W)^2 + E_2 (aM_W)^4 \ . \tag{3.50}$$

The values obtained for physical volumes $3.8 \Leftrightarrow 4.8$, was $E_1 \simeq \Leftrightarrow 0.3$ and $E_2 \simeq \Leftrightarrow 0.3$ for $M_W = M_H$. The volume dependence was found to be exponential decreasing

$$E_{sph}(LM_W, 0) = E_{sph}(\infty, 0) + 18.1 \frac{e^{-M_W L}}{M_W L} \ , \tag{3.51}$$

where $E_{sph}(\infty) = 3.6406 M_W/\alpha$ was found, deviating very little from the continuum calculations. The finite volume effects will tend to increase the energy, whereas the lattice artifacts will decrease the energy.

The needed computer time for obtaining data, was found too large for a detailed study of the sphaleron configuration on the lattice. The main problem being the cooling algorithm for measuring N_{CS}. It was by far the most time consuming element in the program. In particular near the sphaleron configuration a large number of cooling steps were needed to get a final configuration close to a vacuum state, see appendix B figure B.3. An example is shown in figure 3.3. By examining the configuration during the cooling, it was found that after some steps it reach a stable size. The gradient method therefore causes the configuration to approach an eigenstate of the Hamiltonian, where the energy slowly decreases. This made it rather difficult to arrive at any data, and only a few results have been obtained. As an example it took over 1 month of real computer time to obtain the sphaleron configuration for $N = 16$, where I would estimate the measurement of N_{CS} to account for more than 80% of the time. It is also quite difficult to chose the time step for the guidance algorithm. If it is too large N_{CS} will end up far form the target value, and a small time step changes the Chern-Simons number too slowly. It was further

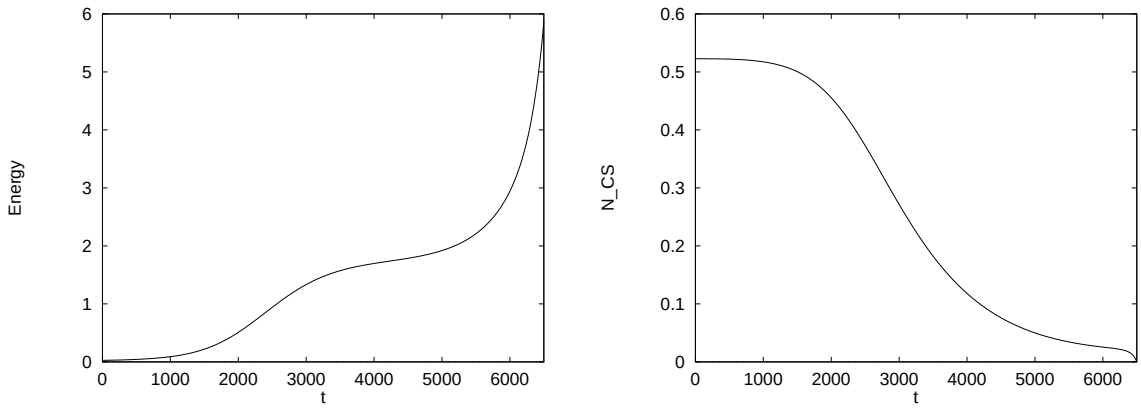

Figure 3.3: Left the energy as a function of the cooling step during a measurement of N_{CS}. Note that the time goes from right to left. Right ΔN_{CS} as a function of the cooling step. The cooling time step was 0.01.

found that the change in N_{CS} was relative large during a constrained cooling step near the sphaleron configuration. Here the derivatives of the fields are large, making the numerical integration less precise, hence N_{CS} is not fixed.

At low value of N_{CS} these problems are not present at the same extend. The constrained cooling is keeping the Chern-Simons number reasonable fixed, and the cooling algorithm for measuring N_{CS} needs less steps to reach a vacuum state. More barrier points are therefore obtained with small Chern-Simons number.

Another note to the technical discussion is that at first it seemed like a reasonable idea to generated the barrier configuration at values of N_{CS} close to one half, by guiding the final sphaleron configuration. This would give the initial configuration a lower energy than if a new lattice was used. But it was found quicker to start from a new configuration, since the sphaleron configuration is very stable.

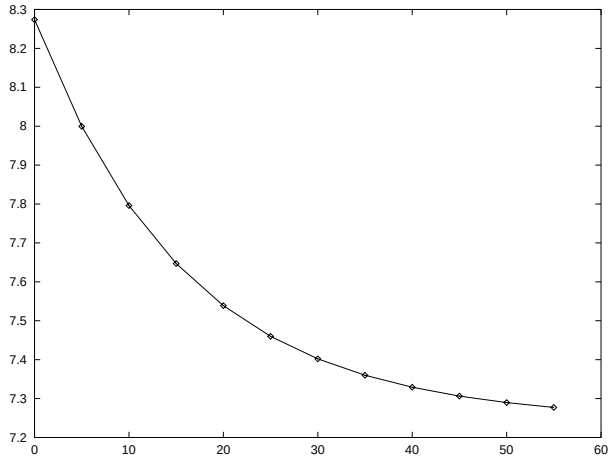

Figure 3.4: The static energy as a function of the cooling step during constrained cooling. Here for $N = 15$, $M_W = 2/3$.

In general the energy falls very rapidly when the constrained cooling is started. After a while the decrease in energy is slowing down considerably. Together with what have

been said above about problems around the sphaleron configuration, make it evident that the sphaleron configuration is hard to obtain. But an estimate of the sphaleron energy can be found, without quite reaching the sphaleron configuration. This is done by extrapolating the energy as a function of the cooling step. An example is provided for $N = 15$, $M_W = 2/3$. By extrapolating the cooling curve 3.4 to an exponential decay

$$f(x) = a + b \exp(\Leftrightarrow c * x) \tag{3.52}$$

the following values of the parameters a, b, c was found

$$\begin{aligned} a &= 7.24428 \quad +/\Leftrightarrow 0.000458614 \\ b &= 0.00198827 \quad +/\Leftrightarrow 1.90333e \Leftrightarrow 05 \\ c &= 0.0625032 \quad +/\Leftrightarrow 9.42603e \Leftrightarrow 05 \end{aligned} \tag{3.53}$$

giving a sphaleron energy $E_{sph}/\frac{M_W}{\alpha} = 3.459$. The curve is seen to fit well with an exponential decrease. This method suffers from the systematic error coming form the change of N_{CS} during the constrained cooling. It was found that this method is only possible if a reunitarization of the link matrices were performed after each constrained cooling step. If the reunitarization is done with a larger interval, the energy was clearly found to be falling due to the reunitarization, as shown in appendix B, figure B.4. An explanation of this can be that boundary link matrices, i.e. the links far from the core of the sphaleron, differs "little" but still sufficiently enough from the identity matrix. This would effect the energy, since the $1 \Leftrightarrow \frac{1}{2}\mathcal{R}\mathrm{e}\ \mathrm{Tr}U_{\Box}$ would not be zero, and this will happen for a lot of boundary matrices.

3.9 The slope of the barrier near the vacuum states

We estimate the slope of the barrier curve close to the vacuum states. In this area we expect that there is a linear dependence of the static energy on the Chern-Simons number. It seems reasonable to assume that the non-abelianity of the theory is not important. Therefore we will simply evaluate the slope for the Abelian $U(1)$ theory, but with the difference to ordinary electromagnetism, that there is a coupling to a Higgs field. Being close to the vacuum states, this coupling simply gives rise to a mass term for the gauge field. In this case the Hamiltonian for static configurations reads

$$H = \tfrac{1}{2}\int d^3x B^2 + \tfrac{1}{2}m_W^2 \int d^3x A_i^2 \ . \tag{3.54}$$

By Fourier transforming to momentum space

$$H = \sum_p \tfrac{1}{2}(p^2 + m_W^2) a^i(p) a^i(\Leftrightarrow p) \ . \tag{3.55}$$

The Chern-Simons number can in the case of a massless gauge field be written as [34]

$$N_{cs} = \frac{1}{4\pi^2 i}\epsilon_{lmn} \sum_p p_m e^i(p)_n e^j(\Leftrightarrow p)_l a^i(p) a^j(\Leftrightarrow p) \ , \tag{3.56}$$

where $a^i(p)$ is the field for a photon with momentum p and transverse polarization e^i. The photon fields obey $a^i(p) = a^i(\Leftrightarrow p)^*$. Now, the massive W-particle also has a longitudinal

polarization state. But gauge invariance of N_{CS}[1] insures us that it is independent of the longitudinal state, so we assume that the given formula is still valid.

The formula for N_{CS} clearly only contributes for $i \neq j$. We want to minimize the Hamiltonian under the constrain that $H = \lambda N_{CS}$, where λ is the slope. Equivalently we want to maximize N_{CS} for fixed energy, and it is sufficient to do this for a separate momentum mode p. For N_{CS} to be real, $a^i(p)a^j(\Leftrightarrow p)$ has to be purely imaginary. We obtain a maximum value of N_{cs} when the modulus of the two fields are the same, and for a reel we have

$$a^1(p) = a \quad , \quad a^2(\Leftrightarrow p) = ia \ . \tag{3.57}$$

Let the three vectors $\vec{p}$, $\vec{e}^{\,2}(p)$ and $\vec{e}^{\,1}(\Leftrightarrow p)$ form a right-handed coordinate system. For simplicity we can take the x-axis to be parallel with the momentum $\vec{p}$. Then we finally get

$$N_{cs} = \frac{1}{2\pi^2}|p|a^2 \ . \tag{3.58}$$

The static energy for this momentum mode is then given by

$$E_{stat} = a^2(p^2 + m_W^2) = \frac{2\pi^2 N_{cs}}{|p|}(p^2 + m_W^2) \ , \tag{3.59}$$

which has its minimum value for $p = m_W$. Plugging this in the slope reads

$$E_{stat} = 4\pi^2 m_W N_{cs} \ . \tag{3.60}$$

On the lattice momenta are discretized, $p = \frac{\pi}{n}$, $n = 1..N$, and it will not always be possible to have a momentum exactly equal to m_W. But since the first Brillouin zone $\mathcal{B} = \{p \mid \Leftrightarrow\pi < p \leq \pi\}$ is dense on the lattices used, the momentum will be close to m_W.

This analysis was carried out in $U(1)$ theory. Roughly speaking we can say that changing to $SU(2)$ only gives another three ways of making the momentum mode $p = m_W$, thereby making the mode degenerate, but which degree is excited is not of importance.

A number of simulation with different lattice size N and $M_W = 1$ was carried out. The final results for the slope are in given below

N	10	12	14	16	18	20
$\lambda/\frac{M_W}{\alpha}$	12.498	12.504	12.547	12.539	12.540	12.518

This fit well with the predicted value $4\pi \simeq 12.5664$.

The result for the slope was obtained for $N_{CS} \simeq 0.01$. For these small values of the Chern-Simons number the curve fits well with a linear form going through $(0, 0)$. Since the constrained cooling algorithm is not keeping N_{CS} totally fixed, the slope was plotted as a function of the constrained cooling step, in order to determine when a constant value was reached. Some of these curves can be seen in appendix B. The results are obtained with a definition of $\tilde{F}F$ including next-to-nearest neighbours. With ΔN_{CS} given by the formula 3.41, the slope was found to be ~ 13.7. For $N = 14$ a rather unusual final configuration was obtain, where it developed two hills, see appendix B figure B.2. It was run with three different initial configurations, without changing the final result.

[1] N_{CS} is gauge invariant in the Abelian theory

3.10 Results

The potential barrier obtained for $N = 16$ is seen in figure 3.5, and for $N = 24$ in figure 3.6. Continuum calculations of the barrier have been done in ref. [17, 16], using

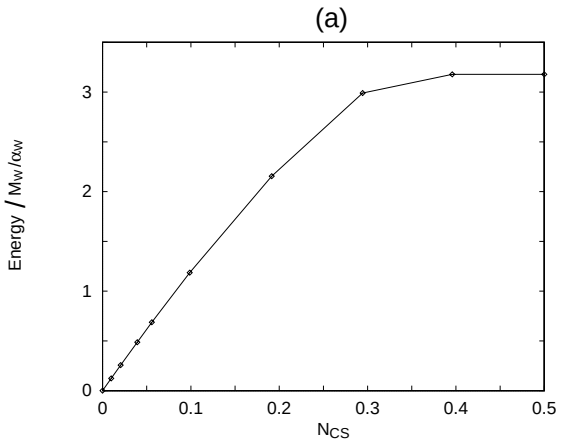

Figure 3.5: The static energy potential for $N = 16$, $M_W = 1$, with $E_{sph} = 3.179 M_W/\alpha$.

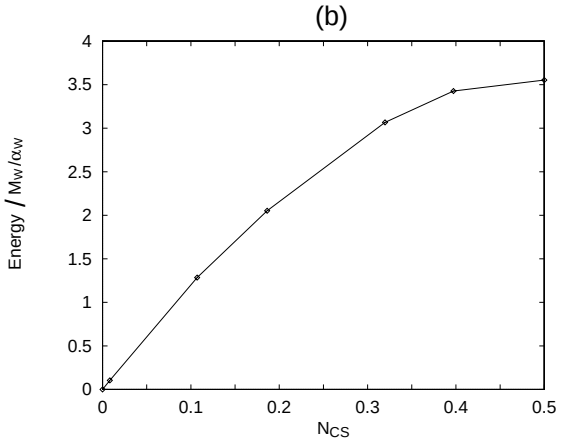

Figure 3.6: The static energy potential for $N = 24$, $M_W = 1/2$, with $E_{sph} = 3.553 M_W/\alpha$.

a spherical symmetric ansatz. The barrier energy is found to deviate more from the continuum results as N_{cs} goes up, with a large discrepancy for $N = 16$ at the sphaleron. The continuum sphaleron energy is 3.64 M_W/α. For small Chern-Simons numbers the results agree well with the continuum calculations, which is also evident from the slope near the vacuum states. Both barriers are close to the extremal path barrier for small Chern-Simons numbers, and are in this region steeper than the gradient barrier, see section 2.8.

The lattice artifacts will lower the energy, because in the discretization energy is lost. In figure 3.7 the final sphaleron configuration for $N = 16$ and $M_W = 1$ is shown by plotting a plane through the core of the sphaleron. The two other possible slices through the core of the sphaleron looks similar, and the sphaleron can be said to be

spherical symmetric, to the extend possible on a lattice. The spherical symmetry is the key assumption in continuum calculations. The Higgs field is very close to its vacuum value at the boundary, and the energy density is close to zero. The finite size effects are therefore small for this configuration. But the lattice artifacts are seen to be large. It is clearly seen that Higgs field is not zero at core, in fact it is ~ 0.3. From the energy density we see that the "top" of the sphaleron is cut off by the discretization. For the sphaleron configuration obtained for $N = 24$ and $M_W = 1/2$, shown in figure 3.8, we see a Higgs field quite close zero at the core, and the energy density has a regular top. By comparing the two sphalerons it is clear that the lattice artifacts tends to decrease the energy of the sphaleron. The configurations for small values of N_{CS} are smoother and consequently a better approximation to the continuum configuration, see appendix B, figure B.7 to B.10. For all barrier points a spherical symmetric configuration was found. We can conclude that the lattice artifacts are increasing as a function of N_{CS}, and a very coarse lattice will consequently have a flat barrier top, as is also seen from the two barriers in figure 3.5 and 3.6. Therefore taking this into account the barrier agrees well with the continuum results.

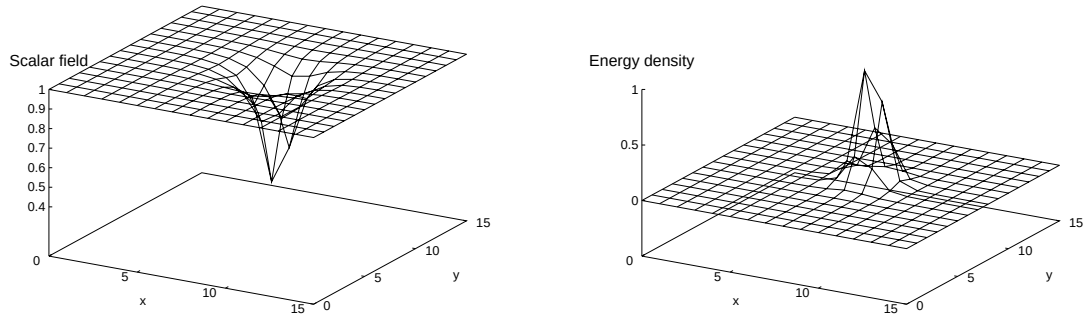

Figure 3.7: A plane through the core of sphaleron configuration for $N = 16$. Left the magnitude of the scalar field. Right the energy density.

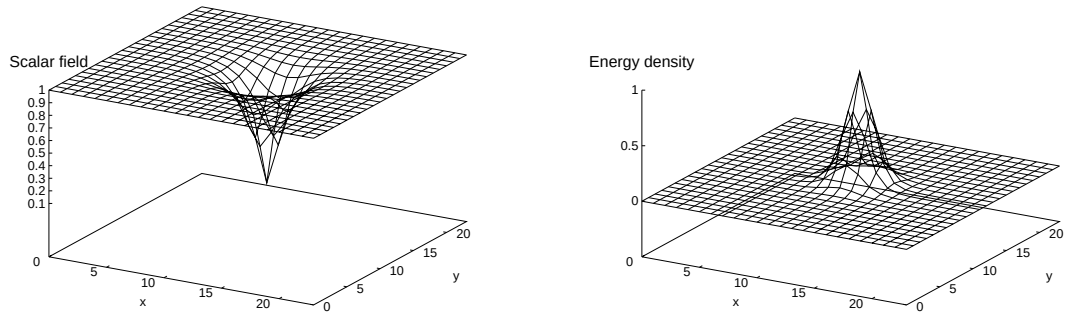

Figure 3.8: A plane through the core of sphaleron configuration for $N = 24$. Left the magnitude of the scalar field. Right the energy density.

The magnitude of the Higgs field at the core of the sphaleron is shown in table 3.1, in the cases where the sphaleron was reached. We see a strong dependence on the coarseness

N	10	12	16	18	24
$M_W a$	1	1	1	2/3	0.5
Min. $\sqrt{\Phi^\dagger\Phi}/v$	0.29604	0.30918	0.30567	0.19268	0.11756

Table 3.1: Magnitude of normalized Higgs field.

N	12	14	16	18	24
$M_W a$	1	6/7	3/4	2/3	1/2
$E_{sph}/\frac{M_W}{\alpha}$	3.223	3.235	3.361	3.4647	3.553

Table 3.2: E_{sph} as a function of the lattice coarseness for physical volume $LM_W = 12$

of the lattice. Both finite volume effect and lattice artifacts will cause the sphaleron to differ from zero at the core, but here the finite size effects are small.

An attempt to estimate the physical sphaleron energy was maid. The volume dependence of the sphaleron energy described by 3.51, gives hardly any notable effect on the energy, for the physical volumes used in the present simulations. For the physical volume $LM_W = 12$, the sphaleron energy as a function of the coarseness of the lattice is shown in table 3.2. Plotting the sphaleron energy as a function of the lattice coarseness, one sees that the curvature changes around $N = 16$. It would be natural that this happens, since the sphaleron energy must approach zero when the coarseness increases, and it will no longer fit the form 3.50. Therefore only the last three points was extrapolated by using 3.50, where the last term is omitted. This rather naive extrapolation yields

$$E(12,0) = 3.7103 \Leftrightarrow 0.60(M_W a)^2 \ . \tag{3.61}$$

For the physical volume $LM_W = 10$, E_{sph} as a function of the the lattice coarseness is shown in table 3.3. Again fitting to a form with just the first term in 3.50 gives

$$E(10,0) = 3.6530 \Leftrightarrow 0.41(M_W a)^2 \tag{3.62}$$

These results are accompanied with a lot of uncertainty. For instance only a few points have been used in the extrapolation. Furthermore there is an uncertainty in the value of N_{CS}, as described in section 3.5, and the method, described in section 3.8, for determining $E_{sph}(LM_W, aM_W)$ suffers from a systematic error. Therefore, within the uncertainty, the energy is most probably in agreement with the continuum value 3.64.

N	10	15	20	25
$M_W a$	1	2/3	1/2	2/5
$E_{sph}/\frac{M_W}{\alpha}$	3.250	3.459	3.552	3.595

Table 3.3: E_{sph} as a function of the lattice coarseness for physical volume $LM_W = 10$

Chapter 4

Baryogenesis

In this chapter we want to consider the possibility of generating a baryon asymmetry within the electroweak theory. The asymmetry is given by the ratio

$$\Delta = \frac{n_b \Leftrightarrow n_{\bar{b}}}{s} \simeq \frac{n_b}{s} = 4 \times 10^{-11} \Leftrightarrow 10^{-10} \ , \tag{4.1}$$

where n_b is the density of baryons, and s the entropy density. In the early Universe, this corresponds to one extra fermion per about one billion fermion-antifermion pair. It was realized by Sakharov, that the asymmetry might be generated dynamically in the early Universe.

4.1 Sakharov's conditions

In his paper [4] Sakharov stated three necessary conditions for a plausible scenario that can explain the asymmetry.

1. **Baryon number non conservation.**
2. **C and CP violation.**
3. **Deviation from thermal equilibrium.**

The first conditions is obvious, if we assume that the Universe started with an equal number of particles and antiparticles.

The second condition can be explained in the following way. C violation is necessary in order to violate the baryon number. Further more, we have that the baryon number $B = b \Leftrightarrow \bar{b}$ transforms under CP as

$$(CP)B(CP)^{-1} = \Leftrightarrow B \ . \tag{4.2}$$

If there is no CP violation the processes which create a net number of baryons, will have the same rate as the processes which create a net number of antibaryons.

If there is thermal equilibrium we have from the CPT theorem that the Hamiltonian H is invariant under CPT. At finite temperature the baryon number is given by a thermal average, and we have

$$\langle B \rangle \quad = \quad \mathrm{Tr}\left(e^{-\beta H} B\right)$$

$$
\begin{aligned}
&= \mathrm{Tr}\left(e^{-\beta H} B (CPT)^{-1} (CPT)\right) \\
&= \mathrm{Tr}\left(e^{-\beta H} (CPT) B (CPT)^{-1}\right) \\
&= \Leftrightarrow \langle B \rangle \,, \qquad (4.3)
\end{aligned}
$$

since the baryon number is odd under (CPT). Hence $\langle B \rangle = 0$ and there must be processes out of thermal equilibrium to create an asymmetry.

The possibility of explaining the baryon asymmetry from a cosmological context has been the subject of much work in past decades. The sphaleron comes into play, when the possibility of electroweak baryogenesis is studied, this is our main interest, although many scenarios have been proposed. The first models used grand unified theories (GUT) to obtain CP violation, and the GUT phase transition to get processes out of thermal equilibrium. In many of these models the decay of lepto-quarks were the source for baryogenesis. It was shown that in some grand unified theories it is indeed possible to create a sufficient amount of baryonic excess. There are various sources, though, that in the cosmological evolution will wash out this asymmetry. The inflationary epoch, where the Universe is exponential expanding, will dilute any previous existing asymmetry by an exponential factor. Therefore if one believes in the inflationary scenario, the asymmetry must be created after inflation. Since the GUT phase transition temperature, is before the inflationary epoch, this will rule out the GUT scenarios, unless the reheating temperature after inflation is again at the GUT scale. This has been shown not to be possible to obtain [2]. A much stronger argument that rules out GUT scenarios is that the baryon violation rate in the standard electroweak model, before the electroweak phase transition, is so high that it will wash out any previously existing asymmetry. Although if a $B + L$ violation is generated at the GUT scale, this will not be erased by electroweak processes, and remains another possibility for explaining the observed asymmetry [24]. Assuming that there is no $B + L$ violation, a scenario for baryon generation, must be realized at or after the electroweak phase transition.

As was realized in ref. [26] the electroweak sector of the minimal standard model has all the required conditions for a baryogenesis scenario. At sufficient high temperature, we expect the electroweak theory to violate the baryon number, as will be described in the following. Experimental confirmation of baryon number violating processes is still lacking, but it is likely that it will be seen in future accelerators due to the instanton tunnelling [3]. The chiral coupling to fermions give C violation and experimentally CP violation has been found for the kaons. If the electroweak phase transition is of first order strong deviations from thermal equilibrium are expected. The electroweak phase transition is probably the latest moment when deviations from thermal equilibrium are sufficiently large for creating the observed asymmetry. The advantage of electroweak baryogenesis is that it mainly relies on known physics. In addition the problem of inflation is no longer present.

4.2 The electroweak phase transition

At sufficiently high temperature, the symmetry of the Higgs potential is restored, giving a vacuum expectation value $v = 0$ for the Higgs field. This phase of the electroweak theory is called symmetric, since the vacuum is invariant under the transformation $\Phi \to U\Phi$. In the broken phase the Higgs field has a vacuum expectation value that differs from zero, and the

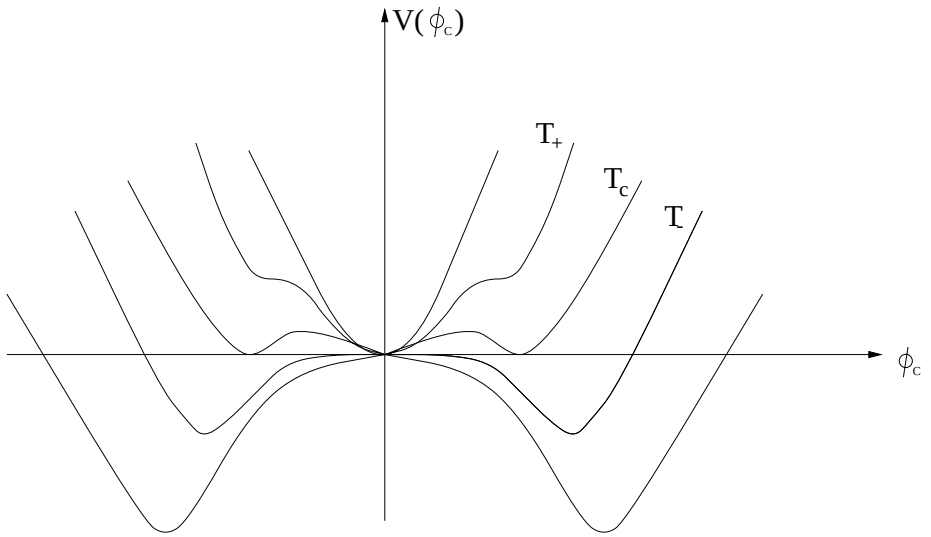

Figure 4.1: The effective potential for a first order phase transition

vacuum is no longer gauge invariant. In the standard cosmological model, with a Big Bang scenario, the Universe evolves from an initial hot stage and cools down as the Universe expands. At some point in the early Universe a phase transition must have occurred, going from the symmetric phase to the broken phase. The order of the electroweak phase transition (EPT) is of crucial importance for the electroweak baryogenesis scenarios. The order parameter is the length of the Higgs field $(\Phi^\dagger\Phi)^{\frac{1}{2}} = \phi$ or, equivalently, the Higgs expectation value v.

A first order phase transition is characterized by a jump in the order parameter when going from one phase to the other. For the EPT the Higgs expectation value is 0 in the symmetric phase, and jumps discontinuously to a value $v \neq 0$ in the broken phase. The evolution of the effective potential for the Higgs field, shown in figure 4.2, starts with a single minimum at $\phi = 0$, but as temperature decreases a new minimum develops. The temperature where it first occurs is denoted T_+. The minimum at $\phi = 0$ is still the global one, and is therefore the classical vacuum state. As temperature drops further the critical temperature T_c is reached, where the two minima for effective potential are degenerate. For a first order phase transition there is an energy barrier between the two minima. For temperatures below T_c, the minimum at $\phi \neq 0$ is the true vacuum state. In the case where the energy barrier between the two minima is sufficiently high, it will cause the Higgs field to be trapped in the former global minimum, which is often called the false vacuum state. The Higgs field will stay there until the barrier becomes so low that the fields can tunnel through or thermally pass the barrier. This phenomenon is known as supercooling. The height of the barrier is a measure of the strength of the transition, and a strong transition has a high barrier. Bubbles of the new phase will emerge at a temperature close to T_-, and expand until they fill the whole Universe. At $T = T_-$ the energy barrier between the two minima disappears and the false vacuum can classically roll down to the global minimum at $v \neq 0$.

In a second order phase transition the picture looks somewhat different. At the critical temperature there is no barrier and the Higgs field will continuously go from the zero

expectation value, to a non-zero expectation value. There is no bubble nucleation, which is the source of non-thermal equilibrium. If a second order transition occurred it has been argued [25] that electroweak baryogenesis is not possible.

A major problem in calculating quantities for the EPT, is that perturbation theory is not reliable for high temperatures, and eventually breaks down in the symmetric phase. At finite temperature the propagator presents a sum of two terms, the standard zero temperature propagator and a temperature dependent term which reflects the presence of particles in a heat bath. The latter term is proportional to the bose distribution function. At finite temperature the relevant expansion parameter is therefore $g^2 n_B(E)$ instead of g^2, where

$$n_B(E) = \frac{1}{e^{E/T} \Leftrightarrow 1} \tag{4.4}$$

is the bose distribution, and E is the typical energy of the process. This accounts for the bose amplification. In the broken phase there is an infrared cutoff coming from the vector boson mass m_W. For processes $E < T$, we have $n_B(E) \sim \frac{T}{E}$, and perturbation theory is valid if $\frac{g^2 T}{E} \ll 1$. In the symmetric phase perturbation theory renders a massless gauge particle, there is no infrared cutoff and the expansion parameter can be arbitrary large, causing perturbation theory to break down. For a small mass of the Higgs boson, perturbation theory of the effective potential of the Higgs field may work up to the critical temperature. We will here look at some perturbative estimates, that give symmetry restoration at high temperature.

The effective potential is given in terms of the classical fields ϕ_c,

$$V(\phi_c) = \Leftrightarrow \sum_{n=1}^{\infty} \frac{1}{n!} \phi_c^n, {}^{(n)}(p_i = 0) \ , \tag{4.5}$$

where , $^{(n)}$ are the 1PI Diagrams. Substituting $\phi = \sqrt{2}(\Phi^\dagger \Phi)$ in equation 1.4, the effective potential for the Higgs field at tree level and with leading orders in temperature is [22, 48]

$$V(\phi, T) = \frac{\lambda}{4}\phi^4 \Leftrightarrow \frac{\lambda}{2} v^2 \phi^2 + \frac{1}{2}\gamma T^2 \phi^2 \ , \tag{4.6}$$

where

$$\gamma = \frac{2M_W^2 + M_Z^2 + 2M_t^2}{4v^2} \ . \tag{4.7}$$

In this calculation all fermions, except the top quark, are neglected. The top quark with mass $M_t = 182$ Gev is by far the heaviest and will give the largest contribution. Here v is the zero temperature expectation value $\simeq 241.6$ GeV. This potential gives rise to a second order phase transition. The temperature dependent term in ϕ^2 has opposite sign with respect to the constant one, and for very large temperatures the mass of the Higgs field becomes positive. The symmetry is no longer broken. The critical temperature when this happens is

$$T_c^2 = \frac{\lambda v^2}{\gamma} \ . \tag{4.8}$$

The Higgs field vacuum expectation value is varying continuously,

$$\langle \phi(T) \rangle = 0 \qquad \text{for} \quad T > T_c \tag{4.9}$$

$$\langle \phi(T) \rangle = v \left(1 \Leftrightarrow \frac{\gamma T^2}{\lambda v^2} \right)^{\frac{1}{2}} \qquad \text{for} \quad T < T_c \ . \tag{4.10}$$

Calculating the effective potential to one loop, yields a first order phase transition, since we get a term with ϕ^3, coming from the interaction with the gauge fields. For a light Higgs boson

$$V(\phi, T) = \frac{\lambda}{4}\phi^4 \Leftrightarrow \frac{\lambda}{2}v^2\phi^2 + \frac{\gamma T^2}{2}\phi^2 \Leftrightarrow M_1 T\phi^3 \ , \qquad M_1 = \frac{2M_W^3 + M_Z^3}{4\pi v^3} \ . \tag{4.11}$$

The critical and lower instability temperature is

$$T_-^2 = \frac{\lambda v^2}{\gamma} \ , \qquad T_c^2 = \frac{T_-^2}{1 \Leftrightarrow 2M_1^2/\lambda\gamma} \ . \tag{4.12}$$

The Higgs field vacuum expectation value will jump discontinuously when reaching the critical temperature. The jump in the order parameter can be characterized with

$$\frac{\phi(T_c)}{T_c} = 2\frac{M_1}{\lambda} \ . \tag{4.13}$$

We see that the strength of the transition gets weaker when the Higgs mass increases. The best perturbative estimate of the critical temperature calculated to two loop level is currently 173.3 GeV for $m_H = 80$ GeV [48]. Qualitatively the perturbative estimate are correct, but the numerical values differs from the non-perturbatively values.

The phase transition can be studied non-perturbatively with lattice gauge theory, and a number of Monte-Carlo simulations have been performed. Many of these simulation are done in the purely bosonic theory, due to problems with treating chiral fermions on a lattice. A great advantage regarding the computer time is obtained by going to dimensionally reduced 3D theory, which should be valid for high temperatures. In general it is possible to integrate out the temperature by going to the Euclidean theory, in this way an effective theory can be obtained. For many theories, including the standard electroweak theory, the effective Lagrangian for the phase transition can then be described by a pure $SU(2) \times U(1)$ gauge group and a Higgs doublet,

$$\mathcal{L}_3 = \frac{1}{4}F_{ij}^a F_{ij}^a + \frac{1}{4}f_{ij}f_{ij} + (D_i\Phi)^\dagger(D_i\Phi) + m_3^2\Phi^\dagger\Phi + \lambda_3(\Phi^\dagger\Phi)^2 \ , \tag{4.14}$$

where the factor of T^{-1} has been scaled into the coupling constants and fields. A special method using both perturbation theory and lattice simulation of the three dimensionally reduced theory has been shown to give very accurate results for the parameters of the phase transition. Concerning the phase transition, only static properties of the bosonic Green's function are relevant, and using the Euclidean Matsubara formulation of finite temperature field theory, it is possible to relate the three dimensional coupling constants to the four dimensional ones. This is done by requiring that the two and four point Green's functions of the two theories, where these are calculated perturbatively, are matching each other to some accuracy [39]. Here effect of fermions are included, since they contribute to the three dimensional coupling constants. Shaposhnikov et. al. [40, 41] have recently calculated latent heat, critical temperature, and order of the transition by simulating the 3D dimensionally reduced theory. Their results yields a first order transition in the minimal standard model for a Higgs mass smaller than the critical value $m_H^* < 80$ GeV, and the strength increasing with decreasing m_H. At the critical mass the transition becomes second order, and above it there is no phase transition but a regular cross over, where the two phases cannot be distinguished.

4.3 Baryon non-conservation at high temperature

In section 1.5 we saw that baryon number changing processes were related to an evolution in the *bosonic* fields. As a first approximation we will therefore neglect the fermions. The baryon violation rate is obtained by calculating the transition rate of the fields between topologically distinct vacua in a pure gauge Higgs theory. At zero temperature the fields will have to tunnel through the barrier and, as shown in section 1.2, the rate is suppressed by a huge factor. At finite temperature there are thermal fluctuations of the fields above the barrier, and it is possible to cross the barrier classically. The fields will be thermally distributed according to the Boltzmann distribution $e^{-E/T}$, and the rate of baryon violation is supposedly unsuppressed when the temperature is comparable to the barrier height.

The height of the barrier varies with temperature. It was shown by Kunz et. al. [22], that the sphaleron energy at finite temperature is well approximated by the formula

$$E_{sph}(T) = E_{sph}(T=0)\frac{v(T)}{v(0)} \tag{4.15}$$

This was obtained using two different temperature dependent potentials for the Higgs field. In the case of the potential given by 4.6, the energy of the sphaleron can be found by scaling the zero temperature sphaleron solution and its energy is given exactly by formula 4.15. Using the potential 4.11 the energy is still in good agreement with this equation. We may write

$$E_{sph}(T) = \frac{M_W(T)}{\alpha} B(\lambda/g^2)\ , \tag{4.16}$$

where the factor B runs from 3.04 at $\lambda = 0$ to 5.44 for $\lambda \to \infty$. The coupling constant should be taken as the temperature dependent running coupling constant.

Clearly the probability rate of crossing the barrier is dominated by configurations passing close to the sphaleron, since these requires the least energy. A simple estimate of the rate at non-zero temperature, when considering Boltzmann suppression, gives

$$,\ \simeq e^{-\beta E_{sph}(T)}\ , \tag{4.17}$$

where $\beta = \frac{1}{T}$. This result is quite clear, since the exponential just counts the number of states with an energy higher than the barrier. The rate in the broken phase is therefore exponentially suppressed. It would give us a rate of order unity when $T \simeq T_c$, since the sphaleron energy goes to zero. Later we will calculate the pre factors to the exponential in 4.17.

Since there is no barrier between the vacua in the symmetric phase, we would expect a very high baryon violation rate in this phase.

4.4 Scenarios for electroweak baryogenesis

A number of scenarios have been proposed, where the electroweak phase transition is used to create an asymmetry. Kuzmin, Rubakov and Shaposhnikov were the first to consider the possibility of electroweak baryogenesis [26]. It is essential for the electroweak baryogenesis scenarios that the phase transition is of first order. For a second order transition, where the Higgs vacuum expectation is varying continuous, any BAU generated

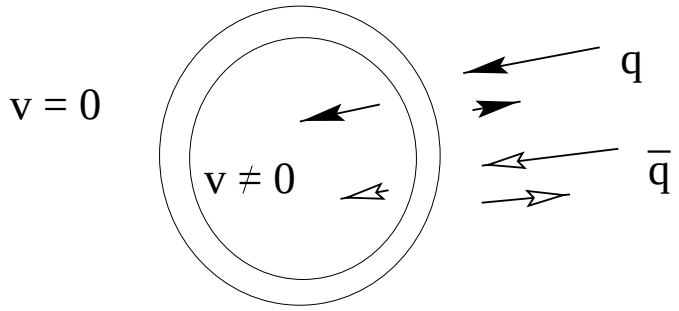

Figure 4.2: CP violation in the bubble wall causes more antiparticles to be reflected than particles.

during the transition will be erased. As will be shown later baryon violating processes in equilibrium tend to equalize the number of baryons and antibaryons. Right after a second order transition the barrier is still absent, and the sphaleron transitions are fast, diluting any BAU. Further more for a second order transition it is hard to create a source for thermal deviation, and it is generally believed that it is not be possible to create enough BAU. A strong first order transition is therefore necessary both for the creation of a BAU and for it to survive. The electroweak baryogenesis scenarios are build on the assumptions that the baryon violation rate is rapid in the symmetric phase, whereas the baryon violating processes in broken phase are practically turned off. In this way a creation of a baryon asymmetry of the Universe (BAU) during the phase transition will not be erased by subsequently sphaleron transitions.

The first order transition will proceed through nucleation of bubbles of the new phase, i.e. the broken phase. The bubbles of broken phase will be created near to the instability point for the minimum at $\phi = 0$, at temperature T_-, and they will expand with a velocity close to the speed of light. There must be an interface wall between the broken phase inside the bubble and the outside where $\phi \simeq 0$. This interface region is called the domain wall, and it is the motion of the wall through the plasma that causes deviations from thermal equilibrium.

A nice mechanism for the generation of the BAU, was suggested by Cohen, Kaplan and Nelson [2], using a CP-violating interaction of fermions with the domain wall of a bubble. In this way, the reflection coefficient of the antifermions is larger than for the fermions (see figure 4.2). The rate of baryon violating processes in the symmetric phase is supposed to be so fast, that the excess of antifermions is strongly diluted, again equalizing the number of fermions and antifermions. The bubble of broken phase is thereby filled with fermions, since the baryon number is assumed to be conserved in this phase. The bubbles expand and will eventually fill the whole Universe, which will be left charge asymmetric. Calculating the exact amount of BAU generated with this mechanism is not easy. The bubble nucleation rate and the structure of the domain wall, their velocity and the density of particles will have to be evaluated. One might wonder if it is at all possible to create enough BAU. One thing among others is the need for sufficiently strong CP violation.

In the minimal standard model the source of CP violation originates from Yukawa couplings between quarks and the Higgs field,

$$\Phi_L K f^{(d)} d_R \phi + \Phi_L I f^{(u)} u_R + \text{h.c.} \tag{4.18}$$

The Kobayashi-Maskawa matrix (K) describes the mixing of the quarks, and contains a CP violating phase δ_{CP}. Experimentally the CP violation from the K matrix is found to be so small that it is hard to generate the observed amount of BAU. In extended versions of the Standard model, other sources for CP violation are possible. In the two Higgs model a CP violating term is generated in the scalar sector.

We see that there are possible mechanisms for creating a BAU at the EPT, if the assumption about the baryon violation rate in the respective phases are for filled. This will be investigated in the following sections.

4.5 The rate in the broken phase

We will estimate the pre factors to the exponential 4.17, by considering small fluctuations around the sphaleron, here the energy functional can be approximated by

$$\mathbf{H} = E_{sph} \Leftrightarrow \frac{1}{2}\omega_-^2 x_-^2 + \sum_i \frac{1}{2}\omega_i^2 x_i^2 + \sum_i \frac{1}{2} p_i^2 \ , \tag{4.19}$$

where x_i, p_i are canonical coordinates for the configuration space. We have $x_- \propto N_{CS}$, since ω_- is the negative mode of the sphaleron,

For each gauge Higgs field configuration $\{A_\mu, \Phi\}$, we can define a gauge sector to which they belong, by cooling the configuration down by the steepest descent equations

$$\frac{\partial A_i}{\partial t} = \Leftrightarrow \frac{dH}{dA_i} \ , \tag{4.20}$$

$$\frac{\partial \Phi}{\partial t} = \Leftrightarrow \frac{dH}{d\Phi^\dagger} \ . \tag{4.21}$$

The equation are started from the initial configuration $\{A_\mu, \Phi\}$, and, as the fictitious time t goes to infinity, the fields will reach a static configuration $A_\mu^\infty, \Phi^\infty$. Some configurations will reach a vacuum state and we define the gauge sector to which they belong by the integer winding number of the vacuum configuration. The sphaleron being a static solution, is also a possible candidate for the final configuration[1]. Configurations ending at the sphaleron, or at one of the gauge copies, are situated on the surface with $x_- = 0$, called the separatrix surface. It is separating the different gauge sectors. If we start out with a configuration on the separatrix, then as time evolves it will almost definitely go to a gauge sector and stay there for a while, according to the projection of its momenta on the normal to the surface. The rate of going from one gauge sector to another, can therefore be calculated from the probability flux through the separatrix. In this section we use a semiclassical method to calculate the probability flux.

First let us regard the case of a system with only one degree of freedom, and a quantum particles in a double well, see figure 4.3. The doublewell is an approximation to the periodic energy barrier in the Chern-Simons number, where we only consider one barrier (see figure 1.1). Supposing that we start with a set of particles in thermal equilibrium in the left vacuum. The rate of passing over the barrier is then given by the probability of being at the barrier and having the right direction times the rate at which the barrier is

[1]The steepest descent equations are imagined to be integrated with infinite precision

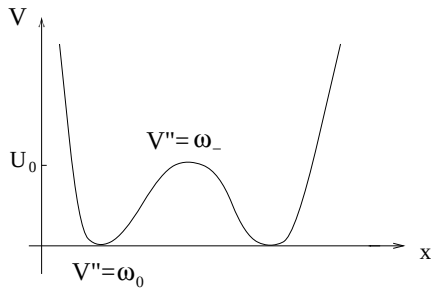

Figure 4.3: Double well

crossed,

$$, = \langle \delta(x_o) p\Theta(p) \rangle \tag{4.22}$$

$$= \frac{\int dpdx \frac{1}{2\pi\hbar} e^{-\beta[\frac{1}{2}p^2+V(x)]} \delta(x_0) p\Theta(p)}{\int dpdx \frac{1}{2\pi\hbar} e^{-\beta[\frac{1}{2}p^2+V(x)]}} . \tag{4.23}$$

Assuming a gaussian form for the potential $V(x) = \frac{1}{2}\omega_0^2 x^2$ around the vacuum, and performing the gaussian integrals we get

$$, = \frac{\omega_o}{2\pi} e^{-\beta U_0} , \tag{4.24}$$

where $V(x_o) = U_0$ is the height of the barrier. This is related to the imaginary part of the free energy. We have the free energy

$$F = T \ln Z , \tag{4.25}$$

where Z is the partition function, and it will pick up a small imaginary part from the contribution of the negative mode. We may write

$$\mathrm{Im}F \approx T \frac{\mathrm{Im}Z_{\mathrm{barrier}}}{Z_0} = T \frac{\int dpdx e^{\frac{1}{2}p^2 - \frac{1}{2}\omega_-^2 x_-^2 + U_0}}{\int dpdx e^{\frac{1}{2}p^2 + \frac{1}{2}\omega_0^2 x^2}} = \frac{\omega_0 T}{2\omega_-} e^{-\beta U_0} , \tag{4.26}$$

where Z_0 is the partition function around the left vacuum. The rate is then

$$, = \frac{\omega_- \beta}{\pi} \mathrm{Im}F = \frac{\omega_-}{\pi} \frac{\mathrm{Im}Z_{\mathrm{barrier}}}{Z_0} . \tag{4.27}$$

Adding more dimensions, the free energy changes as

$$\frac{\int dp_i dx_i \exp(\Leftrightarrow\beta(\frac{1}{2}p_i^2 + \frac{1}{2}\omega_i^2 x_i^2))}{\int dp_i dx_i \exp(\Leftrightarrow\beta(\frac{1}{2}p_i^2 + \frac{1}{2}\omega_{i0}^2 x_i^2))} = \frac{\omega_{i0}}{\omega_i} , \tag{4.28}$$

but the same factor will appear in the expression for the rate , . Hence formula 4.27 can be generalized to field theories. The top of the barrier in our case is represented by the sphaleron, giving

$$, = \frac{\omega_-}{\pi} \frac{\mathrm{Im}Z_{sph}}{Z_0} . \tag{4.29}$$

The rate is therefore given in terms of the partition function around the sphaleron in a gaussian approximation, and of the vacuum partition function.

At high temperature the theory becomes effectively three dimensional. The Euclidean action for the $SU(2)$ Higgs model reads

$$S_E = \int_0^\beta dt \int d^3x \mathcal{L}_E = \int_0^\beta dt \int d^3x (\tfrac{1}{4} F^a_{\mu\nu} F^a_{\mu\nu} + (D_\mu \Phi)^\dagger (D_\mu \Phi) + \lambda (\Phi^\dagger \Phi \Leftrightarrow \frac{v^2}{\sqrt{2}})^2 \ . \quad (4.30)$$

In the high temperature limit $\beta \ll 1$ the integration limit β is very close to zero and the fields can be considered time independent. The integration simply gives a multiplication with β and when scaling the field and coordinate

$$x_\mu \to x_\mu M_W \ , \quad A^a_\mu \to \frac{M_W}{g} A^a_\mu \ , \quad \Phi \to \frac{v}{\sqrt{2}} \Phi \ , \quad (4.31)$$

the three dimensional action becomes

$$S_3 = \frac{\beta M_W(T)}{g^2} \int d^3x (\tfrac{1}{4} F^a_{\mu\nu} F^a_{\mu\nu} + 2 (D_\mu \Phi)^\dagger (D_\mu \Phi) + \tfrac{1}{2} \epsilon^2 (\Phi^\dagger \Phi \Leftrightarrow 1)^2) \ , \quad (4.32)$$

where $\epsilon = \frac{M_H}{M_W} = \frac{2\sqrt{2\lambda}}{g}$. The masses are temperature dependent and this can be taken into account by changing the Higgs expectation value, to its temperature dependent form

$$v(T) = v(0) \left(1 \Leftrightarrow \frac{T^2}{T_c^2} \right)^{\frac{1}{2}} \ , \quad (4.33)$$

which gives a sphaleron energy of the form of equation 4.15. The effective three dimensional coupling constant g_3 is related to the four dimensional one through

$$g_3^2 = \frac{g^2}{\beta M_W(T)} \ . \quad (4.34)$$

For temperatures $T \ll M_W(T)/\alpha$ an expansion in g_3 should be reliable. But also the lower limit $T \gg M_W$ should be imposed in order to justify the three dimensional theory.

Again, we approximating the Lagrangian with a gaussian form around the sphaleron

$$\mathcal{L}_3^{sph} = \mathcal{L}_{3,sph} + (\delta\phi)^\dagger \Omega_{sph} (\delta\phi) \quad (4.35)$$

where ϕ generally denotes the gauge and Higgs fields, and Ω_{sph} is the operator for small fluctuations, defined as the second functional derivative of the action around the sphaleron. We do the same around the vacuum

$$\mathcal{L}_3^0 = (\delta\phi)^\dagger \Omega_0 (\delta\phi) \ . \quad (4.36)$$

Assuming no zero modes we therefore get the following formula,

$$\Gamma \ , \ \simeq \frac{\omega_0}{\pi} \mathrm{Im} \left(\frac{\det \Omega_0^2}{\det \Omega_{sph}^2} \right)^{\frac{1}{2}} e^{-\beta E_{sph}} \quad (4.37)$$

The sphaleron, though, has zero modes, arising from the symmetries of the solution. The sphaleron is translational and rotational invariant, giving rise to 6 zero modes. The integration of the zero modes gives

$$NV = V \prod \left(\frac{1}{2\pi\hbar} \int d^3x (\delta\phi)^2 \right)^{\frac{1}{2}} \ , \tag{4.38}$$

where N is a normalisation factor and V is a factor proportional to the volume of the symmetry group. Since the factors of g^{-2} no longer cancel in the determinants, we get

$$, \ \simeq \frac{\omega_-}{2\pi} (N_{rot} V_{rot}) (N_{tr} V_{tr}) g_3^{-6} \mathrm{Im} \left(\frac{\det \Omega_o^2}{\det{}' \Omega_{sph}^2} \right)^{\frac{1}{2}} e^{-\beta E_{sph}} \tag{4.39}$$

when including the zero modes. The prime on the determinant denotes that the zero modes should be excluded. Further more $V_{tr} = V M_W^3$ when going back to dimensionfull quantities, therefore

$$, \ \simeq \frac{\omega_-}{2\pi} (N_{rot} V_{rot}) N_{tr} V M_W^6 (g^2 T)^{-3} \kappa e^{-\beta E_{sph}} \ , \tag{4.40}$$

where κ is the ratio of the determinants. The zero mode integration factor can be estimated using the sphaleron solution. In [27] the values $N_{tr} = 26$, and $N_{rot} V_{rot} = 5.3 \times 10^3$ was obtained from the integration inserting the sphaleron solution.

In these calculations a number of approximation has been done, and the expression for the rate cannot be trusted near the critical temperature. The main assumption of the calculation is that the dominant contribution to the baryon violation processes passes through configuration in the neighbourhood of the sphaleron. At high temperature the dominating configuration is not necessarily the sphaleron, even though it has the least energy. The size of the sphaleron, being $\sim M_W^{-1}$, is diverging when approaching the critical temperature if we have a second order phase transition. But also for a first order transition will the size of the sphaleron be large, close to the transition. Thermal fluctuations with size $\approx T^{-1}$, might be favoured, having a much smaller size. We see that in this case the energy of the Higgs field can be neglected, since scaling the sphaleron down to a small size will course the energy term involving the Higgs field to decrease rapidly, see equation 2.10. This will put an upper limit on the valid temperature range for the calculation. The gaussian approximation is no longer valid and we have to consider interactions as well. We might also expect a damping effect from the plasma that exists at high temperatures.

4.6 Dilution of the baryon number

So far we have neglected the fermions. Including the fermions, the baryon violating processes will tend to erase any baryonic or antibaryonic excess. The free energy of the fermions created in the transition between the vacuum sectors, will cause the effective potential to raise (see figure 4.4). In the case of a baryonic or leptonic excess, the rates in the the two directions are no longer equal. The excess is described by chemical potentials μ_B for the baryons and μ_L for the leptons. The effective action is modified by

$$\delta S = \Leftrightarrow \beta (\mu_B + \mu_L) N_F N_{CS} \ , \tag{4.41}$$

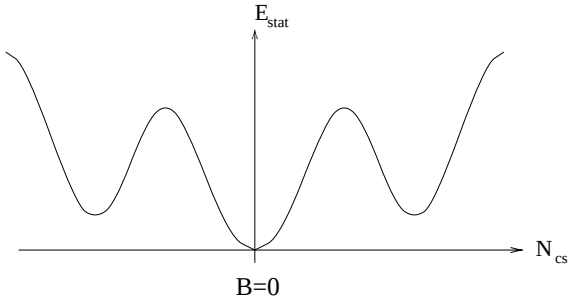

Figure 4.4: The effective potential between the different vacuum sectors when including fermions.

The sphaleron has $N_{CS} = \frac{1}{2}$, as shown in section 2.4. The baryonic increasing/decreasing processes pick up a factor

$$\exp(\pm\beta\frac{N_f}{2}(\mu_B + \mu_L)) \tag{4.42}$$

The difference between the rates, in the case where $\mu/T \ll 1$, is

$$\beta N_f(\mu_B + \mu_L), \quad . \tag{4.43}$$

Each transition changes the baryon number with N_f, so we get the following relation between the baryon number B and the rate , ,

$$\frac{dB}{dt} = \Leftrightarrow\!\!\!\!\!\!\not\beta N_f^2(\mu_B + \mu_L), \tag{4.44}$$

and the chemical potential can be obtained from standard statistical physics [27]

$$\mu_B \simeq \frac{9}{2N_f}\beta^2\frac{B}{V} \ , \qquad \mu_L \simeq \frac{2}{N_f}\beta^2\frac{L}{V} \ . \tag{4.45}$$

Supposing that we have $B \Leftrightarrow L = 0$, then

$$\frac{dB}{dt} = \Leftrightarrow\!\!\!\!\!\!\not\beta^3 N_f\frac{13}{2}\frac{B}{V}, \quad . \tag{4.46}$$

The rate should be compared to expansion rate of the Universe

$$\tau_U^{-1} = 1.66 N_{eff}^{\frac{1}{2}} T^2/M_{pl} \ , \tag{4.47}$$

where M_{pl} is the Planck mass and N_{eff} is the effective number of massless degrees of freedom. If the rate is higher than the expansion rate of the Universe, then the baryon violating processes will be in thermal equilibrium. Baryon violating processes in equilibrium, will equalize the number of baryons and antibaryons. Therefore any asymmetry created in an earlier stage of the Universe would be washed out. We will now consider when, in the cosmological evolution, the baryon violating processes are in equilibrium.

4.7 The rate in the symmetric phase

In the symmetric phase, where the vector bosons are massless, the sphaleron solution does not exist and there is no barrier between the vacua. Due to the infrared divergences it is not possible to do perturbative analytic calculations. The interactions are strongly coupled at small momenta. But in turn we might justify a classical treatment of the baryon violation rate in this phase, for very high temperatures.

To get an idea of the form of the rate at temperature $T > T_c$, the instanton solution at $x_4 = 0$ can be helpful [29, 27],

$$\Phi = 0 \ , \qquad A_i^a = \frac{\epsilon_{ija} x_j}{\vec{x}^2 + \lambda^2} \ , \tag{4.48}$$

where λ is the size of this configuration and its energy the maximum of the instanton energy, $E_{max} \propto \frac{1}{\alpha\lambda}$. This configuration shares a lot of properties with the sphaleron. It is a saddle point of the energy functional, it has one negative mode and it has half integer topological charge. Since this solution is indeed sphaleron-like, we calculate the transitions rate like before, but in addition we must perform integration over the size λ. The rate is estimated by assuming a gaussian form of the Lagrangian. The solution is independent of Euclidean time and we get the three dimensional action

$$S_3 = \frac{\beta}{g^2 \lambda} \int d\xi \mathcal{L}_3(\xi) \ , \qquad \xi = x\lambda \ . \tag{4.49}$$

The sphaleron-like solution has 6 zero modes, but in addition we get another factor of $\frac{\beta}{g^2\lambda}$ in the ratio of the two determinants, since we do not perform a gaussian integration in the λ direction. The rate then reads

$$, \ = \int \frac{d\lambda}{\lambda} \frac{\omega_-}{2\pi} \left(\frac{1}{g^2 T \lambda} \right)^{\frac{7}{2}} \kappa (N_{rot} V_{rot}) (\lambda^{-3} V) N_{tr} e^{-\beta E_{max}} \ . \tag{4.50}$$

The negative mode will have $\omega_- \approx \frac{1}{\lambda}$, and hence

$$\begin{aligned} , \quad &\propto \quad \kappa N_{tr} (N_{rot} V_{rot}) V \ (T\alpha)^4 \int \frac{d\lambda}{\lambda} e^{-\frac{1}{T\lambda\alpha}} \left(\frac{1}{\alpha T \lambda} \right)^{\frac{15}{2}} \\ &= \quad \kappa N_{tr} (N_{rot} V_{rot}) V \ (T\alpha)^4 \int dz e^{-z} z^{\frac{13}{2}} \ , \qquad z = \frac{1}{\lambda \alpha T} \\ &= \quad \kappa N_{tr} (N_{rot} V_{rot}) V \ (T\alpha)^4, \ (\tfrac{15}{2}) \ . \end{aligned} \tag{4.51}$$

The rate get the form

$$\frac{,}{V} = \kappa (\alpha T)^4 \ , \tag{4.52}$$

where the constant factors have been absorbed into κ. This form can be obtained by scaling arguments [28], and it is not just a property of the special solution 4.48. A priori, the numerical value of κ may be so small that fermion number is to a good extend conserved in the symmetric phase. However, a number of simulations of the classical theory suggest that κ is of order 1. This would imply, with the use of equation 4.46 and 4.47, that for temperatures

$$T_c < T < 0.1 M_{pl} \alpha^4 \simeq 10^{12} \text{GeV} \tag{4.53}$$

the electroweak baryon violating processes are in thermal equilibrium, and any excess of baryon or antibaryons will be erased. But can the classical rate be trusted?

We may argue that the dominant transitions can be treated classically. In the non-Abelian theories it is possible to have magnetic screening effects, where a magnetic mass is dynamically generated for the spatial gauge fields. However, it is not possible to calculated such a magnetic mass within perturbation theory, since there will be equal contribution from all orders. It is expected that non-perturbative effects will somehow "heal" the theory by creating a magnetic mass of order $m_{mag} \simeq \alpha T$ [38, 48]. The form can be induced from purely dimensional arguments, since αT is the only relevant scale at low momenta. Lattice simulations in [31] shows that $m_{mag} = 0.47 g^2 T$. This is in very good agreement with simulations of the dimensionally reduced 3D theory [42]. The magnetic mass was found to be constant in the symmetric phase, where $m_H = 80$ GeV was used, which shows that it can be calculated from a pure Yang-Mills theory.

Topological transitions of the gauge fields are believed to be dominated by fields with a typical size $\sim \frac{1}{\alpha T}$. Generally, a configuration having size r will pass an energy barrier of magnitude $E = 1/\alpha r$ and large r will be energetically favoured. It is unlikely, though, that the size of the fields exceeds the inverse of the magnetic mass. We then expect the dominant contribution to come from configurations with size m_{mag}^{-1}. The magnetic mass will again provide a barrier between the different gauge vacuum sectors. The associated Boltzmann suppression factor $e^{-\beta E_s}$, where E_s is the energy of a sphaleron-like configuration in the symmetric phase, is temperature independent, due to the linear dependence of the magnetic mass on the temperature. Since the relevant modes $p = \alpha T$ has a high occupation number, classically being $\frac{T}{E} = \frac{1}{\alpha}$, the rate can be well determined with a classical treatment.

Another indication of the relevance of the classical theory is seen by comparing the effective action for the classical theory and the dimensionally reduced theory, see equation 4.14. It is believed that the leading quantum effects on the rate, can be obtained by using the temperature dependent coupling constants.

4.8 Real time simulations

We see that in the symmetric phase a simplification to the classical theory is reasonable. Unfortunately the classical theory suffers from ultraviolet Raleigh-Jeans divergences, which might turn up in the calculation of the rate. Discretizing space-time by putting the system on a lattice, provide an ultraviolet cutoff $1/a$, where a is the lattice spacing. A natural thing is therefore to do lattice gauge theory simulations of the classical theory, in order to obtain the baryon violation rate. Hopefully κ will not be dependent on the cutoff, otherwise more complicated methods would have to be implemented. It was suggested [36] to integrate out the hard momentum loops and obtain an effective Hamiltonian for small momenta, so as to take properly into account the high momenta modes.

The main idea of the simulation for obtaining κ numerically, is the determination of the time evolution of the topological charge. We know that transitions having $Q(t) = 1$ will be accompanied by baryon violation. But $Q(t)$ will consist of both thermal fluctuations around the vacuum states, that will not give rise to a baryon violation, and an evolution between the different gauge sectors increasing $Q(t)$ by an integer amount. For large t fluctuations not contributing to fermion violations are neglectible in the mean square of

the topological charge. The fields are expected to perform a random walk in the periodic potential and, for large t, we may write

$$\langle (Q(t))^2 \rangle_T \simeq , \, Vt \, , \tag{4.54}$$

where , is the diffusion rate per unit volume. The topological charge is averaged over a classical thermal distributed set of gauge field configurations,

$$\langle (Q(t))^2 \rangle_T = \frac{\int \mathcal{D}A_i e^{-H\beta} Q^2(t)}{\int \mathcal{D}A_i e^{-H\beta}} \, . \tag{4.55}$$

The first micro canonical real time simulations was done of the $SU(2)$ Higgs model in [33]. A configuration consisting of the gauge fields A_i and ϕ, and their canonical conjugate momenta $\frac{dA_i}{dt} = \Pi_i$ and $\frac{d\phi}{dt} = \pi$, was simulated on a lattice. The Hamiltonian in temporal gauge is

$$H = \frac{1}{2} E_i^a E_i^a + \frac{1}{4} F_{ij}^a F_{ij}^a + \pi^2 + D_i \phi^2 + M^2 \phi^2 + \lambda \phi^4 \tag{4.56}$$

The fields are evolved according to the canonical equations of motion. In addition the Gauss constraint, arising from variations with respect to A_0

$$\partial_i E_i^a \Leftrightarrow 2\epsilon^{abc} A_i^b E_i^c = i(\phi^\dagger \sigma^a \pi \Leftrightarrow \pi^\dagger \sigma^a \phi) \, , \tag{4.57}$$

has to be imposed. Since the Gauss constraint commutes with the Hamiltonian, all configurations obtained by classical evolution of the field equations will satisfy the constraint, if the initial configuration does. The set of initial configurations should be created in such a way that they respects the Gauss constraint and further are distributed in accordance with the Gibbs distribution $e^{-H/T}$. This was obtained by the using the standard Monte Carlo technique, where the configurations are updated with the Metropolis algorithm, with a Gauss constraint multiplier added to the Hamiltonian. The Gauss constrained was therefore only for filled to some accuracy, and was a source of uncertainty. The topological charge can be obtained as a function of the discrete time, by calculating the Chern-Simons number, as described in section 3.5. It was found that $Q(t)$ lays in plateaus for a while and then makes rapid transitions to a new plateau. Since, as mentioned in section 3.5, the Chern-Simons number is not a total time derivative on the lattice, the jumps in $Q(t)$ is not exactly giving by an integer number. But the simulations clearly showed that there are transitions between the different vacuum sectors. The simulations was in fine agreement with the random walk picture. The value of κ was extracted using formula 4.52. Due to the noisy data, it was not possible to obtain a continuum limit. However a value $\kappa > 0.4$ was indicated.

The need for a large lattice size, in order to fit the sphaleron in the broken phase, makes it difficult to do simulations in this phase, and compare with the existing analytical calculations. The abelian $U(1)$ Higgs model in 1+1 dimension, has the same quantitative features as the $SU(2)$ Higgs model, with a periodic vacuum structure and fermion violation. Here the numerical simulation have been performed and are in good agreement with analytic calculations of the rate from sphaleron transitions, performed in the same way as described in section 4.5. Naively one would expect the same to be found for the $SU(2)$ Higgs theory.

Ambjørn and Krasnitz [34] has recently obtained the value of κ in the pure $SU(2)$ theory, again by simulations of the classical theory. The Gauss constrain now reads

$$\partial_i E_i^a \Leftrightarrow 2\epsilon^{abc} A_i^b E_i^c = 0 \tag{4.58}$$

The initial set of fields were thermalized by a Langevin set of equation [35], obeying the Gauss constrain exactly. The rate fitted the form 4.52 well and κ was found to be independent of the lattice spacing for sufficiently small values, which indicated that the finite continuum limit was reached. Further finite size effects was eliminated. Let N denote the number of lattice site in one direction. When $\frac{N}{\beta}$, exceeded twice the magnetic mass, κ was found to be independent of this ratio, which fits well with the idea of the dominant contribution coming for configurations with size $\approx m_{mag}$. These are strong arguments for the reliability of the value, and it was numerically given by

$$\kappa = 1.09 \pm 0.04 \tag{4.59}$$

At very high temperature $T \gg T_c$ the scalar field decouples, having a thermal mass $\approx gT$, much greater than g^2T, justifying a pure Yang-Mills theory in this limit. It is therefore well established that the topological transitions are fast enough to wash out any baryonic excess in the symmetric phase.

In ref. [37] the diffusion rate was calculated in the $SU(2)$ Higgs model, by using an effective classical Hamiltonian, where the parameters was determined by comparison with dimensional reduction. The results was in agreement with the value found in [34] for the pure $SU(2)$ theory, in the symmetric phase. A value of $M_H = M_W$ was used. In the broken phase it was found that the rate only decreased a factor 5, which is a factor of 650 higher than the existing analytic calculations, as described in section 4.5. The rate was not found to be dependent on the lattice spacing. The sphaleron energy enters exponentially in the transition rate, and since it is decreasing with the coarseness of the lattice, a coarse lattice would tend to make the rate higher. The question is whether this can explain the discrepancy. From the lattice artifacts of the sphaleron energy in [19], a factor of less than 2 of systematic error in the value of κ is indicated. The large factor between the analytic result calculated from the sphaleron transitions, and the results from the computer simulations cannot be explained by the lattice artifacts of the sphaleron. But since the dimensional reduction is not a good approximation in the broken phase, because the temperature is low in this phase, the validity of the method is unclear. Furthermore dimensional reduction is what indicates that the quantum rate is well approximated by the classical one. The authors stated other sources of uncertainty. A finite renormalization factor was neglected, and this might give a substantial correction. It definitely needs some clarification, before the result in [37] can be trusted. If these results are to be trusted, the baryon violation rate get a significant contribution by non-sphaleron processes, causing the rate to be high enough, even in the broken phase, to eliminate a surplus of baryons. This would force a plausible scenario to take place later than the electroweak phase transition, or by $B + L$ violation at an earlier stage.

4.9 Bounds on the Higgs mass

In order that a BAU created at the EPT is kept till now, it is necessary that the baryon violation rate by sphaleron transitions after the phase transition is sufficiently low. This can give us a bound on the Higgs mass. Experimentally the lower bound for the Higgs mass is currently $m_H > 65$ GeV.

We saw in section 4.5, that the suppression factor after the EPT is proportional to $e^{-\beta E_{sph}}$. The sphaleron energy given by formula 4.15 will increase for a larger vacuum

expectation value of the Higgs field, and we understand that a high v is needed after the phase transition. This is equivalent to a strong phase transition, since a high barrier will keep the Higgs field in the false vacuum for a long time, and the expectation value of Higgs field increases with decreasing temperature. The transition to the true vacuum will take place close to the temperature T_- where the barrier disappears. However, the energy, gained from the transition to the true vacuum will reheat the system, and these effects will have to be included when the temperature T^* right after the phase transition is estimated.

Requirering that the sphaleron transitions decouples, by going out of thermal equilibrium, right after the transitions Shaposhnikov derived bound

$$\frac{E_{sph}(T^*)}{T^*} > 45 \ , \tag{4.60}$$

which has to be satisfied for a BAU to survive till now. This is found by using equation 4.40 and 4.47. The inequality is not satisfied for the minimal standard model. The simulation of the EPT for the dimensionally reduced theory by Shaposhnikov et. al., shows that the EPT for the minimal standard model is not strong enough to generate the observed BAU, for any value of the Higgs mass [3]. The fact that the minimal standard model cannot explain the observed asymmetry has been established for some time, since the bound on the Higgs mass was already in disagreement with experiments.

This turn us to search for extensions of the standard model, where a stronger phase transition is possible. Both the two-Higgs model and some supersymmetric models have an area of parameter space, where this is realized.

Conclusion

From the study of electroweak baryogenesis it is nowadays believed, that the minimal standard model is not capable of explaining the observed baryon asymmetry of the Universe. The bounds on the Higgs mass from demanding the sphaleron transition rate to be turned off after the phase transition, cannot be satisfied in the minimal standard model. The baryon violation rate for the electroweak processes in the symmetric phase, at least for temperatures far above the critical temperature, is well established to be so high that it will wash out any preexisting asymmetry. The rate in the broken phase is mainly determined by the sphaleron energy, but the numerical value of the rate is still to be obtained by real time simulations. Extended models, like the two Higgs doublet theory, can give an upper bound on the lowest Higgs mass, within the experimental limit.

The remaining possibilities for explaining the observed baryon asymmetry, is therefore including extensions of the standard model where electroweak baryogenesis is used, and a GUT model where $B + L$ violating processes are present.

Acknowledgements

I would like to thank my supervisor J. Ambjørn for various discussions and advise. I am grateful to A. Krasnitz for providing me with the computer code used for the simulations, and for many enlightening conversations. Furthermore I would like to thank Sune and Alberto for reading through and commenting on the manuscript.

Appendix A

A.1 Energy of the sphaleron

The energy is given by

$$E = \int d^3x \tfrac{1}{4} F_{ij}^{\alpha} F_{ij}^{\alpha} + (D_i\Phi)^{\dagger}(D_i\Phi) + \lambda(\Phi^{\dagger}\Phi \Leftrightarrow \frac{v^2}{2}) \ . \tag{A.1}$$

We want to show that for these ansätze 2.22 and 2.23 the energy density is spherical symmetric. Starting with the pure gauge field contributions. The expressions for the field strength tensor is to long to be quoted, and only the final energy density is written

$$\begin{aligned} \mathcal{E}(A) &= \Leftrightarrow \frac{1}{2g^2} \mathrm{Tr}(F_{ij}F_{ij}) \\ &= \Leftrightarrow \frac{1}{2g^2}(\Leftrightarrow \frac{8}{r^4})\Big(2[f(1 \Leftrightarrow f)]^2 + 2yz\partial_z f \partial_y f + 2xz\partial_x f \partial_z f + 2xy\partial_y f \partial_x f \\ &\quad + x^2(\partial_x f)^2 + y^2(\partial_y f)^2 + z^2(\partial_z f)^2\Big) \\ &= \frac{4}{r^4 g^2}([2f(1 \Leftrightarrow f)]^2 + r^2(\frac{df}{dr})^2) \ . \end{aligned} \tag{A.2}$$

Changing to $\xi = gvr$ we obtain

$$\int \mathcal{E}(r) d^3x = \int \mathcal{E}(r) 4\pi r^2 dr = \int \frac{16\pi v}{\xi^2 g}(2[f(1 \Leftrightarrow f)]^2 + \xi^2(\frac{df}{d\xi})^2) d\xi \ , \tag{A.3}$$

which is the first two terms in formula 2.25. The covariant derivative term gives rise to the contribution to the energy density

$$\mathcal{E}(\Phi, A) = \frac{v^2}{r^2}([h(1 \Leftrightarrow f)]^2 + \tfrac{1}{2} r^2(\frac{dh}{dr})^2) \tag{A.4}$$

and we get

$$\int \mathcal{E}(r) d^3x = \int \frac{4\pi v}{g}([h(1 \Leftrightarrow f)]^2 + \tfrac{1}{2}\xi^2(\frac{dh}{d\xi})^2) d\xi \ , \tag{A.5}$$

which is the next two term in the energy. The potential energy term for the Higgs field is easily seen to give

$$\mathcal{E} = \lambda(\frac{v^2}{2}h^2 \Leftrightarrow \frac{v^2}{2})^2 = \frac{v^4}{\lambda}(h^2 \Leftrightarrow 1)^2 \tag{A.6}$$

and we see that the last term in equation 2.25 is obtained.

A.2 Topological charge of sphaleron

The topological charge, given by

$$Q = \Leftrightarrow\frac{g^2}{16\pi^2}\int d^3x\epsilon_{ijk}\left(A_i^a\partial_j A_k^a + \frac{1}{3}g\epsilon_{abc}A_i^a A_j^b A_k^c\right) , \tag{A.7}$$

is calculated for the sphaleron configuration

$$A_i^a = A(r)\epsilon_{iae}\hat{x}_e + B(r)(\delta_{ia}\Leftrightarrow\hat{x}_i\hat{x}_a) + C(r)\hat{x}_i\hat{x}_a , \tag{A.8}$$

where

$$A(r) = \frac{[1\Leftrightarrow 2f(gvr)]\cos\Theta(r)\Leftrightarrow 1}{gr} , \tag{A.9}$$

$$B(r) = \frac{[1\Leftrightarrow 2f(gvr)]\sin\Theta(r)}{gr} , \tag{A.10}$$

$$C(r) = \frac{1}{g}\frac{d\Theta}{dr} . \tag{A.11}$$

First we will evaluate the term

$$\epsilon_{ijk}A_i^a\partial_j A_k^a . \tag{A.12}$$

Using $\partial_j\hat{x}_k = \frac{1}{r}(\delta_{jk}\Leftrightarrow\hat{x}_i\hat{x}_k)$ we get

$$\begin{aligned}\partial_j A_k^a &= (\partial_j A)\epsilon_{kad}\hat{x}_d + (\partial_j B)(\delta_{ka}\Leftrightarrow\hat{x}_k\hat{x}_a) + (\partial_j C)\hat{x}_k\hat{x}_a \\ &+ \frac{A}{r}\epsilon_{kad}(\delta_{jd}\Leftrightarrow\hat{x}_j\hat{x}_d) + \frac{C\Leftrightarrow B}{r}[(\delta_{jk}\Leftrightarrow\hat{x}_k\hat{x}_i)\hat{x}_a + (\delta_{ja}\Leftrightarrow\hat{x}_j\hat{x}_a)\hat{x}_k] .\end{aligned} \tag{A.13}$$

However when contracting with $\epsilon_{ijk}A_i^a$ a lot of the term gives zero. For instance we get for the term with $(\partial_j A)$

$$\epsilon_{ijk}A_i^a(\partial_j A)\epsilon_{kad}\hat{x}_d = (\partial_j A)A_i^a(\delta_{ia}\delta_{jd}\Leftrightarrow\delta_{id}\delta_{ja})\hat{x}_d = (\partial_j A)A_i^a(\delta_{ia}\hat{x}_j\Leftrightarrow\delta_{ja}\hat{x}_i) . \tag{A.14}$$

But we have

$$(\delta_{ia}\hat{x}_j\Leftrightarrow\delta_{ja}\hat{x}_i)\epsilon_{iae}\hat{x}_e = \Leftrightarrow\epsilon_{ije}\hat{x}_i\hat{x}_e = 0 , \tag{A.15}$$

since ϵ_{ije} is antisymmetric in i and e and $\hat{x}_i\hat{x}_e$ is symmetric. There will be no contribution from the A term in A_i^a. Further

$$(\delta_{ia}\hat{x}_j\Leftrightarrow\delta_{ja}\hat{x}_i)\hat{x}_i\hat{x}_a = (\hat{x}_j\Leftrightarrow\hat{x}_j) = 0 \tag{A.16}$$

$$(\delta_{ia}\hat{x}_j\Leftrightarrow\delta_{ja}\hat{x}_i)\delta_{ia} = 3\hat{x}_j\Leftrightarrow\hat{x}_j = 2\hat{x}_j , \tag{A.17}$$

and we get the contribution $2x_j B(\partial_j A)$.

The term with $(\partial_j B)$ is non-zero only for the A term in A_i^a

$$\epsilon_{ijk}A\epsilon_{iae}\hat{x}_e(\partial_j B)\delta_{ka} = A(\partial_j B)\epsilon_{ija}\epsilon_{iae}\hat{x}_e \tag{A.18}$$

$$= A(\partial_j B)(\Leftrightarrow 2)\delta_{je}\hat{x}_e = \Leftrightarrow 2\hat{x}_j A(\partial_j B) . \tag{A.19}$$

The term with $(\partial_j C)$ is easily seen to give zero, since the structure in the $\hat{x}$'s is always symmetric in some indices, and contracted with the ϵ symbol this gives zero.

Now the term with $\frac{A}{r}$, we get

$$\epsilon_{ijk}A_i^a\frac{A}{r}\epsilon_{kad}(\delta_{jd}\Leftrightarrow\hat{x}_j\hat{x}_d) = A_i^a\frac{A}{r}(\delta_{ia}\delta_{jd}\Leftrightarrow\delta_{id}\delta_{ja})(\delta_{jd}\Leftrightarrow\hat{x}_j\hat{x}_d) \quad (A.20)$$

$$= A_i^a\frac{A}{r}(3\delta_{ia}\Leftrightarrow\delta_{ia}(\hat{x})^2\Leftrightarrow\delta_{ia}+\hat{x}_a\hat{x}_i) \quad (A.21)$$

$$= A_i^a\frac{A}{r}(\delta_{ia}+\hat{x}_a\hat{x}_i)\ . \quad (A.22)$$

We have

$$(\delta_{ia}+\hat{x}_a\hat{x}_i)\ \epsilon_{iae}\hat{x}_e = 0 \quad (A.23)$$

$$(\delta_{ia}+\hat{x}_a\hat{x}_i)\ \hat{x}_a\hat{x}_i = 2 \quad (A.24)$$

$$(\delta_{ia}+\hat{x}_a\hat{x}_i)\ \delta_{ai} = 4\ , \quad (A.25)$$

given a contribution $2\frac{A}{r}(C+B)$.

The term with $\frac{C-B}{r}$ gives a similar result. Noting that $\epsilon_{ijk}(\delta_{jk}\Leftrightarrow\hat{x}_k\hat{x}_i)\hat{x}_a = 0$, we are left with

$$\epsilon_{ijk}A_i^a\frac{C\Leftrightarrow B}{r}(\delta_{ja}\Leftrightarrow\hat{x}_j\hat{x}_a)\hat{x}_k = A_i^a\frac{C\Leftrightarrow B}{r}\epsilon_{iak}\hat{x}_k\ , \quad (A.26)$$

and we have

$$\epsilon_{iak}\hat{x}_k\epsilon_{iae}\hat{x}_e = 2\hat{x}^2\ . \quad (A.27)$$

This gives us the contribution $2\frac{C-B}{r}A$. The rest of the term gives zero. In total we may therefore write

$$\epsilon_{ijk}A_i^a\partial_jA_k^a = 4\frac{AC}{r}+2\hat{x}_j[B(\partial_jA)\Leftrightarrow A(\partial_jB)] \quad (A.28)$$

$$= 4\frac{AC}{r}+2[B(\partial_rA)\Leftrightarrow A(\partial_rB)]\ , \quad (A.29)$$

since $\partial_jA(r) = \hat{x}_j\partial_rA(r)$ by the chain rule.

Now we will calculate the term

$$\epsilon_{ijk}\epsilon_{abc}A_i^aA_j^bA_k^c\ . \quad (A.30)$$

An investigation yields that all cubic terms vanish, and from the cross terms we get the following contributions. From the term with two A's and one C

$$\epsilon_{ijk}\epsilon_{abc}\epsilon_{iad}\hat{x}_d\epsilon_{jbe}\hat{x}_e\hat{x}_k\hat{x}_c = \epsilon_{ijk}\epsilon_{jbe}(\delta_{ic}\hat{x}_b\Leftrightarrow\delta_{ib}\hat{x}_c)\hat{x}_e\hat{x}_k\hat{x}_c \quad (A.31)$$

$$= (\delta_{ie}\delta_{kb}\Leftrightarrow\delta_{ib}\delta_{ke})(\delta_{ic}\hat{x}_b\Leftrightarrow\delta_{ib}\hat{x}_c)\hat{x}_e\hat{x}_k\hat{x}_c \quad (A.32)$$

$$= (\delta_{ce}\hat{x}_k+\delta_{ke}\hat{x}_c)\hat{x}_e\hat{x}_k\hat{x}_c = 2\ . \quad (A.33)$$

This will appear three times, so in total we get the contribution $6A^2C$. From the term with two B's and one C

$$\epsilon_{ijk}\epsilon_{abc}(\delta_{ia}\Leftrightarrow\hat{x}_i\hat{x}_a)(\delta_{jb}\Leftrightarrow\hat{x}_j\hat{x}_b)\hat{x}_k\hat{x}_c = \epsilon_{ijk}\epsilon_{abc}\delta_{ia}\delta_{jb}\hat{x}_k\hat{x}_c \quad (A.34)$$

$$= \epsilon_{abk}\epsilon_{abc}\hat{x}_k\hat{x}_c = 2\ . \quad (A.35)$$

Hence this give rise to $6B^2C$, and the final result yields

$$\epsilon_{ijk}\epsilon_{abc}A_i^aA_j^bA_k^c = 6(A^2+B^2)C\ . \quad (A.36)$$

Indeed we see that the topological charge density is spherical symmetric

$$Q = \Leftrightarrow\frac{g^2}{16\pi^2}\int 4\pi r^2 dr \left(6(A^2+B^2)C + 4\frac{AC}{r} + 2[B(\partial_r A) \Leftrightarrow A(\partial_r B)]\right) . \tag{A.37}$$

It it easily seen that g drops out, and by redefining the function $A \to gA$ and the same for B and C, we may write

$$(\partial_r A) = \frac{1}{r}\left(\Leftrightarrow 2f'\cos\Theta \Leftrightarrow (1\Leftrightarrow 2f)\sin\Theta\frac{d\Theta}{dr} \Leftrightarrow A\right) , \tag{A.38}$$

and

$$(\partial_r B) = \frac{1}{r}\left(\Leftrightarrow 2f'\sin\Theta + (1\Leftrightarrow 2f)\sin\Theta\frac{d\Theta}{dr} \Leftrightarrow B\right) . \tag{A.39}$$

We get

$$B(\partial_r A) \Leftrightarrow A(\partial_r B) = \frac{1}{r^2}\left(\Leftrightarrow 2f'\sin\Theta \Leftrightarrow (1\Leftrightarrow 2f)^2\frac{d\Theta}{dr} + (1\Leftrightarrow 2f)\cos\Theta\frac{d\Theta}{dr}\right) . \tag{A.40}$$

Further

$$(A^2+B^2)C = \frac{1}{r^2}\left((1\Leftrightarrow 2f)^2 + 1 \Leftrightarrow 2(1\Leftrightarrow 2f)\cos\Theta\right)\frac{d\Theta}{dr} , \tag{A.41}$$

and

$$\frac{AC}{r} = \frac{1}{r^2}\left((1\Leftrightarrow 2f)\cos\Theta \Leftrightarrow 1\right)\frac{d\Theta}{dr} . \tag{A.42}$$

The gives the following integrand

$$I = \frac{1}{r^2}\left(2(1\Leftrightarrow 2f)\cos\Theta\frac{d\Theta}{dr} \Leftrightarrow 2\frac{d\Theta}{dr} \Leftrightarrow 4f'\sin\Theta\right) , \tag{A.43}$$

and the topological charge reads

$$Q = \Leftrightarrow\frac{1}{4\pi}\int dr \left(2(1\Leftrightarrow 2f)\cos\Theta\frac{d\Theta}{dr} \Leftrightarrow 2\frac{d\Theta}{dr} \Leftrightarrow 4f'\sin\Theta\right) . \tag{A.44}$$

We have that $\Theta(\infty) = \pi$, $\Theta(0) = 0$, $f(0) = 0$ and $f(\infty) = 1$, hence by partial integrating the last term the surface term will vanish

$$\int dr(\Leftrightarrow 4f'\sin\Theta) = \Leftrightarrow 4[f\sin\Theta]_0^\infty + \int dr 4f(\sin\Theta)' = \int dr 4f\cos\theta\frac{d\Theta}{dr} . \tag{A.45}$$

The remaining integral cancels with the $f\cos\Theta$ term in A.44, hence

$$Q = \Leftrightarrow\frac{1}{4\pi}\int dr 2(\cos\Theta\Leftrightarrow 1)\frac{d\Theta}{dr} = \Leftrightarrow\frac{1}{2\pi}\left[\sin\Theta\Leftrightarrow\Theta\right]_0^\infty = \frac{1}{2\pi}\pi = \frac{1}{2} . \tag{A.46}$$

The topological charge of the sphaleron is a half integer.

Appendix B

Data

Data obtain from the program is shown in this appendix.

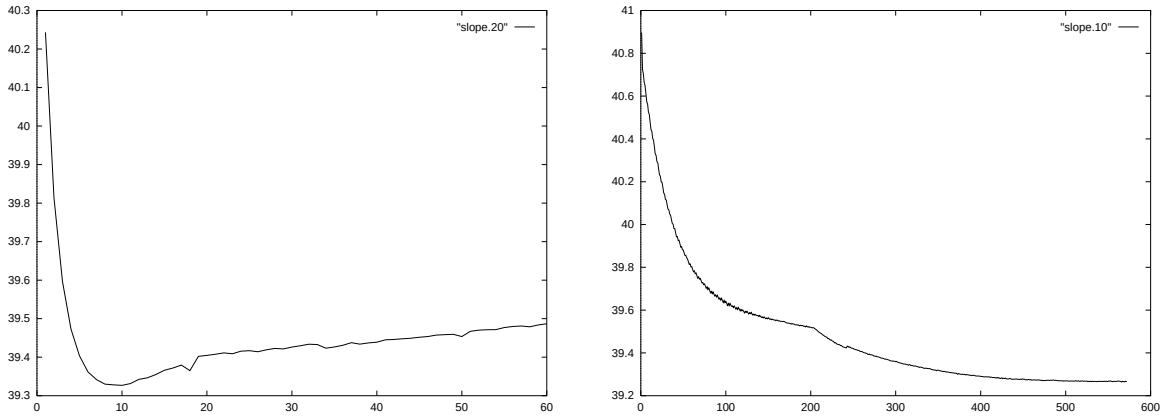

Figure B.1: The slope as a function of the cooling step . The left graph is for $N = 20$, $M_W = 1$ The right graph is for $N = 10$, $M_W = 1$. Here the change in the curve is due to change of the cooling step parameter in the program.

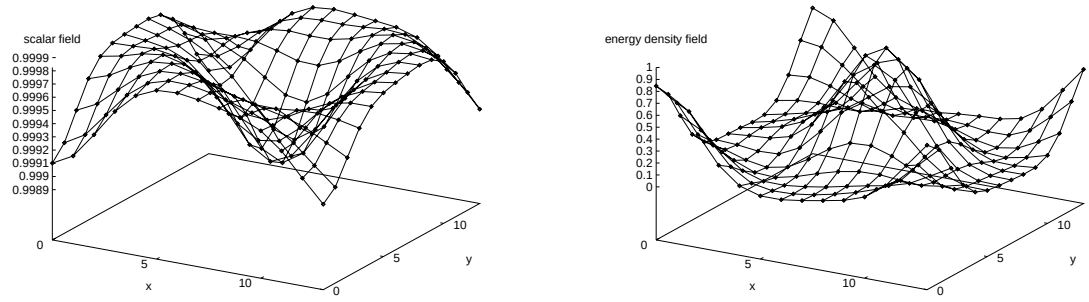

Figure B.2: A configuration with $N_{CS} \simeq 0.1$ for $L = 14$, $M_W = 1$ Left the normalized scalar field squared. Right the energy density.

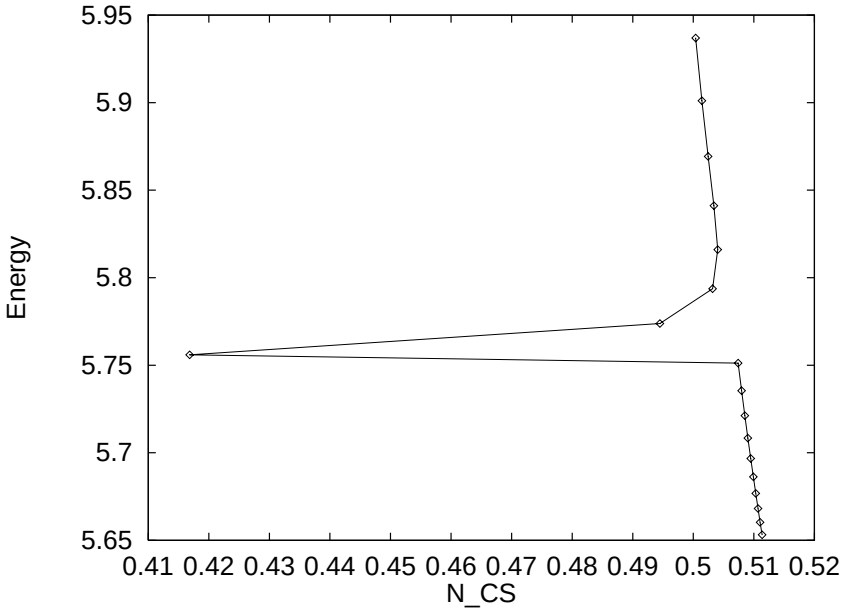

Figure B.3: The static energy as a function of N_{CS} during the constrained cooling. Around the sphaleron configuration the measurement of the Chern-Simons number is extremely difficult. The maximum step-size for the cooling algorithm is 7500, and still to low for a correct value of N_{CS}. For the point with $N_{CS} \simeq 0.415$, the cooling algorithm reaches a final configuration far from a vacuum state ($E_{stat} = 0.43$). Since N_{CS} goes outside the allowed region, going from $N_{CS} \simeq 0.415$ to $N_{CS} \simeq 0.517$ in the lower "nearly" horizontal line, guidance is used and not constrained cooling.

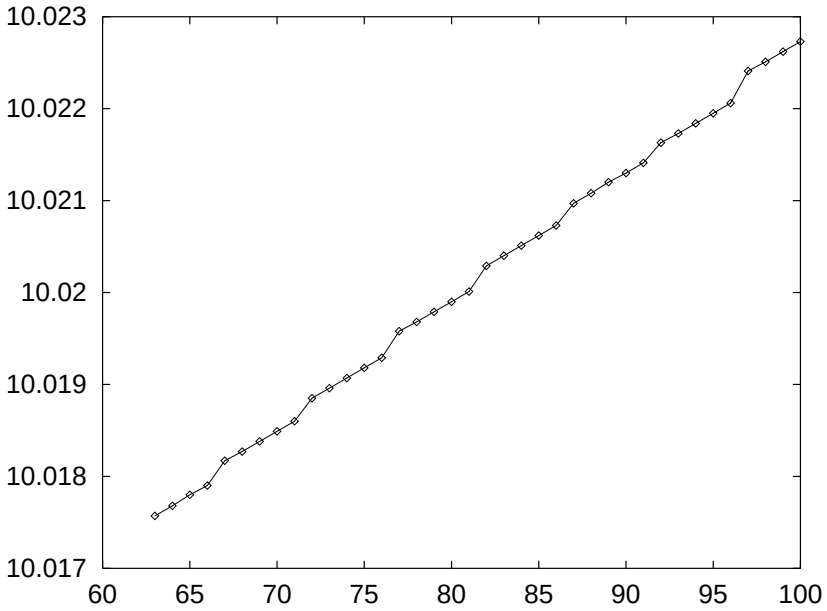

Figure B.4: The static energy as a function of time, during the constrained cooling, with time going from right to left. Clear jumps are seen every fifth time, corresponding to the reunitarization of the link matrices.

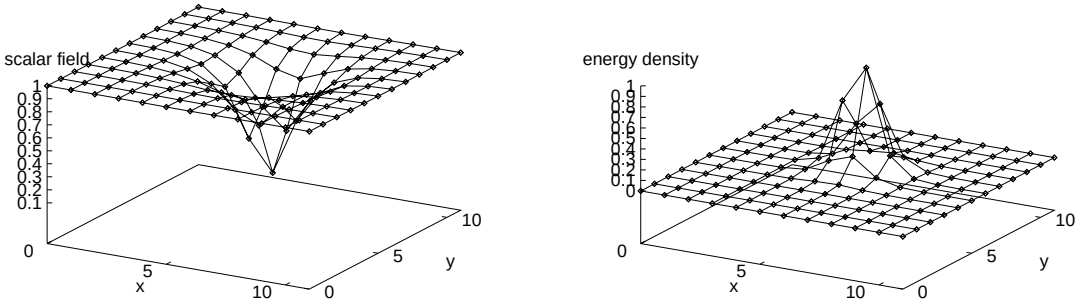

Figure B.5: The sphaleron configuration for $N = 12$ and $M_W = 1$. Mininimum value of $(\Phi^\dagger\Phi)^{\frac{1}{2}}/v = 0.30918$. Energy of configuration $E_{sph} = 3.223 M_W/\alpha$. Chern-Simons number $N_{CS} = 0.500$. Left the normalized magnitude of scalar field squared. Right the energy density, which is does not vanish at the boundary.

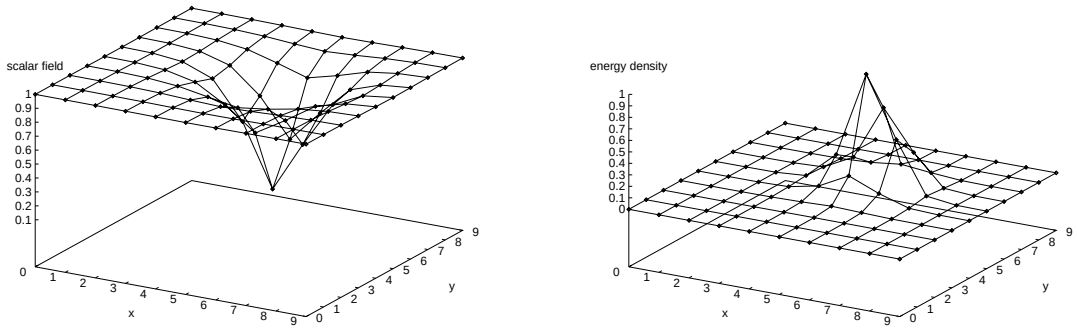

Figure B.6: The sphaleron configuration for $N = 10$ and $M_W = 1$. Mininimum value of $(\Phi^\dagger\Phi)^{\frac{1}{2}}/v = 0.29604$. Energy of configuration $E_{sph} = 3.250 M_W/\alpha$. Chern-Simons number $N_{CS} = 0.506$. Left the normalized magnitude of scalar field squared. Right graph the energy density, which is different from zero at the boundary.

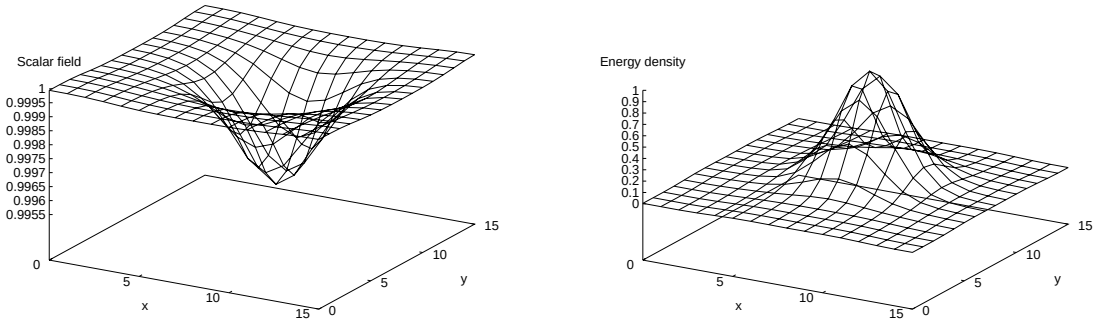

Figure B.7: A configuration on the barrier for $N = 16$ and $M_W = 1$ with $N_{CS} = 0.0098$. Energy of configuration $E = 0.123 M_W/\alpha$. Left the normalized magnitude of scalar field squared. Right the energy density.

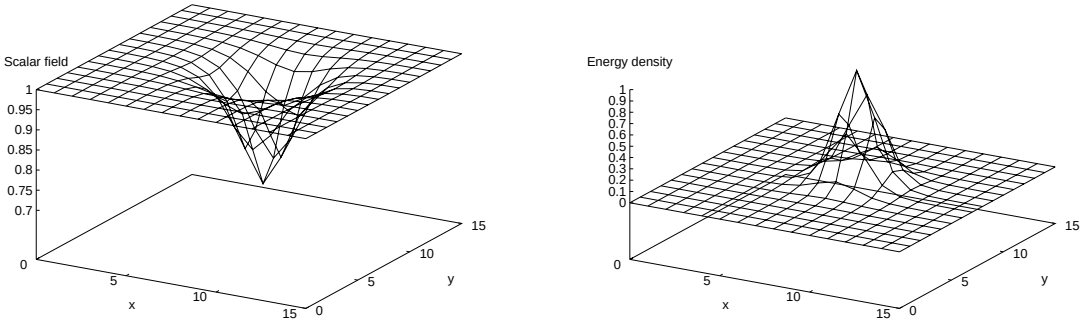

Figure B.8: A configuration on the barrier for $N = 16$ and $M_W = 1$ with $N_{CS} = 0.191$. Energy of configuration $E = 2.152 M_W/\alpha$. Left the normalized magnitude of scalar field squared. Right the energy density.

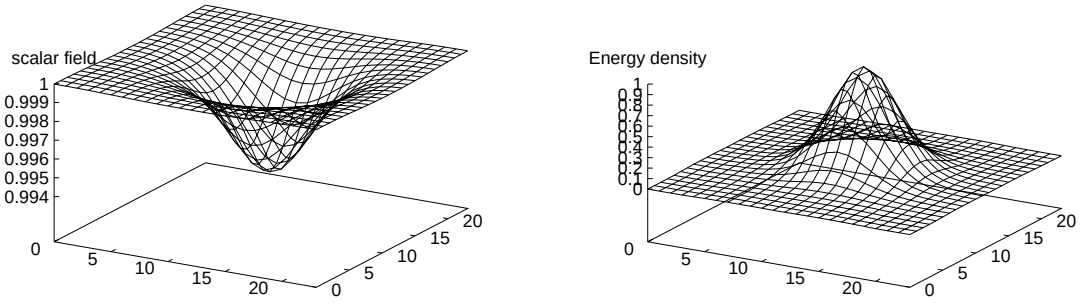

Figure B.9: A configuration on the barrier for $N = 24$ and $M_W = 1/2$ with $N_{CS} = 0.0083$. Energy of configuration $E = 0.104 M_W/\alpha$. Left the normalized magnitude of scalar field squared. Right the energy density.

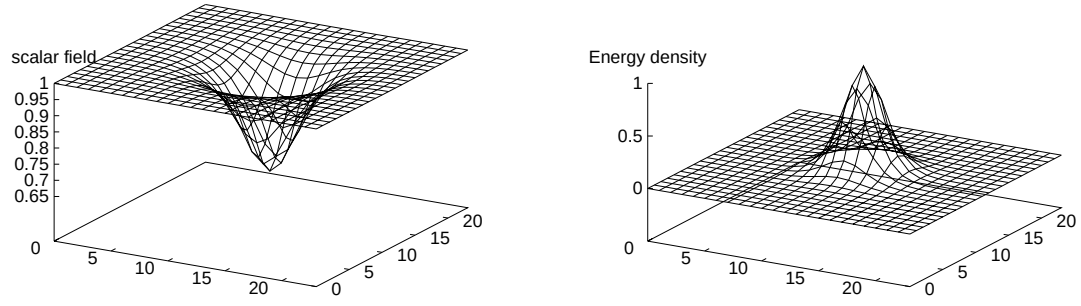

Figure B.10: A configuration on the barrier for $N = 24$ and $M_W = 1/2$ with $N_{CS} = 0.186$. Energy of configuration $E = 2.05 M_W/\alpha$. Left the normalized magnitude of scalar field squared. Right the energy density.

Bibliography

[1] M. E. Shaposhnikov, *Anomalous Fermion Number Non-conservation* (1991).

[2] A.G. Cohen, D.B. Kaplan, A.E. Nelson, **Annu. Rev Nucl. Part. Sci 43 27** (1993), *Progress in Electroweak Baryogenesis.*

[3] V.A. Rubakov, M.E. Shaposhnikov, **hep-ph/9603208** (1996). *Electroweak baryon number non-conservation in the Early Universe and in high energy collisions.*

[4] A.D. Sakharov, **ZhETF Pis'ma, no. 1, 32-35** (1967). *Violation of CP invariance, C asymmetry, and baryon asymmetry of the Universe.*

[5] G. 't Hooft, **Phys. Rev. D14 3432** (1976). *Computation of the quantum effects due to a four-dimensional pseudoparticle.*

[6] K. Fujikawa, **Phys. Rev. Lett. 42 1195** (1979). *Path-integral measure for gauge-invariant fermion theories.*

[7] R. F. Dashen, B. Hasslacher, A. Neveu, **Phys. Rev. D10 4138** (1974). *Nonperturbative methods and extended-hadron models in field theory. III. Four-dimensional non-abelian models.*

[8] N.S. Manton, **Phys.Rev D28 2019** (1983). *Topology in the Weinberg-Salam theory.*

[9] F. R. Klinkhamer, N.S. Manton, **Phys.Rev. D30 2212** (1984). *A saddle-point solution in the Weinberg-Salam theory*

[10] B. Kleihaus, J. Kunz, Y. Brihaye, **Phys. Lett B273 100** (1991). *The electroweak sphaleron at physical mixing angle.*

[11] J. Kunz, Y. Brihaye, **Phys. Lett. B216 353** (1989). *New sphalerons in the Weinberg-Salam theory.*

[12] A. Ringwald, **Phys. Lett B213 61** (1988). *Sphaleron and level crossing.*

[13] G. Nolte, J. Kunz, B. Kleihaus, **hep-ph/9507369** (1995). *Nondegenerate fermions in the background of the sphaleron barrier.*

[14] T. Akiba, H. Kikuchi, T. Yanagida, **Phys. Rev D38 1937** (1988). *Static minimum-energy path from a vacuum to a sphaleron in the Weinberg-Salam model.*

[15] L. Yaffe, **Phys. Rev. 40 3463** (1989). *Static solutions of $SU(2)$-Higgs theory.*

[16] Y. Brihaye, S. Giler, P. Kosinski, J. Kunz, **Phys. Rev. D42 2846** (1990). *Configuration space around the sphaleron.*

[17] J. Kunz, G.P. Korchemsky, **Nucl. Phys. B437 127** (1995). *Gradient approach to the sphaleron barrier.*

[18] B. Young, **hep-ph/9503298** (1995). *Some recent developments in sphalerons.*

[19] M. Garcia Perez, P. van Baal, **hep-lat/9512004** (1995). *The electroweak sphaleron on the lattice.*

[20] G. D. Moore, **hep-lat/9605001** (1996). *Improved Hamiltonian for Minkowski Yang-Mills theory.*

[21] G. D. Moore, **hep-th/9603384**. *Motion of Chern-Simons Number at High Temperatures under a Chemical Potential.*

[22] J. Kunz , S. Braibant, Y. Brihaye, **hep-ph/9302314** (1993). *Sphalerons at finite temperature.*

[23] J. Kunz, Y. Brihaye, **hep-ph/9304256** (1993). *Electroweak bubbles and sphalerons.*

[24] K. Kainulainen, **hep-ph/9503335** (1995). *Primordial baryon asymmetry and sphalerons.*

[25] T. Prokopec, R. Brandenberger, A. Davis, **hep-ph/9601327** (1996). *The impossibility of baryogenesis at a second order electroweak phase transition.*

[26] V.A. Kuzmin, V.A. Rubakov, M.E Shaposhnikov, **Phys. Lett. 155B 36** (1985).

[27] P. Arnold, L. McLerran, **Phys. Rev. D36 581** (1987). *Sphalerons, small fluctuations, and baryon-number violation in electroweak theory.*

[28] S. Yu. Khlebnikov, M.E. Shaposhnikov, **Nucl. Phys. B308 885** (1988). *The statistical theory of anomalous fermion number non-conservation.*

[29] L. McLerran, E. Mottola, M. E. Shaposhnikov, **Phys. Rev. D43 2027** (1991). *Sphaleron and axion dynamics in high-temperature QCD.*

[30] D. Diakonov, M. Polyakov, P. Sieber, J. Schaldach, K. Goeke, **hep-ph/9502245** (1995). *Sphaleron transitions in the minimal standard model and the upper bound for the Higgs mass.*

[31] U. Heller, F. Karsch, J. Rank, **Phys. Lett. B355 511-517** (1995). (1995). *The gluon propagator at high temperature.*

[32] J. Ambjørn, M. Laursen, M.E. Shaposhnikov, **Phys. Lett. 197B 49** (1987). *Baryon asymmetry of the Universe. Monte Carlo study on the lattice.*

[33] J. Ambjørn, T. Askgaard, H. Porter, M. E. Shasposhnikov, **Phys Lett. B244 479** (1990). *Lattice simulations of electroweak sphaleron transitions in real time.*
Nucl. Phys. B353 346 (1991). *Sphaleron transitions and baryon asymmetry: A numerical, real-time analysis.*

[34] J. Ambjørn, A. Krasnitz, **Phys. Lett. B** (1995). *The classical sphaleron transition rate exists and is equal to* $1.1(\alpha_w T)^4$.

[35] A. Krasnitz, **NBI-HE-95-25** (1991). *Thermalization algorithms for classical gauge theories.*

[36] D. Bödeker, L. McLerran, A. Smilga, **hep-th/9504123** (1995). *Really computing non-perturbative real time correlation functions.*

[37] W. Hung Tang, Jan Smit, **hep-lat/9605016** (1996). *Chern-Simons diffusion rate near the electroweak phase transition for* $m_H \approx m_W$.

[38] O. Philipsen, **hep-ph/9506478** (1995). *The sphaleron rate in the symmetric electroweak phase.*

[39] K. Kajantie, M. Laine, K. Rummukainen, M. Shaposhnikov, **hep-ph/9508379** (1995). *Generic rules for high temperature dimensional reduction and their application to the standard model.*

[40] K. Farakos, K. Kajantie, M. Laine, K. Rummukainen, M. Shaposhnikov, **hep-lat/9509086** (1995). *Results from 3D electroweak phase transition simulation.*

[41] K. Kajantie, M. Laine, K. Rummukainen, M. Shaposhnikov, **hep-ph/9605288** (1996). *Is there a hot electroweak phase transition at* $m_H \gtrsim m_W$ *?*

[42] M. Gürtler, E. Ilgenfritz, J. Kripfganz, H. Perlt, A Schiller, **hep-lat/9607063** (1996). *Physics of the electroweak phase transition at* $M_H \leq 70$ *GeV in a 3-dimensional* $SU(2)$*-Higgs model.*

[43] J. Ambjørn, K. Farakos, **Phys. Lett. B294 248** (1992). *Topography of the hot sphaleron transition.*

[44] J. Ambjørn, K. Farakos, M. E Shaposhnikov, **Nucl. Phys. B393 633** (1993), *Parity breaking at high temperature and density.*

[45] M. Gleiser, **DART-HEP-94/03** (1994). *Baryogenesis in brief.*

[46] E. Farhi *et al.*, **hep-ph/9410365** (1995). *Fermion Production in the background of Minkowski space classical solution in spontaneously broken gauge theory.*

[47] J. Ambjørn, J. L. Petersen, lecture notes, University of Copenhagen. *Quantum field theory.*

[48] J. C. Romao, F. Freire, *Electroweak physics and the early Universe.* Plenum publishing corporation ISBN 0-306-44909-9.

[49] I. Montvay, G. Münster, *Quantum fields on a lattice.* Cambridge University Press ISBN 0-521-40432-0.

[50] L. Ryder, *Quantum field theory.* Cambridge University Press ISBN 0-521-33859.